Seismic Damage Assessment of Reinforced Concrete Frame Buildings in Canada

By

Abdullah Al Mamun

A thesis submitted to the Faculty of Graduate and Postdoctoral Studies in partial fulfillment of the requirements for the degree of

Doctor of Philosophy

in

Civil Engineering

Department of Civil Engineering
Faculty of Engineering
University of Ottawa
June 2017

EXECUTIVE SUMMARY

The emphasis on seismic design and assessment of reinforced concrete (RC) frame structure has shifted from force-based to performance-based design and assessment to accommodate strength and ductility for required performance of building. RC frame structure may suffer different levels of damage under seismic-induced ground motions, with potentials for formation of hinges in structural elements, depending on the level of stringency in design. Thus it is required to monitor the seismic behaviour and performance of buildings, which depend on the structural system, year of construction and the level of irregularities in the structural system. It is the objective of the current research project to assess seismic performance of RC frame buildings in Canada, while developing fragility curves as analytical tools for such assessment. This was done through dynamic inelastic analysis by modelling selected building structures and using PERFORM-3D as analysis software, while employing incremental dynamic analysis to generate performance data under incrementally increasing seismic intensity of selected earthquake records. The results lead to probabilistic tools to assess the performance of buildings designed following the National Building Code of Canada in different years of construction with and without irregularities. The research consists of three phases; i) regular buildings designed after 1975, ii) regular buildings designed prior to 1975, and iii) irregular buildings designed prior to 1975. The latter two phases address older buildings prior to the development of modern seismic building codes. All three phases were carried out by selecting and designing buildings in Ottawa, representing the seismic region in eastern Canada, as well as buildings in Vancouver, representing the seismic region in western Canada. Buildings had three heights (2; 5; and 10-stories) to cover a wide range of building periods encountered in practice. The resulting fragility curves indicated that the older buildings showed higher probabilities of exceeding life safety and/or collapse prevention performance levels. Newer buildings showed higher probabilities of exceeding target performance levels in western Canada than those located in the east.

ACKNOWLEDGEMENTS

The journey begins when I leave my country with a dream of higher studies, six and a half years ago. On the verge of completing my Master degree, I started dreaming to obtain the highest degree in Earthquake Engineering. Though it was hard to take the decision as the future was vague to me and it is indeed a long term commitment. The decision was much easier when I got an offer from Dr. Murat Saatcioglu, who was always in my dream to come true. Today, after a long, adventurous and enjoyable journey, I come to complete the final requirement to acquire the Doctor of Philosophy degree in Civil Engineering. At this stage, I am grateful to acknowledge the contributions of my well-wishers.

At first, I would like to thank Dr. Murat Saatcioglu who trusted me as a potential researcher and gave me freedom to use my judgement and opinion in my research work. You will always be in my mind for your guidance, expertise, motivation and above all, polite behaviour.

I would like to remember my father, who died in my first year of PhD, for his dream and inspiration to motivate me to pursue a PhD in Civil Engineering. I would also like to thank my mother and sisters for their support and inspiration.

To my wife, Israt Jahan, this journey could not come true if I did not get courage, mental support and love from you. Thanks for your patience on taking care of our children alone in home and helping me to put more efforts to complete the research and course-work in a timely manner.

As a colleague, I like to thank Yasamin Rafie Nazari and Farah Hafeez to share their knowledge, idea and experience to enhance my research ability. I would also like to thank all of my friends at the University of Ottawa and elsewhere for their well wishes.

As this journey ends, a new journey starts again, with a new dream and new hope……

TABLE OF CONTENTS

LIST OF FIGURES

LIST OF TABLES

CHAPTER 1

1. INTRODUCTION

1.1 Seismic Vulnerability of Structures

Buildings are commonly designed for lateral forces due to wind and earthquakes. The level of design force depends on the geographic location of the building and the seismicity of the region specified in buildings codes. In Canada, the National Building Code of Canada (NBCC) is used to design buildings. NBCC defines structural loads for which buildings are designed. The code requirements change over the years as more information become available and structural analysis and design techniques advance. Older buildings, designed prior to the ductile design requirements of modern building codes lack proper seismic design and detailing. These buildings may be vulnerable to seismic forces. Figure 1.1 illustrates typical failures in reinforced concrete frame elements.

a) Reinforcement splice failure (Ref 1.)

b) Column shear failure (Ref 2.)

Fig 1.1 (Con'd)

c) Shear failure in short column (Ref 3.)

d) Beam diagonal tension failure (Ref 4.)

e) Beam yielding (Ref 5.)

f) Beam-column joint failure (Ref 6.)

Fig 1.1 Reinforced concrete frame failures under earthquake loading

In Canada, the first National Building Code was published in 1941. It contained seismic design provisions based on the 1937 edition of the Uniform Building Code (UBC) in the U.S. The earthquake design force was defined as a fraction of building weight (seismic coefficient). The same approach remained in the NBCC with gradually improving computation of seismic coefficient. In 1953 the seismic coefficient included the effect the number of stories. In 1960 the effects of site soil condition and the type of construction were introduced, with the latter parameter indirectly reflecting available ductility in the structural system, without explicitly addressing the requirements for ductile detailing. This parameter was expanded in 1970. The 1970 NBCC also included the effects of different seismic zones in Canada with a multiplier. It was not until 1975 NBCC, which made reference to the 1973 CSA Standard A23.3, “Design of

Concrete Structures for Buildings" (CSA) and contained ductile design and detailing requirements for concrete frame buildings, that ductile design was implemented in Canada. These requirements and expected building performance have improved since then, with significant improvements introduced in the 1985 NBCC and associated CSA A23.3-84 with the adoption of "Capacity Design" concept. The buildings were then designed to promote ductile flexural response, as opposed to brittle shear distress. Figure 1.2 illustrates the performance of ductile and brittle reinforced concrete building response.

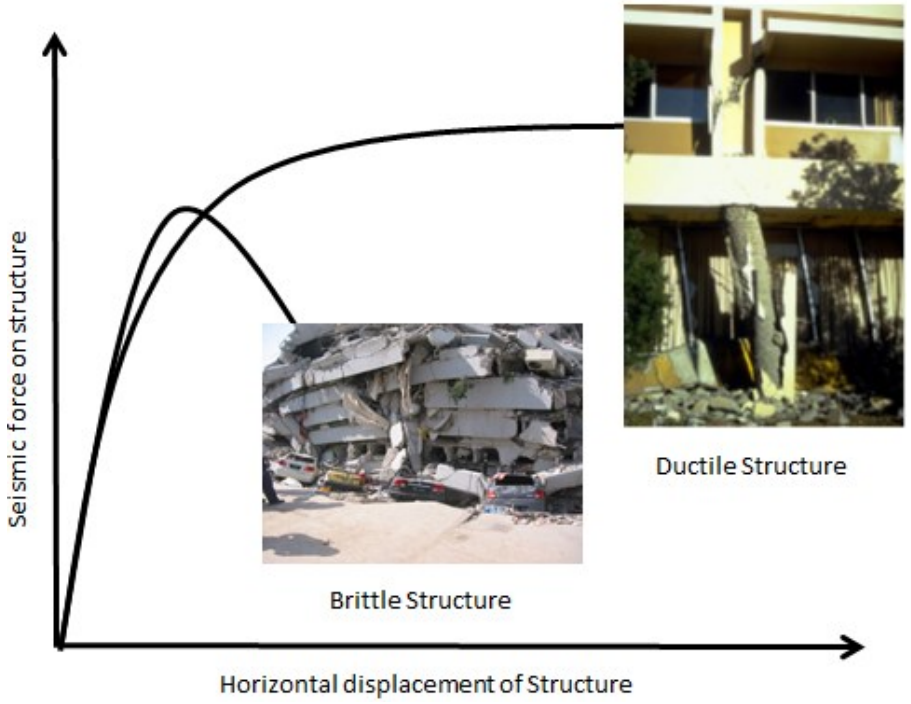

Fig 1.2 Ductile versus brittle response (Ref 7., Ref 8.)

An important aspect of seismic response of buildings is the regularity of the structural system. It has consistently been observed after previous earthquakes that buildings having irregularities have higher seismic demands. These buildings suffer significantly more damage than those that have regular floor plans, without discontinuities. Recent codes generally address the design of buildings having irregularities. In addition, restrictions have been specified to prevent designs that would lead to increased seismic force and deformation demands. As an example, the NBCC since 2005 does not permit the use of soft storeys in hospital buildings. Other buildings with irregularities must be designed to account for increased seismic demands. Figure 1.3 shows damage to irregular buildings, observed during previous earthquakes.

a) Soft storey collapse (Ref 9.)

b) Loss of a storey due to vertical discontinuity (Ref 10.)

c) Damage associated with setback (Ref 11.)

d) Torsional failure (Ref 12.)

Fig 1.3 Seismic behaviour of irregular buildings

It becomes clear from the forgoing discussion that reinforced concrete frame buildings designed and built prior to 1975 may be vulnerable to earthquake forces. Buildings designed after 1975 may also experience seismic damage, especially if subjected to strong earthquakes. Indeed, the design philosophy of NBCC is to maintain life safety of the occupants, with potentially significant damage in buildings under strong earthquakes, repairable damage under medium size earthquakes and insignificant damage in the event of minor earthquakes so that the

buildings could be re-occupied immediately after the earthquake. Different performance of buildings after earthquakes prompted "performance-based design and assessment" of buildings in recent years. Irregular buildings are especially susceptible to seismic forces. Existing buildings may need to be assessed against different levels of performance for proper seismic mitigation measures. Seismic evaluation of existing buildings can best be determined through dynamic inelastic response history analysis. However, this may not always be feasible if the building inventory at hand is large. An alternative to individual building analysis is the fragility analysis of buildings. Fragility analysis provides information on the probability of exceedance of pre-defined performance objectives under different earthquake intensity measures. Such an analysis results in fragility curves, which when available for buildings of different structural characteristics, provide convenient seismic assessment tools.

Fragility curves for different buildings designed in different eras, with different lateral load systems lack in Canada. A comprehensive research program is currently underway at the University of Ottawa to develop fragility curves for reinforced concrete and masonry buildings in Canada, reflecting the Canadian design practice. The current research is a research project that intended to fill this gap in the area of reinforced concrete frame buildings. Companion projects include reinforced concrete shear wall buildings, and masonry buildings.

According to NBCC 2010, design seismic shear force in irregular frame structures should be equal to or greater than that established by equivalent static loads, whereas design seismic forces in regular frame structures can be reduced by 20% through dynamic analysis. NBCC 2010 defined 8 types of irregularity in frame structures with no quantification was made to differentiate the effect of irregularity type on seismic design force. Guidelines were not provided in NBCC prior to 1985 to calculate seismic base shear for buildings with irregularities. Lack of study was observed to quantify the effect of irregularity on seismic design forces in Canada. Hence a detailed initiative has been taken in this research project to identify the effect of selected irregularitiess on seismic behaviour of code-complied reinforced concrete frame structures in eastern and western Canada constructed prior to 1975.

1.2 Objective

The overarching goal of this research project is to evaluate the seismic performance of existing reinforced concrete frame structures in Canada through fragility analysis. Since Canada exhibits two distinctly different seismically active regions; one in the west, resulting in earthquakes associated with active fault lines likely to cause strong ground excitations; and the other in the east, believed to be caused by crustal weaknesses and likely result in medium size earthquakes, the characteristics of both regions are considered. More precisely, the objectives of this research project include the development of fragility curves for reinforced concrete buildings in Canada; i) with ductile design characteristics, conforming building codes after 1975, ii) with brittle design of pre-1975 era but regular structural layouts, and ii) with brittle design of pre-1975 era with irregularities. The following forms the milestones of the research project:

- Identify seismic performance and failure modes of ductile reinforced concrete frame buildings designed after 1975.
- Identify performance levels of post-1975 reinforced concrete frame buildings.
- Develop fragility response and fragility curves for post-1975 reinforced concrete frame buildings.
- Identify seismic performance and failure mode of pre-1975 reinforced concrete frame buildings.
- Develop fragility response and fragility curves for pre-1975 reinforced concrete frame buildings.
- Compare performance of pre-1975 and post 1975 frame buildings.
- Identify seismic performance and failure modes of pre-1975 reinforced concrete frame buildings with stiffness, geometric and torsional irregularities, effects of which were not accounted for as stringently as newer buildings.
- Develop fragility response and fragility curves for the above reinforced concrete frame buildings with irregularities.
- Quantify effects of irregularity type on seismic behaviour of older buildings with irregularities.
- Identify the effects of building height and associated building period, age of construction, irregularities and the seismicity of the region on fragility response of reinforced concrete frame buildings.

1.3 Methodology and Scope

The research methodology follows the following scope:

- *Literature review:* A detailed literature review was conducted to identify research needs, building selection, seismic record selection, analysis method and Finite Element (FE) model, performance criteria, effects of parameters (flexure/shear) on failure modes, development of fragility curves and effects of irregularity on building seismic performance.
- *Selection of building plan and dimensions:* Frame buildings with different heights were selected to cover a wide range of structural period.
- *Design of frame buildings:* Frame buildings selected in this study were designed for both Ottawa in eastern Canada and Vancouver in western Canada as moderately ductile and ductile structures, respectively.
- *Selection of seismic records:* Synthetic seismic records compatible with UHS of NBCC 2010 were selected for dynamic analysis of structures.
- *Selection of suitable non-linear software*: PERFORM-3D (CSI 2013) was selected as software to model the buildings designed, and to perform non-linear dynamic analysis under selected ground motions.
- *Verification of numerical models and dynamic analysis:* The analytical model developed for PERFORM-3D and the analysis results were verified by using other well-known non-linear computer software.
- *Performing Incremental Dynamic Analysis (IDA):* Seismic records were incrementally reduced and amplified to cover a range of earthquake intensities to develop IDA curves and identify seismic behaviour and failure modes of buildings.
- *Identification of performance levels:* Maximum inter-storey drift level was considered as a damage indicator in this study to define performance levels. Drift demands for performance levels were selected based on available standards and literature.
- *Development of fragility curves*: Fragility responses were computed and fragility curves were developed for selected performance levels in terms of spectral accelerations through IDA.

A graphical view of the research methodology is shown in Fig. 1.4.

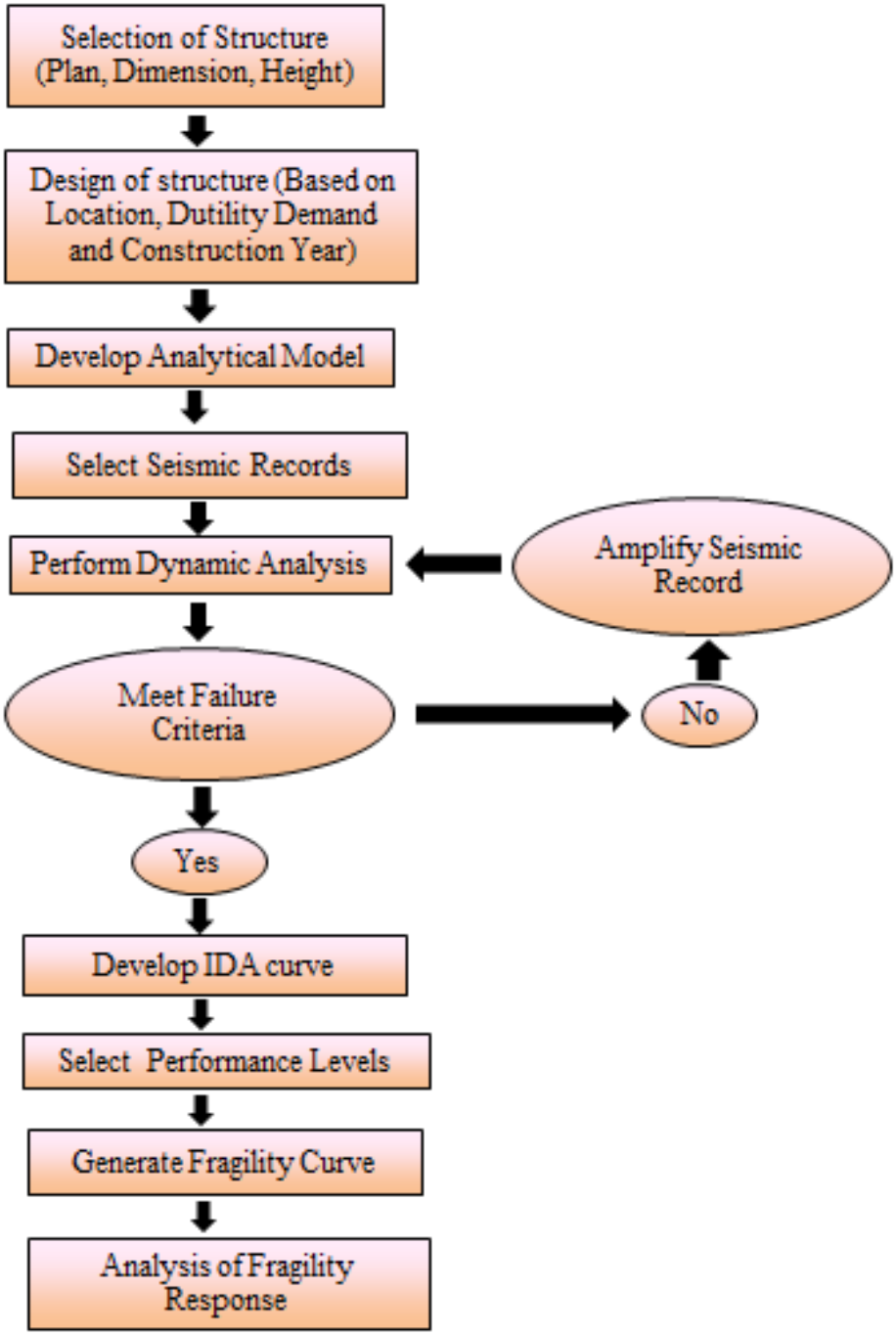

Fig 1.4 Flow chart of research methodology

1.4 Presentation of Thesis

The thesis consists of 7 Chapters. The details of each chapter are described below:

- *Chapter 1*: Introduction chapter where research needs are summarized and the objective and methodology of research are described.
- *Chapter 2*: Literature Review chapter where seismic vulnerability assessment techniques used by previous researchers are reviewed. Since fragility analysis was selected as the research approach, the emphasis is placed on the review of previous research on fragility analysis. Since the effects of structural irregularities are studied, observations and findings of previous research on both regular and irregular frame buildings are included.

- *Chapter 3*: This chapter represents the journal article "Seismic Performance Evaluation of RC Frame Structures Using PERFORM-3D", provisionally accepted for publication in *Earthquake Spectra* (Manuscript ID: 081016EQS131M). Detailed description of structural model development techniques with PERFORM-3D software and the effects of different modelling parameters on fragility response are discussed in this chapter.
- *Chapter 4*: This chapter presents the journal article "Seismic Fragility Curves for Reinforced Concrete Frame Buildings in Canada Designed After 1985" published in *Canadian Journal of Civil Engineering* (Online on May 1st 2017, DOI: 10.1139/cjce-2016-0388). Structural design and fragility analysis of 2, 5 and 10-storey reinforced concrete frame buildings designed according to the 2010 NBCC for Ottawa and Vancouver with regular structural layout is presented. Detailed descriptions of the procedure employed to generate IDA curves, selection of seismic records, failure modes of structures and effects of structural period on fragility response are also presented.

- *Chapter 5*: This chapter presents the journal article "Seismic Fragility Analysis of Pre-1975 Conventional Concrete Frame Buildings in Canada", under review in *Canadian Journal of Civil Engineering* (Manuscript ID: cjce-2017-0238). Structural design and fragility analyses of 2, 5 and 10-storey reinforced concrete frame buildings, designed according to the 1965 NBCC for Ottawa and Vancouver with regular structural layout, are presented. Detailed descriptions of fragility curves and seismic performance assessment are also described.

- *Chapter 6:* This chapter presents the journal article "Seismic Performance Assessment of Pre-1975 Irregular Concrete Frame Buildings in Canada", intended to be submitted to *Earthquake Spectra.* Structural design and fragility analysis of 5-storey irregular reinforced concrete frame buildings designed according to the 1965 NBCC for Ottawa and Vancouver are presented. Detailed descriptions of the effects of irregularities on fragility response, and performance assessment of buildings are discussed.
- *Chapter 7:* This chapter presents summary and conclusions of the research project.
- *Appendix A:* Describes seismic vulnerability assessment of a 6-storey frame building in Canada by using the fragility curves developed in this research study.

1.5 References for Chapter 1

Canadian Standards Association (CSA). 1973. Design of concrete structures. CSA standards update service. CSA A23.3-1973. Mississauga, Canada.

Canadian Standards Association (CSA). 1984. Design of concrete structures. CSA standards update service. CSA A23.3-1984. Mississauga, Canada.

Computers and Structures, Inc (CSI), 2013. *PERFORM-3D. Version 5.0.1*. Berkeley, CA.

NBCC. (1970). National building code of Canada 1970. *National Research Council of Canada*, Ottawa, Ont.

NBCC. (1975). National building code of Canada 1975. *National Research Council of Canada*, Ottawa, Ont.

NBCC. (1985). National building code of Canada 1985. *National Research Council of Canada*, Ottawa, Ont.

NBCC. (2005). National building code of Canada 2005. *National Research Council of Canada*, Ottawa, Ont.

NBCC. (2010). National building code of Canada 2010. *National Research Council of Canada*, Ottawa, Ont.

Ref 1. Available at "http://www.drgeorgepc.com/Tsunami1976Phillipines.html".

Ref 2. Available at "https://www.fhwa.dot.gov/publications/research/infrastructure/structures/11029/003.cfm".

Ref 3. Available at "http://db.world-housing.net/pdf_view/15/".

Ref 4. Available at “http://www.arch.virginia.edu/~km6e/tti/tti-summary/part-2.html”.

Ref 5. Available at “http://nees-anchor.ceas.uwm.edu/wenchuan_earthquake/eeri_lfe_wenchuan.html”.

Ref 6. Available at “http://peer.berkeley.edu/grandchallenge/news/successful-nees-grand-challenge-tests-on-non-ductile-beam-column-joints-experiencing-axial-collapse-under-simulated-seismic-loading/”.

Ref 7. Available at “https://sites.google.com/a/ualr.edu/operation-rabbit-hole-where-did-the-towers-go/the-collapse-story”.

Ref 8. Available at “http://db.world-housing.net/pdf_view/111/”.

Ref 9. Available at “https://failures.wikispaces.com/1999+Kocaeli-Golcuk+%26+Duzce-Bolu+Turkey+Summary+%26+Lessons+Learned”.

Ref 10. Available at “https://www.slideshare.net/javeduet/module-2-53880998”.

Ref 11. Available at “http://www.nation.co.ke/photo/1951220-2559334-1a1hox/index.html”.

Ref 12. Available at “http://www.canadianunderwriter.ca/features/shaken-and-stirred/”.

UBC. (1937). Uniform Building Code 1937. *International Conference of Building Officials*, Whittier, California, USA.

CHAPTER 2

2. LITERATURE REVIEW

2.1 Introduction

Losses due to earthquakes have increased dramatically during the last decade. This is explained by the concentration of populations in urban centres and the development of cities in high seismic areas (Smolka et al. 2004). According to the CEDIM 2011 report, 20,475 fatalities occurred due to earthquakes in 2011 alone, leaving 1.108 million people homeless. The economic loss due to the 2011 Tohoku Earthquake was $144 billion. An economic loss caused by the 2011 Christchurch Earthquake was over $20 billion, the 2011 Van Earthquake in Turkey was $2.2 billion and the 2011 Sikkim Earthquake in India was $1.7 billion.

Reinforced concrete buildings are a significant percentage of the building stock in all over the world. Therefore, seismic vulnerability assessment of reinforced concrete buildings is essential by developing seismic assessment tool (Masi & Vona. 2012). The seismic tool is not only important to predict the economic and structural impact of potential earthquake, but also can perform a significant role on seismic hazard mitigation and rehabilitation solutions. The tool can also be used to assess the seismic vulnerability of buildings designed and constructed based on recent building codes. The seismic assessment tool assesses the vulnerability of buildings by considering the site specific seismic hazard, structural system, failure criteria and inelastic properties of structural members. From the analysis and damage state of structure it is possible to calculate the loss and repair cost of a building stock. (Calvi et al. 2006).

Loss of structure due to potential earthquake can be quantified with proper selection of site specific ground records and vulnerability assessment of building. (Angeletti et al. 1988). Figure 2.1 shows a chart to evaluate the seismic vulnerability of buildings.

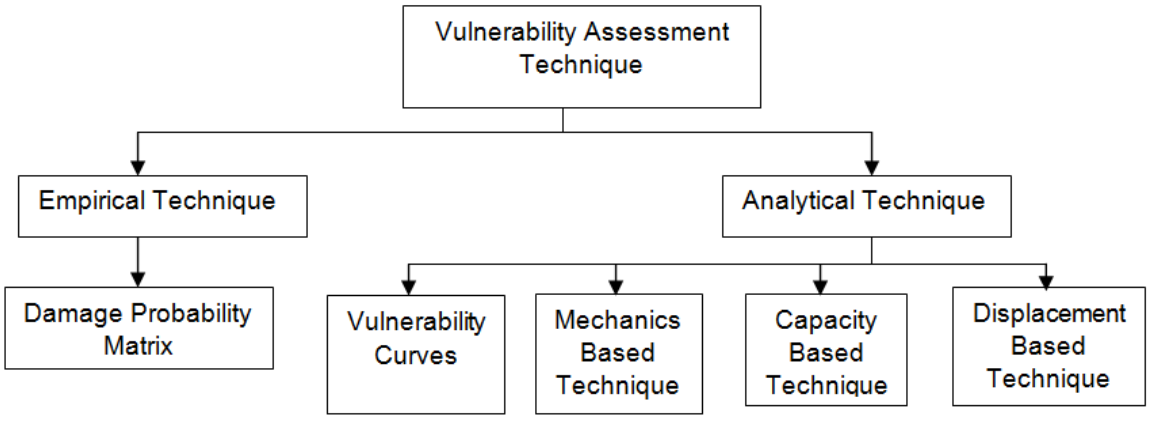

Fig 2.1 Assessment technique to evaluate the vulnerability of buildings

2.2 Vulnerability Assessment Techniques

2.2.1 Empirical Technique - Damage Probability Matrix

Okada and Takai (2000) developed damage vulnerability functions with consideration of ground motion intensity and structural damage relation for various types of structures. They proposed a chart, as shown in Figure 2.2, for describing building damage patterns by seismic vulnerability so as to help investigators to classify building damage without a gross error. In the proposed damage scale, damage was defined on a scale of 0.0 (No damage) to 1.0 (Total collapse). For D2 (Moderate damage) buildings damage index values of 0.2 to 0.4 were assigned which was equivalent to damage associated with falling plasters. Structural damage in buildings were classified as D3 (Substantial to heavy damage) and the index values were assigned to 0.4 to 0.6. This level of damage was associated with large and deep cracks in walls of unreinforced masonry and reinforced concrete buildings, and warping of wall boards in wood frame buildings. For the significant damage condition of buildings where repair is impossible, damage index of 0.6 to 0.8 was assigned, and the damage grade was classified as D4. Damage grade D5 (Damage index 0.8 to 1.0) was assigned to totally collapsed buildings where the stories of buildings have disappeared.

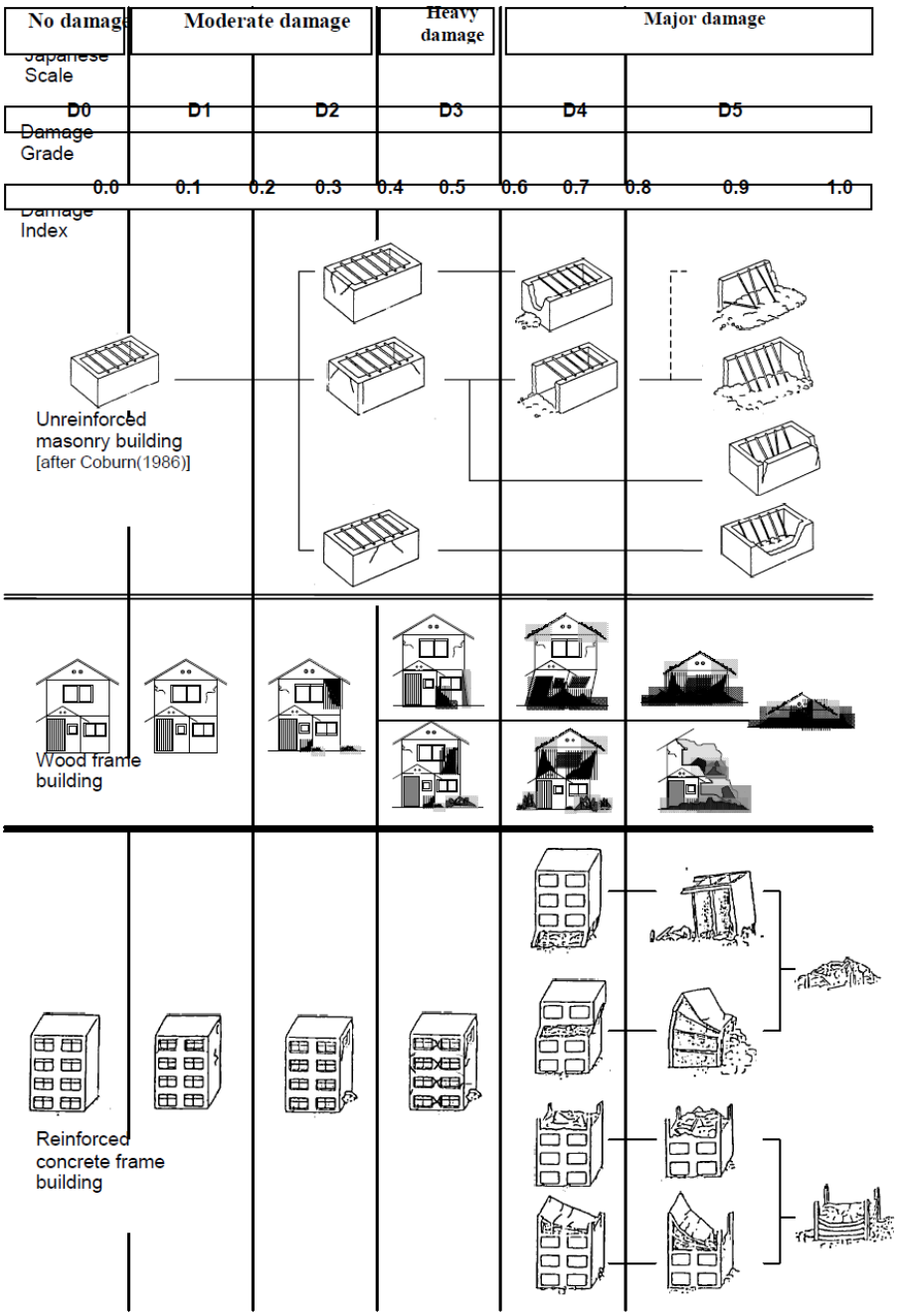

Fig 2.2 Damage Pattern Chart (Okada and Takai, 2000)

European Macroseismic (EM) Scale (EMS-98) includes an Intensity Scale ranging from V to XII for six different classes of decreasing vulnerability (from A to F). In the EM scale, it was attempted to move closer to classes directly representing vulnerability. Table 2.1 shows that the well-built and well-performed structures are defined as class D and F, whereas structures designed to resist seismic force defined as class F.

Table 2.1 Differentiation of structures (buildings) into vulnerability classes (EMS-98)

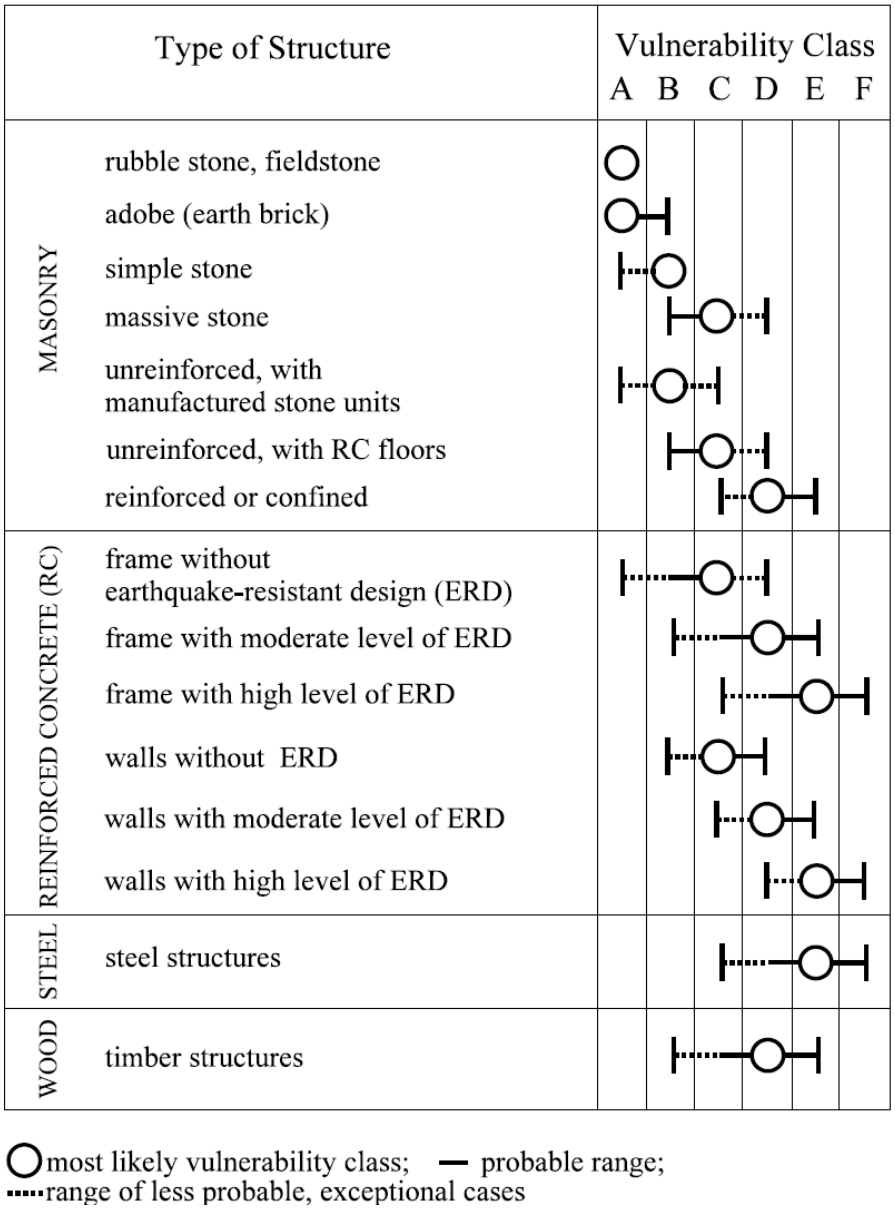

EMS-98 described “Few”, “Many” and “Most” to define damage grades associated with the intensity levels as shown in Table 2.2.

Table 2.2 Damage Model for Vulnerability Class C as Presented in EMS-98 (Calvi et al. 2006).

Damage Level Intensity	Damage Grade				
	1	2	3	4	5
V					
VI	Few				
VII		Few			
VIII		Many	Few		
IX			Many	Few	
X				Many	Few
XI					Many
XII					Most

2.2.2 Analytical Techniques

Analytical procedures involve development of response for building where ground motion due to earthquake considers as intensity measure and deformation of the structure consider as damage measure indicator. Damage state of the building can be identified for different performance level from the response curves. This method is suitable to forecast the potential damage condition for a building stock during earthquakes. (Manzur and Noor, 2006).

2.2.2.1 Analytically-Derived Vulnerability Curves and DPMs

Rajeev and Tesfamariam (2012) developed vulnerability curves for RC buildings, which have either poor quality of construction on different irregularities such as weak storey, soft storey, plan irregularities. Soft storey (SS) and quality of construction (CQ) was taken into consideration to develop fragility based seismic vulnerability of structures. Nonlinear finite element analysis was used to develop probabilistic seismic demand model (PSDM) for gravity load designed structures, considering the interactions between SS and CQ. The fragility curves were developed by considering SS, CQ and of their interactions as a measure of risk-informed decision-making. Figure 2.3 shows the fragility curve of a three storey-three bay frame for three different limit states where the Immediate Occupancy (IO) level described as the structure can be occupied safely without significant repair, the SD level occurs at significant damage to the structure but a substantial margin remains against incipient collapse, and the Collapse Prevention (CP) level

defined collapse of the frame due to either severe degradation in strength of members or excessive lateral deformations.

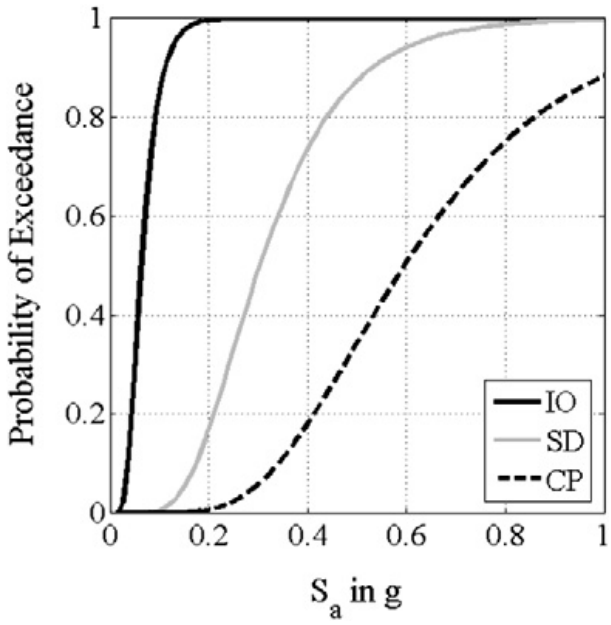

Fig 2.3 Seismic fragility curve for three storey-three bay frame (Rajeev and Tesfamariam,2012)

Singhal and Kiremidjian (1996) developed a method to obtain fragility curves and damage probability matrices for reinforced concrete frames. Nonlinear properties of structures and nonstationary characteristics of ground motions were considered to develop fragility curves and damage probability matrices. Modified Mercalli intensity was used as the ground motion parameter for damage probability matrices. Monte Carlo-simulation technique was used to evaluate probabilities associated with different damage states at a specified ground motion level. The nonstationary autoregressive moving average (ARMA) model was used to generate earthquake time histories. Figure 2.4 and Table 2.3 show fragility curves and a damage probability matrix for a sample high-rise building. A fragility curve for a particular damage state for various levels of ground motion was obtained by computing the conditional probabilities of reaching or exceeding that damage state. The conditional probabilities were defined as follows:

$P_{ik} = P[D \geq d_i \mid Y = y_k]$

Where P_{ik} = probability of reaching or exceeding a damage state at ground motion y_k;

D = damage random variable defined on damage state vector; D = $\{d_1, d_2, \ldots\ldots d_n\}$;

Y = ground motion random variable.

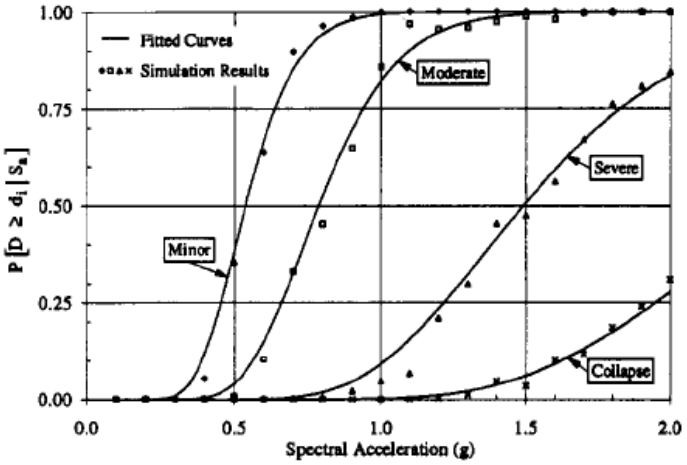

Fig 2.4 Fragility Curves for Sample High-Rise Building (Singhal and Kiremidjian, 1996)

Table 2.3 Damage Probability Matrix for Sample High-Rise Building (Singhal and Kiremidjian, 1996)

Damage state (1)	Modified Mercalli Intensity VI (2)	VII (3)	VIII (4)	IX (5)	X (6)	XI (7)	XII (8)
None	100.0	99.7	93.0	35.3	0.2	—	—
Minor	—	0.3	5.7	35.3	3.3	—	—
Moderate	—	—	1.3	26.9	45.9	0.7	—
Severe	—	—	—	2.4	38.9	11.8	—
Collapse	—	—	—	0.1	11.7	87.5	100.0

2.2.2.2 Collapse Mechanism-Based Methods

Cosenza et al. (2005) developed a mechanical based approach to assess seismic capacity of buildings and derived capacity curves in terms of ultimate strength and deformation capacities. The approach allowed changing the mechanical properties and geometric configurations of RC building to evaluate the relative influence on the capacity.

For a pre-defined collapse mechanism (i=1,2..n) (Fig. 2.5) for each structural model, equilibrium equations were used to determine base shear, $V_{b,i}$. Horizontal seismic force, F_i

distribution was assumed as linear. Ultimate roof displacement, $\Delta_{u,i}$ was determined as a function of the minimum ultimate rotation, θ_u. The global seismic behaviour was then represented by the base shear coefficient, $C_{b,i}$ (i.e., base shear $V_{b,i}$ divided by seismic weight W) and the corresponding lateral drift, $\Delta_{u,i}$ (i.e., roof displacement divided by building height, H_n).

$$V_{b,1} = \frac{\sum M_c^k + \sum_{i=k+l}^{n} \sum M_b}{\sum_{i=k+1}^{n} H_i \cdot (H_i - H_k)} \sum_{i=1}^{n} H_i,$$

$$V_{b,2} = \frac{\sum M_c^l + \sum M_c^k + \sum_{i=2}^{k-l} \sum M_b}{\sum_{i=1}^{k-l} H_i^2 + \sum_{i=k}^{n} H_k H_i} \sum_{i=1}^{n} H_i,$$

$$V_{b,3} = \frac{2 \cdot \sum M_c^k}{\sum_{i=k}^{n} H_i \cdot (H_k - H_{k-1})} \sum_{i=1}^{n} H_i.$$

$$\Delta_{u,1} = \theta_u \cdot (H_n - H_k),$$
$$\Delta_{u,2} = \theta_u \cdot H_k,$$
$$\Delta_{u,3} = \theta_u \cdot (H_k - H_{k-l})$$
$$C_{b,i} = \frac{V_{b,i}}{W},$$
$$(\text{drift}_u)_i = \frac{\Delta_{u,i}}{H_n}$$

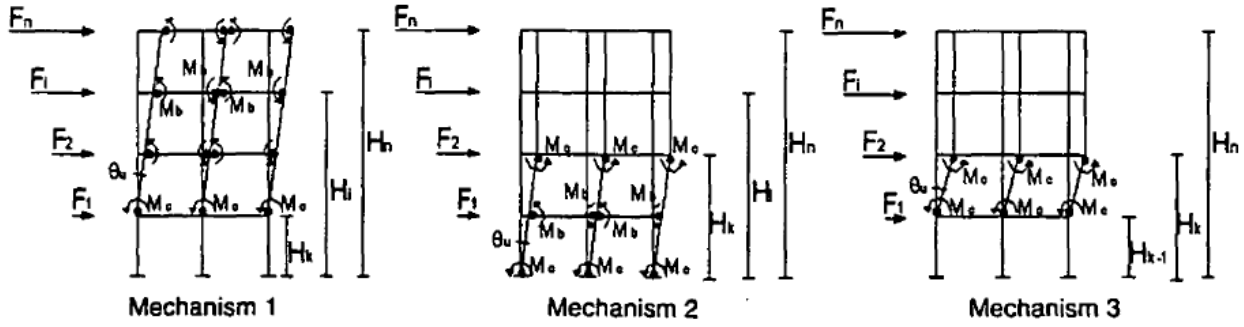

Fig 2.5 Analyzed collapse mechanism types (Cosenza et al. 2005).

D'Ayala and Speranza (2002) incorporated collapse mechanism at failure and load factors to assess seismic vulnerability of masonry building. The collapse mechanics included effect of boundary condition and construction material quality. The mechanism considered both in-plane and out of plane failure mode of walls, whereas only out of plane failure mode was considered for roof and floor elements. Figure 2.6 shows the schematic failure mode of out of plane collapse.

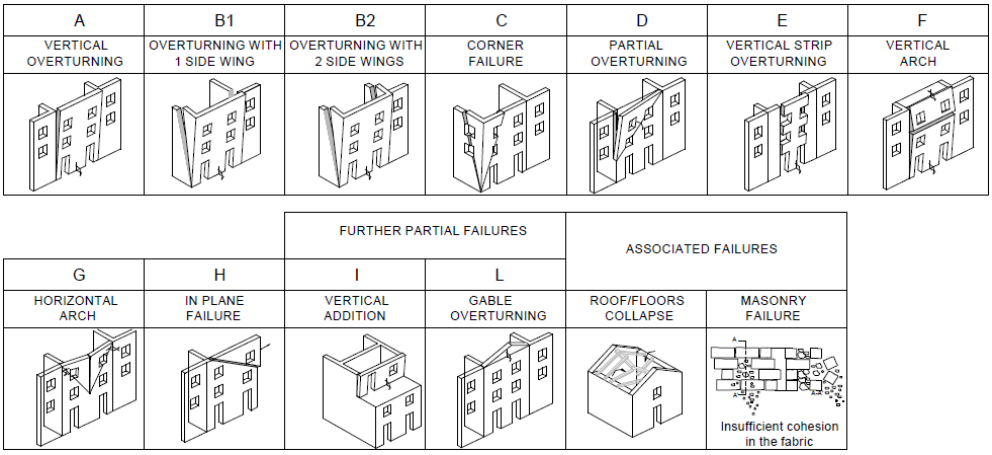

Fig 2.6 Schematic failure mode of out of plane collapse mechanism (D'Ayala and Speranza 2002)

2.2.2.3 Capacity Spectrum-Based Methods

Capacity Spectrum Method (CSM) was first developed as a rapid evaluation method for a pilot seismic risk project of the Puget Sound Naval Shipyard for the U.S. Navy by Freeman (1998). It was assumed that the structure consisted of hysteresis behaviour. The global stiffness degradation was also considered. The capacity spectrum consisted of spectral acceleration, S_a and spectral displacement, S_d and the secant period, T along the curve was calculated by the following:

$$T = 2\pi(S_d \div S_a g)^{1/2} .$$

A bilinear idealized curve consisted of yield and inelastic peak point was calculated from the capacity spectrum. Earthquake response spectra were used to represent the demand curve as shown in Fig. 2.7.

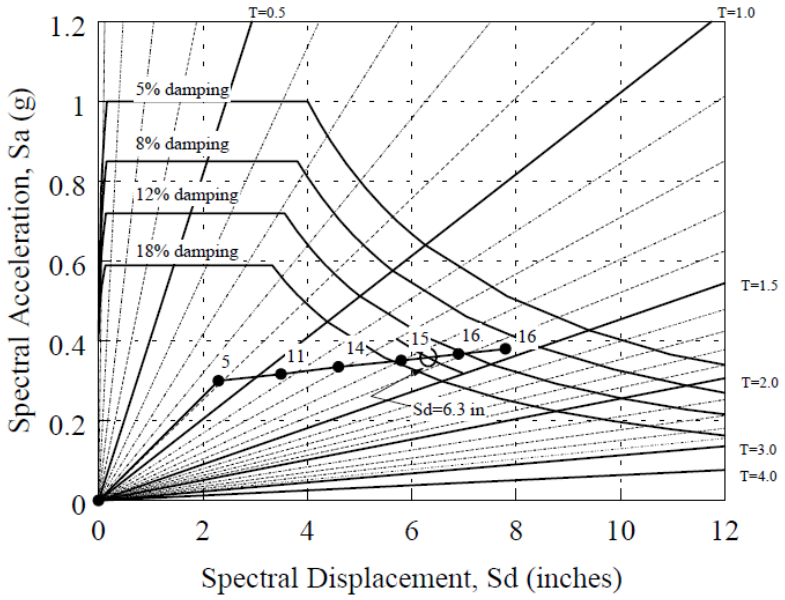

Fig 2.7 CSM graphical solution (Freeman, 1998)

Kircher et al. (1997) described the earthquake loss estimation methodology developed by Whitmen et al. (1997) to estimate the probability of discrete states of structural and non-structural damage to buildings for FEMA/NIBS. In this method, base shear was converted to spectral acceleration and the roof displacement was converted to spectral displacement in order to facilitate direct comparison with spectral demand. Building capacity curves were defined by two control points: (a) yield capacity, and (b) ultimate capacity. The yield strength of the building represented the lateral strength which accounted for design strength, redundancies and conservatism in building codes and strength of materials whereas ultimate capacity represents the maximum strength of building when the structural system reached to full mechanism. The intersection point of the demand spectrum for different intensity ground motion and the building capacity curve indicated the seismic response of the building as shown in Fig. 2.8.

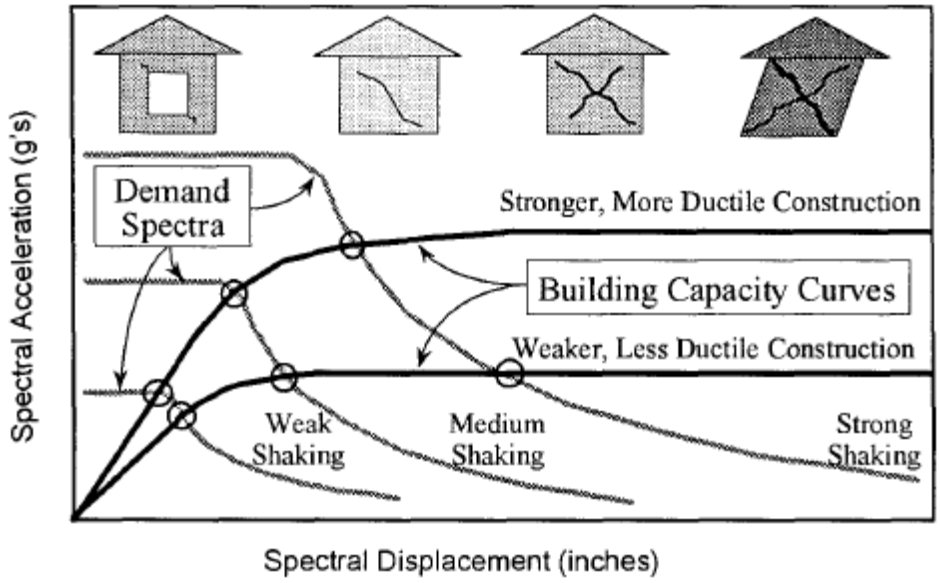

Fig 2.8 Plotting of demand spectra and building capacity curves (Kircher et al. 1997)

Fajfar (1999) developed a more straightforward approach for the determination of seismic demand which was based on the use of inelastic strength and displacement spectra and could be obtained directly by time-history analyses of inelastic SDOF systems, or indirectly from elastic spectra. In this modified capacity spectrum method, the base shear-top displacement relationship was determined by pushover analysis. It was assumed that the lateral force, P_i in the i th storey was proportional to the displacement shape, ϕ_i weighted by the storey mass, m_i

$$P_i=m_i\phi_i$$

Then the force-displacement relationship of the MDOF transformed into that of an equivalent SDOF system.

$$Q = \Gamma Q^*$$

$$\Gamma = (\sum m_i\phi_i)/ (\sum m_i\phi_i^2)$$

Where Q^* represented the quantities (force, displacement and hysteretic energy) in the equivalent SDOF system and Q represented the corresponding quantities (base shear, top displacement and hysteretic energy) in MDOF system. Graphical procedure was used to idealize the force-displacement relationship of the equivalent SDOF system into an elastic-perfectly plastic form. Reduction factor was defined as the ratio of the required elastic strength to the yield

strength. In the demand spectra, the influence of moderate strain hardening was incorporated. The elastic period of SDOF system was determined as

$T^* = 2\pi\sqrt{(m^*D_y^*/F_y^*)}$

Where D_y^* and F_y^* were the yield displacement and strength.

The intersection point of the elastic stiffness of SDOF system and the elastic demand spectrum determined the strength required for elastic behaviour and the corresponding elastic displacement demand. The ductility demand was then calculated by

$$\mu = (R\mu - 1)\frac{To}{T*} + 1$$

Where $R\mu$ = Reduction factor and T_o = Transition period. The displacement demand was determined as $D^* = S_d = \mu D_y^*$

The displacement then transformed back from the SDOF to the MDOF system and the performance at maximum displacement was evaluated on the global and local level. Figure 2.9 shows a pushover curve and corresponding capacity spectrum for a 4-storey RC frame and Fig. 2.10 shows demand and capacity spectra.

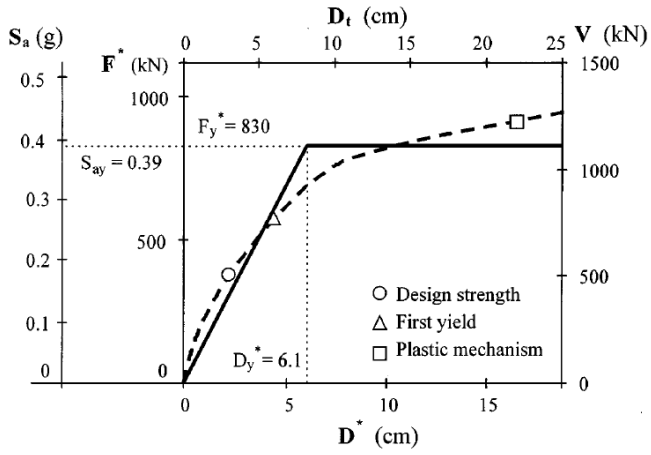

Fig 2.9 Pushover curve and corresponding capacity spectrum for a 4-storey RC frame (Fajfar, 1999)

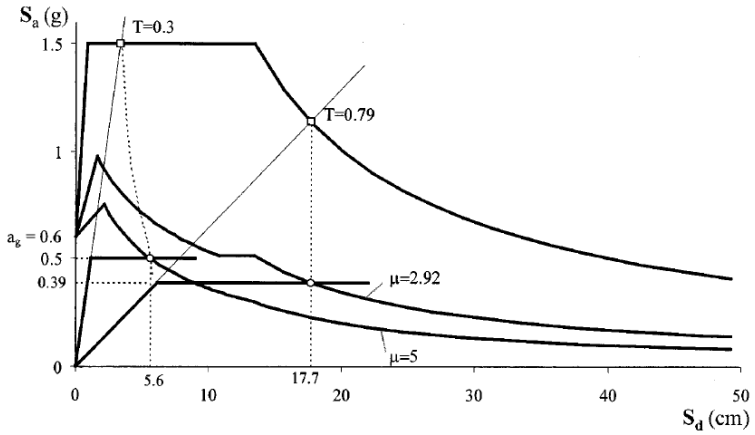

Fig 2.10 Demand and capacity spectra (Fajfar, 1999)

FEMA (2003) developed analytical tool to estimate damage condition of building in seismic event. This damage tool included the development of (1) fragility curves and (2) building capacity curves. Fragility curves showed the probability of exceeding limit states for a Potential Earth Science Hazards (PESH). The intensity measure used to develop fragility curve was spectral displacement, spectral acceleration, peak ground acceleration or peak ground displacement. Spectral displacement or spectral acceleration was used to derive fragility response associated with PESH. Peak ground acceleration was used to assess the vulnerability of buildings with high importance. Height, displacement and flexibility of building effect the fragility response developed with peak spectral damage.

Building response was characterized by building capacity curves. These curves described the push-over displacement of each building type and seismic design level as a function of laterally-applied earthquake load. The Methodology used a technique to estimate peak building response as the intersection of the building capacity curve and the response spectrum of PESH shaking demand at the building's location (demand spectrum). The demand spectrum was the 5%-damped PESH input spectrum reduced for higher levels of effective damping (e.g., effective damping included both elastic damping and hysteretic damping associated with post-yield cyclic response of the building). Figure 2.11 illustrates the intersection of a typical building capacity curve and a typical demand spectrum. Peak building response (either spectral displacement or spectral acceleration) at the point of intersection of the capacity curve and demand spectrum was the parameter used with fragility curves to estimate damage state probabilities.

According to FEMA (2003), building displacements is the cause of building damage rather than lateral seismic force level. The severity of damage state depends on the extent and location of structural displacements in nonlinear stage. Hence, the assessment of seismic vulnerability depends on the prediction of inelastic displacement of structures. Push-over analysis can predict the non-linear displacement of structure through capacity spectrum method (CSM).

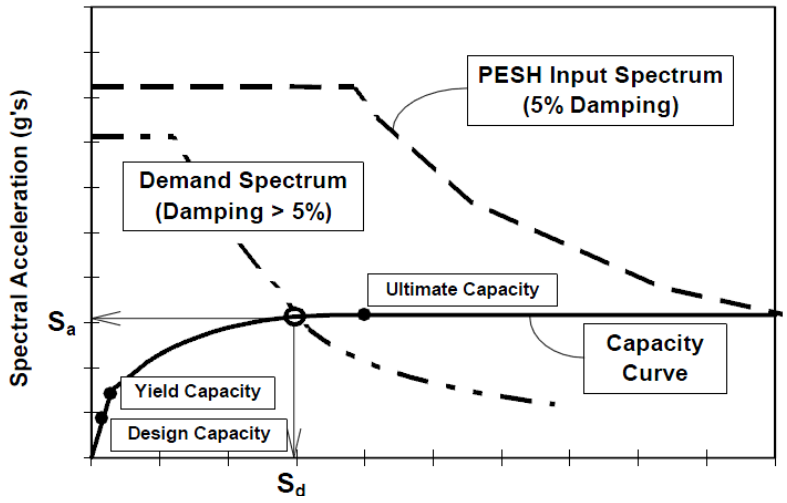

Fig 2.11 Building Capacity Curve and Demand Spectrum (FEMA, 2003)

The probability of exceeding a damage state can be calculated from the lognormal distribution for a spectral displacement, S_d :

$$P[dsIS_d] = \Phi\,[(1/\beta_{ds})\,\ln(S_d/\bar{S}_{d,ds})]$$

where: $\bar{S}_{d,ds}$ = median value of spectral displacement at expected damage state, ds,

β_{ds} = standard deviation of the logarithmic value of spectral displacement at damage state, ds, and

Φ = standard normal cumulative distribution function

The total variability associated with the structural damage state, β_{Sds}, consisted of three damage variable β_C, β_D and $\beta_{M(Sds)}$, as described in following Equation:

$$\beta_{Sds} = \sqrt{\{(CONV[\beta_c,\beta_D, \bar{S}_{d,ds}])^2 + (\beta_{M(Sds)})^2\}}$$

where: β_{Sds} = total variability associated with structural damage, ds,

β_C = capacity curve variable,

β_D = variability of the demand spectrum,

$\beta_{M(Sds)}$ = uncertainty associated with the estimation of the median value of structural damage state, ds.

2.2.2.4 Displacement Based Methods

Calvi (1999) developed a unique approach to evaluate the seismic vulnerability of buildings based on an estimation of their displacement and energy dissipation capacity. In the approach, the displacement capacities of different buildings were evaluated as a function of relevant limit states and were compared with displacement demands computed entering appropriate displacement spectra with equivalent period of vibration. A multi-degree-of-freedom (MDOF) structure was modeled as a single DOF system (Fig. 2.12) and different displacement profiles were accounted for according to the failure mechanism or displacement profile at a given limit state.

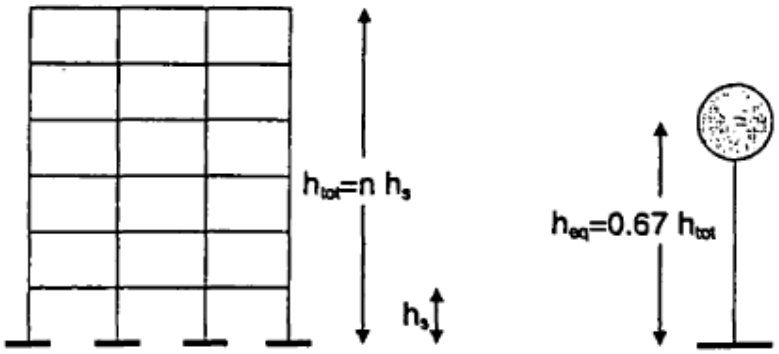

Fig 2.12 A representation of a single-degree-of-freedom (SDOF) model equivalent to the real structure (Calvi, 1999)

Figure 2.13 presents displacement capacities of column-sway (soft-storey) and beam-sway (distributed damage) failure mechanisms for reinforced concrete frames and Fig. 2.14 presents different in-plane failure modes for masonry structures.

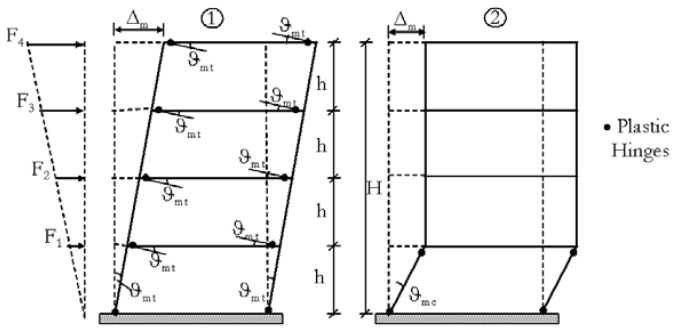

Fig 2.13 Distributed damage/beam-sway (left) and soft-storey/column-sway (right) response mechanisms (Calvi, 1999)

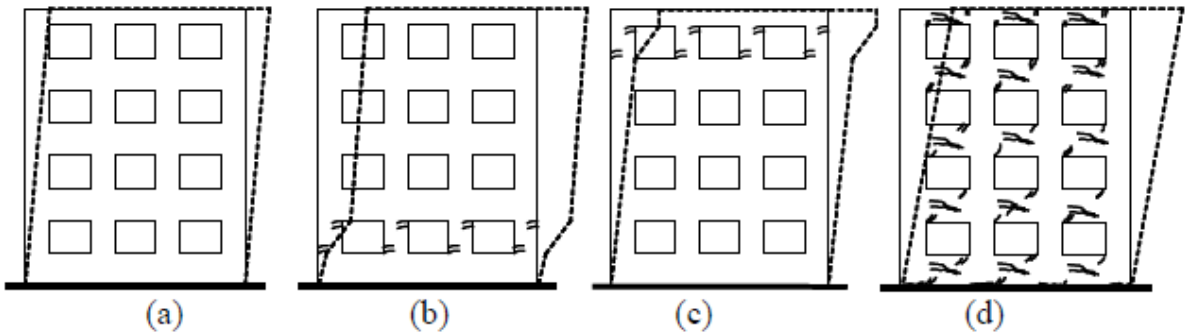

Fig 2.14 Deformed shapes for different limit states and in-plane failure modes (Calvi, 1999)

In the approach the elastic displacement response spectra was defined as a function of assumed return period, geographical location and local soil condition. Then a set of limit states and simplified structural models for different building types were defined as a function of available data. Minimum and maximum expected displacement capacity and period of vibration were computed and a displacement demand reduction factor as a function of the expected energy dissipation level was evaluated for each building type. A probability density function was defined over the rectangles, defined by the displacement and period values calculated at point on the relevant displacement spectrum as shown in Fig. 2.15. The computed probability could be interpreted as the percentage of the total number of similar buildings represented by the rectangle attains the corresponding limit state.

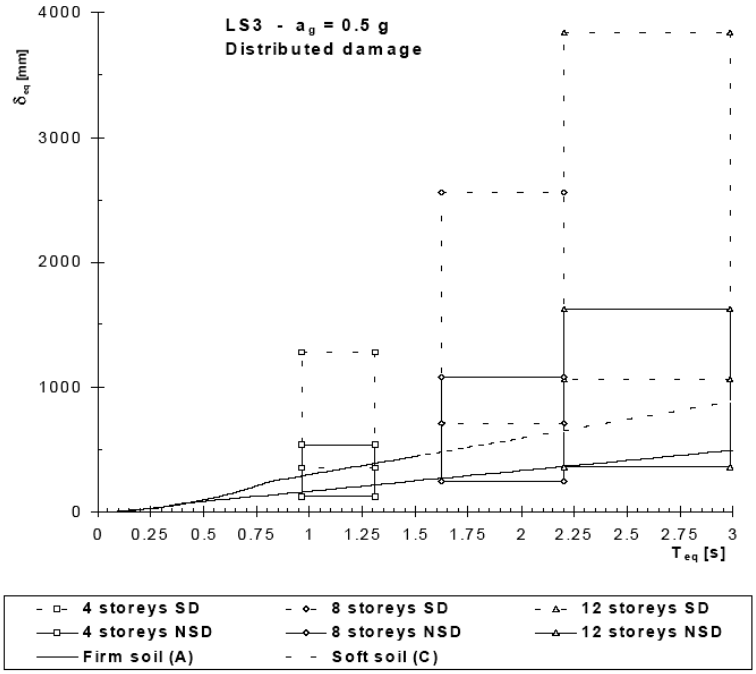

Fig 2.15 Intersection of capacity areas and demand spectrum (Calvi, 1999)

Glaister and Pinho (2003) introduced a relationship between the different qualitative damage states usually defined in loss estimation studies and inter-storey or global drifts (displacements as a proportion of storey or total height) of buildings. Capacity curves for different limit states in terms of period and displacement was developed using analytical relationships between displacement capacity and height (Fig. 2.16), and empirical relationships between height and elastic period. The boundaries of the various limit states (LSi) were defined by the intersection between any given displacement spectrum, scaled by a damping factor (η_{LSi}) in correspondence to the ductility demand (μ_{LSi}), and its corresponding drift capacity curves, indicate the periods (T_{LSi}).

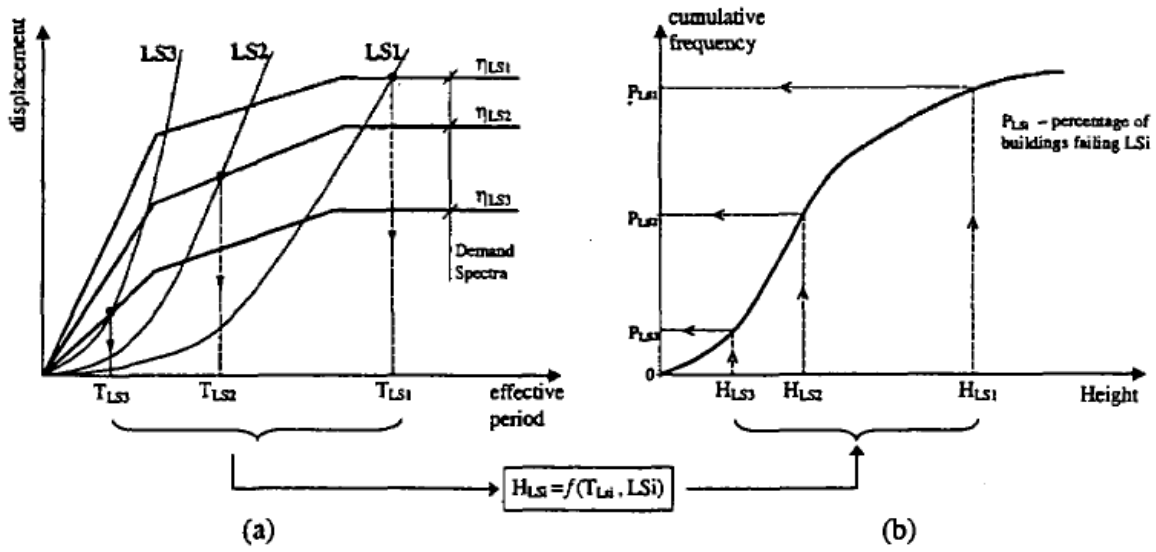

Fig 2.16 Proposed methodology: (a) displacement capacity/demand curves (b) CDF of building stock. (Glaister and Pinho, 2003)

These periods were then transformed into their equivalent heights (H_{LSi}) and plotted across a cumulative distribution function (CDF) of buildings with height to find the proportions of the exposed building stock failing each limit state using the period-height relationships. Thus, by identifying these relationships between natural period, height and displacement capacity it is possible to use this approach to estimate directly the distribution of damage states across a particular class of buildings at a specific location and for any given earthquake ground motion.

Crowley et al (2004) developed a probabilistic framework to bring the displacement based method one step closer to practical application. The treatment of the uncertainty in the displacement demand and capacity had been incorporated with the inclusion of a fully probabilistic framework. A brief preliminary study regarding the probabilistic distributions that should be applied to the parameters used within the displacement capacity formulae had been presented.

For Pre-yield limit state, the building height (H_T) simply defined in terms of the yield period (T_y):

$H_T = 10T_y$

In the case of beam-sway RC frames, the yield capacity equation (the formula for the yield displacement capacity, Δ_{Sy} in terms of height) was as follows:

$\Delta_{Sy}=5ef_h T_y \varepsilon_y l_b/h_b$

For column-sway RC frames, the yield displacement equation was as follows:

$\Delta_{Sy}=4.3ef_h T_y \varepsilon_y h_s/h_c$

Where,

ef_h effective height coefficient

ε_y yield strain of the reinforcement

l_b length of beam

h_b depth of beam section

h_s height of storey

h_c depth of column section

The probability, P_f that the displacement demand, D greater than the displacement capacity of a building class, for a given limit state, was given by

$$P_f = \int_y \int_x [1-F_D(x/T_{Lsi}=y)] f_{\Delta LSi} / T_{LSi}\,(x / T_{Lsi}=y)\, f_{TLSi}\, dxdy$$

The joint probability density function (JPDF) , $f_{\Delta LSi}T_{LSi}\,(x, y)$, was defined as the product of the probability density function of $_{\Delta LSi}$, conditioned to T_{Lsi} , and the probability density function of T_{Lsi}. Figure 2.17 shows the JPDF of capacity for a four storey column-sway RC building class.

2.3 Approach to determine seismic vulnerability of irregular structures

Ellul and D'ayala (2004) used displacement based design to estimate the realistic performance of medium height reinforced concrete infilled frames. Simple frame concrete structure was modeled with infill partition walls which mortared against the narrow side of the column, between the frame without any positive connection to the latter and offered a simple means of providing external cladding and internal partitions to the frame structure. Non-linear push-over analysis for the bare frame was performed for a variety of loading conditions. It was observed that the regular infilled configuration had extra strength over the bare frame for the same displacement capacity. A marked increase in stiffness caused attracting forces to parts of the structure that have not been designed to resist them. Inherent weaknesses in such structures usually included the presence of weak storeys triggered by an uneven distribution of the infills in elevation which result in an irregular stiffness distribution.

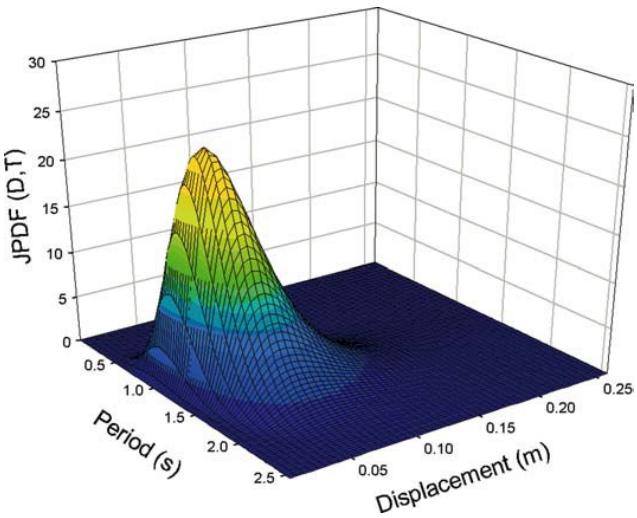

Fig 2.17 JPDF of capacity for a four storey column-sway RC building class. (Crowley et al. 2004)

D'ambrisi et al. used modified pushover analysis developed by Fajfar et al. [2005] to evaluate the seismic performance of an existing school building which consisted of both vertical and plan irregularities. The results were than compared with the inelastic dynamic response of the structure. In the modified pushover analysis, the elastic modal analysis was used to predict the shape of top lateral displacements in plan, i.e., non dimensionalized with respect to the top lateral displacement at the mass center, thus providing amplification factors of top lateral displacements to be applied to those obtained from conventional pushover analysis. It was shown that vertical irregularity did not affect significantly the ability of modified pushover analysis to correlate results from inelastic dynamic analysis, as the Fajfar's procedure is intrinsically formulated to account exclusively for plan irregularity. Only at failure, modified pushover analysis becomes slightly unconservative due to development of a local (floor) mechanism as shown in Fig. 2.18.

Arede and Pinto (1996) performed nonlinear analyses of vertically irregular eight storey R/C building using global element model which was based on the flexibility formulation and used force shape functions instead of displacement shape functions. Mechanic based approach was considered as collapse mechanism. The local probability of failure was computed using damage vulnerability functions. The convolution integral of damage distribution with that of the damage capacity yields the local probability of failure. Then, the bounds of the probability of failure

associated to each mechanism were computed from the local failure and the final bounds of the structure probability of failure were obtained from them.

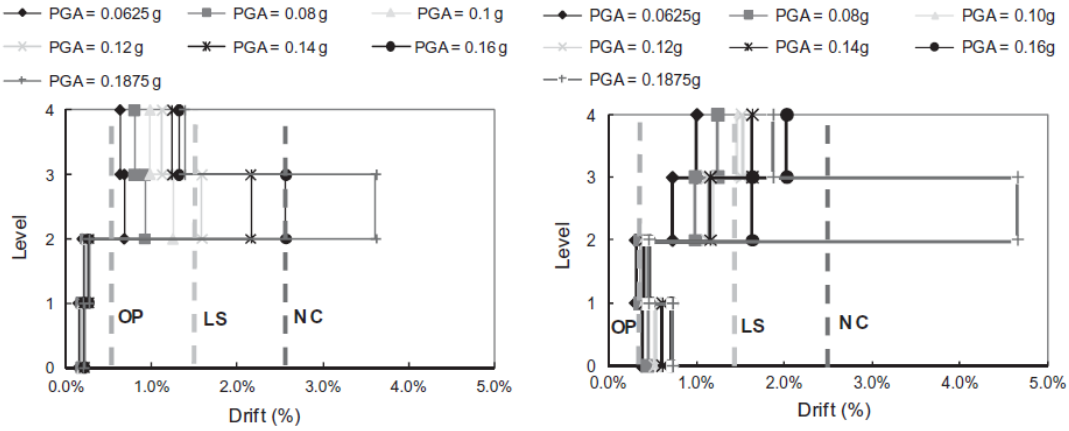

(a) (b)

Fig 2.18 Mean vertical profiles of interstorey drift ratios obtained with: (a) modified pushover analysis; and (b) inelastic dynamic analysis

2.4 Damage assessment of RC frame with fragility curve

Jeong et al. (2012) designed 12 regular RC frame structures according to Eurocode 8 (1995). The structures had been designed to confirm strong-column weak-beam system and failure modes were controlled by allowing plastic hinge in beams while all columns remained elastic except ground level. Fiber-based finite element program ZEUS (Elnashai et al. 2010) was utilized to develop model where shear failure of the structural elements were prohibited by ensuring strength exceeds the required strength at plastic hinge region. Inelastic dynamic simulations with twenty natural records from the European Strong-motion Database (Ambraseys et al. 2004) were used for deriving fragility relationships. All the seismic records were set as 5% damped viscous damping ratio and PGA of the records were ranging in between 0.1 to 0.8g. To identify various damage characteristics and damage states through Incremental Dynamic Analysis (IDA), input seismic ground motions were scaled to 12 different intensity levels, ranging from PGA of 0.1g to 1.9g. Maximum inter-storey drift demand was selected as seismic demand measure and structural responses were defined as a relationship between 5% damped spectral acceleration at the effective period and maximum inter-storey drift ratio where effective period was calculated based on the secant stiffness from bilinear idealization of the capacity curve developed from inelastic static pushover analysis. ASCE/SEI 41-06 (ASCE 2007)

approach had been used to define the performance levels for the fragility analysis. Immediate Occupancy (IO) performance level was defined as the drift value beyond which any structural member started to yield. Life Safety (LS) and Collapse Prevention (CP) performance level was determined as an inter-storey drift ratio of 2% and 4% of structures respectively. This paper concluded that the probability of exceeding a limit state by a structure decreased with the decrease of design peak ground acceleration (PGA) and buildings designed for higher PGA and ductility levels had higher probability of exceeding a limit state as compared with their lower ductility counterparts.

Ellingwood et al. (2007) developed fragility response for RC frame due to the potential impact of earthquake in low-to moderate seismicity region of Central and Eastern United States where building design and construction followed gravity load design without providing provision for earthquake resistance. Three-storey and six-storey frame buildings were designed according to ACI 318 (ACI 1989) for gravity with load combination 1.4D + 1.7L with no consideration of seismic resistance. Open source program Opensees (Opensees 2007) was used to model the frames where fibre approach nonlinear uniaxial constitutive concrete and steel model were used to develop element/section. Shear and bond-slip were considered in modelling the joints. Synthetic uniform hazard ground motions for Central and Eastern United States were selected from Mid-America Earthquake Center. 10 ground motions were generated using attenuation models from each 10%/50 year and 2%/50 year hazard level ground motions developed by Wen-Wu (2001) for both hard rock and representative soil sites. 10 ground motions were also generated using attenuation models from each 10%/50 year, 5%/50 year and 2%/50 year hazard level ground motions developed by Rix-Fenandez (Fernenandez and Rix 2006). Nonlinear static pushover analysis was performed for each structure to identify system behaviour, development of initial yield and plastic hinge locations followed by application of different sets of synthetic records to assess the seismic demand. Maximum inter-storey drift was considered as demand variable and 5% damped spectral acceleration at fundamental period was adopted as ground motion intensity measure. IO performance level was defined as the drift at which pushover analysis started nonlinear behaviour; LS performance level was considered as 2% inter-storey drift and CP performance level was considered as drift limit at which collapse of the frame initiated due to strength degradation of members or significant p-delta effects from excessive lateral deformations and found 4% and 4.8% for three and six- storey building respectively.

Researchers concluded that gravity-designed concrete frames may suffer severe damage or collapse with current design-basis ground motions.

Ramamoorthy et al. (2006) also developed fragility response of a two-storey RC concrete frame building designed for gravity load in Mid-America (Memphis) region without providing seismic provisions. Reinforcement of the structure was detailed according to ACI 318 (ACI 2002). IDASS analysis platform (Kunnath 2003) was used to develop 2-D numerical model of the building consisted of nonlinear member properties with degrading hysteretic behaviour. 180 synthetic seismic records were selected from ground motions developed for the Memphis region under Mid-America earthquake center research program. Maximum inter-storey drift was considered as seismic demand whereas 5% damped elastic response spectral acceleration at fundamental period was considered as intensity measure. Though FEMA-356 (FEMA 2000) was used to defined performance level, reduced drift value was considered for the limit states i.e., 0.5% for IO, 1% for LS and 2% for CP. Fragility analysis of the building found structurally vulnerable to seismic events and the researchers concluded that the buildings in Mid-America region which designed and constructed without providing proper seismic provision has potential seismic damage.

Kircil and Polat (2006) developed fragility curves for mid-rise RC frame buildings designed followed by 1975 Turkish design code in Istanbul. 3, 5 and 7storey RC frame buildings were considered as reference structures which designed according to 1975 Turkish design code and followed the common practice in Istanbul. 2-D non-linear dynamic analysis was performed for sample building using IDARC (IDARC 1996) computer package. 12 synthetic ground motions generated with computer program developed in Kandilli Observatory and Earthquake Research Institute (KOERI) at Bogazici University were used to determine seismic performance of the structures. A magnitude of 7.5 with fault distance 20, 30, 40 and 50 km was used to generate 40 second duration artificial ground motions. All the records had probability of 10%/50 year. Spectral acceleration was increased at a step of 0.05g to identify capacity of the structure through IDA. Maximum inter-storey drift and 5% damped elastic spectral acceleration was defined as demand and intensity measure to develop fragility curves. Yield capacity of the structures were defined as drift at which IDA curve leaves linear path, whereas collapse capacity were defined as drift corresponding to dynamic instability as a result of non-converging run or 3% inter-storey

drift. Two limit states were used to determine performance criteria; IO was defined as inter-storey drift corresponding to 5% yield probability of sample buildings with 95% confidence level and CP was defined as inter-storey drift corresponding to 5% collapse probability of sample buildings with 95% confidence level. From the fragility curves developed for the buildings, effect of number of stories on fragility curve was observed and the researchers proposed relationship between limit states values based on spectral displacement and number of stories that could preliminary used to evaluate seismic behaviour of mid-rise RC frame structures designed according to 1975 Turkish seismic design code.

Goulet et al. (2007) assessed seismic performance of RC moment frame buildings designed according to 2003 International Building Code (IBC) through fragility analysis. Eight types of design were considered for a four-storey RC frame structure based on the variation of structural system, beam strength and strong-column weak-beam ratio. Two element models were developed using Opensees: fiber model to capture cracking and initial behaviour and plastic hinge model to assess strength and stiffness deterioration and collapse. Elastic shear and bond-slip was considered in fiber element model whereas bond-slip and column yielding response lumped into hinge. Shear failure was not considered in plastic hinge model. Moment-chord rotation envelope with post-peak response was considered in plastic hinge model. Seismic records were selected from PEER strong motion database based on the magnitude and fault distance and disaggregation of the records were performed to identify suitable records at seven hazard levels of intensity magnitude. IDA was performed with 68 seismic records having 2%/50 year probability. The research work found that probability of exceeding collapse performance level by a structure is highly sensitive to structural modelling uncertainties and plastic chord rotation capacity of structural member should be realistic to accurately predict collapse performance.

Erberik (2008) assessed fragility response of typical low-rise and mid-rise RC frame buildings in Turkey where two and three stories were considered as low-rise and four to six stories were considered as mid-rise. SAP2000 (CSI 2000) was used to model each building as equivalent single degree-of-freedom system on the basis of period, strength ratio and post-yield to initial stiffness ratio. Site specific adjusted 100 seismic records with magnitude 5.1 to 7.8 around the world were used to generate fragility curves where peak ground velocity (PGV) was used as

intensity measure and structural displacement was considered as demand. Serviceability limit state was taken as drift ratio corresponding to structural period increased by 20% of its initial period; Damage control limit state was defined as 75% of CP limit state and CP limit state was defined as minimum of 75% of ultimate deformation or drift value where strength of structure reduced by 20% of maximum strength. Researcher of this paper found that variability of low-rise building is more significant than mid-rise building in terms of period and strength ratio; post-elastic stiffness ratio has little effect whereas uncertainty in capacity and degradation characteristics has higher effect on developing fragility functions.

Liel et al. (2011) examined seismic collapse safety of non-ductile RC frame buildings designed according to seismic provisions of 1967 Uniform Building Code and compare with recent code-conforming special ductile RC moment frame in California. Twelve RC frame buildings were designed with regular elevation and plan. Ductile frames were designed according to International Building Code (ICC 2003), ASCE 7 (ASCE 2002) and ACI 318 (ACI 2005). Nonlinear analysis models were developed with OpenSees where moment-rotation monotonic backbone properties were assigned both for ductile and non-ductile structure. Plastic rotation capacity of ductile column was 2.7 times greater than non-ductile column and post-capping rotation capacity was also larger for ductile column. Linear elastic shear was assumed for code-conforming ductile structures whereas inelastic spring with monotonic backbone and hysteresis rule was assigned to model shear behaviour of non-ductile column. Elastic fundamental period was calculated using cracked stiffness of beams and columns. 80 ground motions were selected to perform IDA and seismic collapse was defined as the intensity of each record at fundamental period of the structure caused excessive inter-storey drift. The research work concluded that ductile RC frames seismic performance is substantially superior as compared to non-ductile RC frame. More deformation capacity with ability of standing at higher intensity seismic records was observed for ductile structures. Also collapse margin ratio was three times larger for ductile structures.

Ozer et al. (2006) carried out research to find the seismic performance of code conforming RC frame structures and compare the results with non-code conforming structures in Turkey. 3,5,7 and 9-storey frame structures were selected for the analyses. The structures had 3 meters storey height and 5 meters bay and designed with SAP2000 according to TS500 (2000), TSC

(1998) and ACI Building Code (ACI 2002). Analytical model of the structures were developed using IDARC-2D. Sixty ground motions were selected for analysis based on the Peak Ground Velocity (PGV) and compatible with FEMA 356 design spectra. PGV was considered as intensity measure of seismic hazard and maximum inter-storey drift ratio was considered as demand measure to develop fragility relationship. Limit states were defined as IO, LS and CP where Softening Index (SI), developed by DiPasquale and Cakmak (1987), was used to find the drift value for the limit states. IO and LS performance level was defined as drift corresponding to 20% and 50% reduction of structural stiffness respectively and CP performance level was determined from pushover analysis. From analyses it was observed that probability of collapse for code-conforming structure was negligibly small for the selected records whereas non-code conforming structures showed substantial damage which worsen with the increase of storey height by reducing safety margin between the limit states.

Heidebrecht and Naumoski (1999) investigated the seismic performance of six-storey ductile moment resisting structure designed and detailed according to the seismic provisions of NBCC (1995). The structure was located in Vancouver and consisted with six transverse moment-resisting frames. Inelastic dynamic analysis program IDARC (Kunnath et al. 1992) was used to generate inelastic model of the structures. Rigid zones were assigned at the end of beams and columns except bottom of first-storey column. A trilinear moment-curvature relationship was assigned to the fiber analysis used to model beam and column sections where stiffness degradation and pinching effects were taken into consideration through hysteretic model. 15 seismic records having similar spectral shape of Vancouver was used for dynamic analysis of the structures. Peak ground velocity was used to scale the seismic records. Inter-storey drift ratio was used to quantify the seismic damage of a building and to define performance criteria. 0.5%, 1.5% and 2.5% inter-storey drift was used to define operational, life safety and near collapse performance level respectively. The research work found that behaviour of structure subjected to strong seismic motions could not be simulated with pushover analysis, base or top floor column strength reduction did not increase the deterioration of structures in terms of storey or member deformation and damage states of gravity dominated frames were less in compared to seismic dominated frame.

Tesfamariam et al. (2012) investigated seismic vulnerability of modern code-conformed RC frame structures in China. 3, 6 and 9-storey RC frames were designed according to 2010 CCSDB (NSPRC 2010), Chinese Code for Design of Concrete Structure (NSPRC 2002) and Chinese Load Code for Design of Building Structures (NSPRC 2006). SAP2000 software was used to model 2-D frame with fiber plastic hinge at end of column element. Inelastic deformations in beams and columns, effect of axial load on stiffness and strength and p-delta effect was considered in 2-D model. Moment-rotation flexural hinges with FEMA 356 default rotational values were assigned at end of beam elements. 4 to 9 moment magnitude 30 seismic records with source to site distance 0 to 200km were selected from Pacific Earthquake Engineering Research Center's Next Generation Attenuation (NGA) database. Seismic intensity and soil condition were considered and records compatible with 2-3%, 10% and 63% probability in 50 years Uniform Hazard Response Spectrum (UHRS) in 2010 CCSDB were selected for dynamic analysis. Maximum inter-storey drift and 5% damped spectral acceleration at fundamental period was considered as demand and intensity magnitude respectively to develop seismic fragility curve. It was observed from the research work that RC frame structures designed according to 2010CCSDB did not collapse at target seismic intensity and considered appropriate for corresponding UHRS. It was also found that maximum inter-storey drift concentrated on the floor where column section reduced and thus effect of column size reduction had significant effect on lateral stiffness of structure along height.

El-Kholy et al. (2012) evaluated seismic vulnerability of R/C buildings with vertical irregularity. A seven storey R/C frame building was considered for the analysis. The building was designed for gravity load according to pre-1992 Egyptian design code considering three types of irregularity i.e., vertical, mass and setback. Computer program 2-D IDARC was considered for modeling of structures and performing nonlinear dynamic analysis. Beams and columns were modeled as inelastic elements with spread plasticity. Hysteretic behaviour with tri-linear monotonic envelope was assigned to the elements. 5% damped 14 seismic records from PEER was selected for time-history dynamic analysis of the structures and the records were scaled from 0.1 to 1.5g based on PGA. Inter-storey drift limit stated in FEMA 356 was used to define IO, LS and CP limit states in this study. The research work concluded that existing RC frame buildings, designed for gravity load, are seismically vulnerable. Irregular frame structures

were vulnerable based on the location of irregularity and buildings with setbacks were more vulnerable in compared to vertical and mass irregularity.

Athanassiadou (2007) evaluated the seismic performance of ten-storey RC irregular frame structure. The structure was designed as high and medium ductile frame according to the seismic provisions of 2004 Eurocode 8. Setback was introduced as irregularity at bottom six stories of the structures. DRAIN-2000 (Kappos and Dymiotis 2000) was used to develop FE model and perform inelastic dynamic analysis of the structures. Structural members were modeled with hinge consisted with bi-linear hysteresis properties. Moment-axial load interaction was account for only exterior columns and reduced stiffness for beams and columns were considered to develop model of the structures. 4 natural seismic records were selected and normalized equal to or double the intensity of design spectrum for dynamic analysis. The researcher observed that seismic performance of frame buildings with setback irregularity was not inferior as compared to regular buildings for both high and medium ductility, most of the energy dissipated through formation of plastic hinge in beams, EC8 code requirement with regard to irregular structure in elevation was sufficient to protect failure of setback storeys, the over-strength ratio of irregular structure was similar to regular structure and both high and medium ductility structures performed satisfactorily during the design earthquake.

Rajeev and Tesfamariam (2012) investigated seismic performance of irregular old frame buildings designed for gravity load only. 3, 5 and 9-storey RC frame structures were considered for the analysis and designed for gravity load in addition to lateral load which was calculated as 8% of weight of the structure. FE software Opensees was used to generate model where flexure-shear interaction and joint hysteretic response was incorporated. Multilinear shear force-deformation envelope was adopted with considering cracking, peak and residual strength and hysteretic behaviour with pinching effect due to bond slip and shear cracking was assigned in joint modeling. 30 seismic records with magnitude and source-to-site distance 5.5-7.9 and 0-97km respectively from European Strong Motion Database were used for dynamic analysis. The researchers found that irregularity in frame buildings had significant influence on developing fragility response and seismic risk assessment of structures.

2.5 Concluding Remarks

A significant effort had been implemented in this research work to identify the available damage assessment technique to evaluate seismic performance of RC structures and identify suitable option to be used in this study to evaluate seismic performance of RC frame structure accurately and more precisely. Literature review of this chapter also revealed important information on analytical model development technique, selection criteria of seismic records, IDA and fragility curve development techniques, failure mode of structures and performance levels. Though more literatures were reviewed to identify effect of shear and flexure on hinge formation, determining rotational and displacement capacity at hinges, assigning hysteretic behaviour of concrete members and effect of period and height on fragility responses, following chapters addressed the literature where necessary. A few literatures describing the effect of irregularity on frame structures are also presented in this chapter.

The current research complements the existing seismic vulnerability studies for frame buildings in Canada. It provides a comprehensive set of seismic assessment tools for older and newer buildings in Canada for the first time in the literature.

2.6 References for Chapter 2

ACI. (1989). "Building code requirements for structural concrete and commentary." ACI-318, *American Concrete Institute*, Farmington Hills, Mich.

ACI. (2002). "Building code requirements for structural concrete and commentary." ACI-318, *American Concrete Institute*, Farmington Hills, Mich.

ACI. (2005). "Building code requirements for structural concrete." *American Concrete Institute* . ACI 318, Farmington Hills, MI.

Ambraseys, N., Douglas, J., Rinaldis, D., Berge-Thierry, C., Suhadolc, P., Costa, G. (2004). Dissemination of european strong-motion data, Vol. 2. Engineering and Physical Sciences Research Council, Swindon, U.K.

Angeletti, P., Bellina, A., Grandori. E. G., Moretti, A., Petrini, V. (1988). "Comparison Between Vulnerability Assessment and Damage Index, Some Results". *Proceedings of the Ninth World Conference on Earthquake Engineering.* August 2-9, 1988. Tokyo, Japan (Vol VII)

Arede, A., Pinto, A.V. (1996). "Performance of R/C Buildings Designed for Different Ductility Classes". *Proceedings of 11th World Conference on Earthquake Engineering*. Paper No. 1877. ISBN 0080428223

ASCE. (2002). "Minimum design loads for buildings and other structures." *American Society of Civil Engineers*. ASCE 7-02, Reston, VA.

ASCE (2007). "Seismic evaluation and retrofit of existing buildings". *American Society of Civil Engineers*. ASCE/SEI 41-06.

Calvi, G.M. (1999). "A Displacement-Based Approach for Vulnerability Evaluation of Classes of Buildings", *Journal of Earthquake Engineering*, Vol. 3, No. 3, pp. 411-438.

Calvi, G.M., Pinho, R., Magenes, G., Bommer, J.J., Restrepo-Vélez, L.F., Crowley. H. 2006." Development of Seismic Vulnerability Assessment Methodologies over the past 30 years". *ISET Journal of Earthquake Technology,* Paper No. 472, Vol. 43, No. 3, September 2006, pp. 75-104.

Cosenza, E., Manfredi, G., Polese, M. and Verderame, G.M. (2005). "A Multi-Level Approach to the Capacity Assessment of Existing RC Buildings", Journal of Earthquake Engineering, Vol. 9, No. 1, pp. 1-22

CSI (2000). SAP2000 nonlinear. *Computers and Structures, Inc.* Berkeley, CA.

D'ambrisi, A., Steffano, M., Tanganelli, M. (2009). "Use of Pushover Analysis for Predicting Seismic Response of Irregular Buildings: A Case Study". *Journal of Earthquake Engineering*, 13:1089–1100, ISSN: 1363-2469 print / 1559-808X online. DOI: 10.1080/13632460902898308

D'Ayala, D. and Speranza, E. (2002). "An Integrated Procedure for the Assessment of Seismic Vulnerability of Historic Buildings", *Proceedings of the 12th European Conference on Earthquake Engineering,* London, U.K., Paper No. 561

Daniell, J., Vervaeck, A. (2011). "Damaging Earthquake Database 2011-The Year in Review". *CEDIM Report 2011*.

DiPasquale, E., Çakmak, A.S., (1987), "Detection and assessment of seismic structural damage". *Technical Report NCEER–87–0015*, State University of New York, Buffalo, NY.

Ellingwood, B.R.., Celik, O.C., Kinali, K. (2007). "Fragility assessment of building structural systems in Mid-America". *Earthquake Engineering and Structural Dynamics.* Volume 36, Issue 13, Pages 1935-1952.

Ellul, F., and D'ayala, D. (2004). "On the Vulnerability Assessment of Modern Low Technology Engineered Residential Construction", *Proceedings of 13th World Conference on Earthquake Engineering*. Vancouver, B.C., Canada. August 1-6, Paper No. 880.

Elnashai, A., Papanikolaou, V., Lee, D. (2010). "ZEUS NL – a system for inelastic analysis of structures", user's manual. *Mid-America Earthquake (MAE) Center*, Department of Civil and Environmental Engineeering. University of Illinois at Urbana- Champaign, Urbana, IL.

Erberik, M.A. (2008). "Fragility-based assessment of typical mid-rise and low-rise RC buildings in Turkey". *Engineering Structures.* Volume 30, Issue 5, pages 1360-1374.

El-Kholy, S.A., El-Assaly, M.S., Maher, M. (2012). "Seismic Vulnerability Assessment of Existing Multi-Storey Reinforced Concrete Buildings in Egypt". *Arabian Journal for Science and Engineering.* Vol 37, Page 341-355. DOI 10.1007/s13369-012-0170-0

Eurocode 8. (1995). "Design provisions for earthquake resistance of structures". *European Committee for Standardization.* ENV 1998-1-Parts 1, 2, 3.

European Macroseismic Scale. EMS-98. (1998). *European Seismological Commission*. Luxembourg.

Fajfar, P., Marusˇic´, D., and Perus, I. (2005) ''Torsional effects in the pushover-based seismic analysis of buildings,'' *Journal of Earthquake Engineering*. Vol 9, Issue 6, page: 831–854

Fajfar, P. (1999). "Capacity Spectrum Method Based on Inelastic Demand Spectra". *Earthquake Engineering and Structural Dynamics.* 28, 979-993

FEMA (2000). "Prestandard and commentary for the seismic rehabilitation of buildings." *Federal Emergency Management Agency.* FEMA 356.

FEMA (2003). "HAZUS-MH Technical Manual", *Federal Emergency Management Agency*, Washington, DC, U.S.A.

Fernandez, JA., Rix, GJ. (2006). "Soil attenuation relationships and seismic hazard analyses in the Upper Mississippi Embayment". *Proceedings of the Eighth U.S. National Conference on Earthquake Engineering*, San Francisco, CA, 18–22 April 2006.

Freeman, S.A. (1998). "The Capacity Spectrum Method as a Tool for Seismic Design", *Proceedings of the 11th European Conference on Earthquake Engineering*, Paris, France.

Glaister, S., Pinho, R. (2003). "Development of a Simplified Deformation-Based Method for Seismic Vulnerability Assesment**".** *Journal of Earthquake Engineering,* Vol. 7, Specid Issue 1 (2003) 107-140

Goulet, C.A., Haselton, C.B., Mitrani-Reiser, J., Beck, J.L., Deierlein, G.G., Porter, K.A., Stewart, J.P. (2007). "Evaluation of the seismic performance of a code-conforming reinforced-concrete frame building—from seismic hazard to collapse safety and economic losses". *Earthquake Engineering & Structural Dynamics*. Volume 36, Issue 13, pages 1973–1997.

Heidebrecht, A.C., Naumoski, N. (1999). "Seismic performance of ductile medium height reinforced concrete frame buildings designed in accordance with the provisions of the 1995 National Building Code of Canada". *Canadian Journal of Civil Engineering*. Vol 26, Page 606-617

ICC. (2003). International Building Code. *International Code Council*. Falls Church, VA.

IDARC-2D (1996). Computer program. Inelastic damage analysis of RC building structures, State University of New York; 1996. Developed by Park YJ, Reinhorn AM, Kunnath SK.

Jeong, S.H., Mwafy, A.M., Elnashai, A.S. (2012). "Probabilistic seismic performance assessment of code-compliant multi-storey RC buildings". *Engineering Structures.* Volume 34, January 2012, Pages 527-537.

Kappos AJ, Dymiotis C. (2000). DRAIN-2000: A program for the inelastic timehistory and seismic reliability analysis of 2-D structures. *Heriot-Watt University*. Edinburgh (UK).

Kircil, M.S., Polat, Z. (2006). "Fragility analysis of mid-rise R/C frame buildings." *Engineering Structures.* Volume 28, Issue 9, July 2006, Pages 1335-1345.

Kircher, Charles A., Nassar, Aladin A., Kustu. O., Holmes, William T. (1997). "Development of Building Damage Functions for Earthquake Loss Estimation". *Journal of Earthquake Spectra*. Vol 13. No. 4. Page 663-682

Kunnath, S. K. (2003). "IDASS." (http://cee.engr.ucdavis.edu/faculty/ Kunnath)

Kunnath, S.K., Reinhorn, A.M., Lobo, R.F. (1992). IDARC Version 3.0: a program for inelastic damage analysis of reinforced concrete structures. *National Center for Earthquake Engineering Research*, Buffalo, Report NCEER-92-0022, N.Y.

Liel, A.B., Haselton, C.B., Deierlein, G.G. (2011). "Seismic collapse safety of reinforced concrete buildings. II: Comparative assessment of nonductile and ductile moment frames". *Journal of the Structural Engineering, ASCE.* Volume 137, Issue 4, pp. 492-502.

Manzur, T., Noor. Munaz A. (2006). "Displacement Based Fragility Curves for R.C.C. Frame Structures in Context of Dhaka, Bangladesh". *Proceedings of the 6th Asia-Pacific Structural Engineering and Construction Conference* (APSEC 2006), 5 – 6 September 2006, Kuala Lumpur, Malaysia.

Masi, A., Vona, M. (2012). "Vulnerability Assessment of Gravity-Load Designed RC Buildings: Evaluation of Seismic Capacity Through Non-Linear Dynamic Analyses". *Journal of Engineering Structures*. 45 (2012) 257-269

National Standard of the People's Republic of China (NSPRC) (2002), Chinese Concrete Structure Design Code (GB 50010-2002), *Ministry of Construction of Peoples Republic of China*, Beijing, China.

National Standard of the People's Republic of China (NSPRC) (2006), Chinese Load Code for the Design of Building Structures (GB 50009-2001), *Ministry of Construction of Peoples Republic of China,* Beijing, China.

National Standard of the People's Republic of China (NSPRC) (2010), Chinese Code for Seismic Design of Buildings (GB50011-2010), *Ministry of Construction of Peoples Republic of China*, Beijing, China.

NBCC. (1995). National building code of Canada 1995. *National Research Council of Canada*, Ottawa, Ont.

Okada, S., Takai, N. (2000). Classifications of Structural Types and Damage Patters of Buildings for Earthquake Field and Investigation. *Proceedings of the Twelfth World Conference on Earthquake Engineering.* Auckland, New Zealand.

OpenSees. (2007). Open System for Earthquake Engineering Simulation. *Pacific Earthquake Engineering Research Center*, University of California: Berkeley, CA.

Ozer AY, B. Erberik, M.A., Akkar, S. (2006). "Fragility Based Assessment of the Structural Deficiencies in Turkish RC Frame Structures". *First European Conference on Earthquake Engineering and Seismology*. Geneva, Switzerland. Paer no. 593.

Ramamoorthy, S., Gardoni, P., Bracci, J. (2006). "Probabilistic Demand Models and Fragility Curves for Reinforced Concrete Frames". *Journal of the Structural Engineering, ASCE.*, Volume 132, Issue 10, pages 1563–1572.

Rajeev, P., Tesfamariam, S. (2012). "Seismic Fragilities for Reinforced Concrete Buildings with Consideration of Irregularities". *Journal of Structural Safety.* 39 (2012). Page 1–13

Tesfamariam, D.Wu., Stiemer, S.F., Qin, D. (2012). "Seismic fragility assessment of RC frame structure designed according to modern Chinese code for seismic design of buildings". Earthquake Engineering and Engineering Vibration. Volume 11, No. 3, Page 331-342

TS 500. (2000). "Requirements for Design and Construction of RC Structures", *Turkish Standards Institute*, Ankara, Turkey.

TSC. (1998), "Specifications for Structures to be Built in Disaster Areas", *Ministry of Public Works and Settlement,* Ankara, Turkey.

Wen, YK., Wu, CL. (2001). "Uniform hazard ground motions for Mid-America cities." *Earthquake Spectra.* Volume 17 Issue 2, Page: 359–384.

CHAPTER 3

3. SEISMIC PERFORMANCE EVALUATION OF RC FRAME STRUCTURES USING PERFORM-3D

Abstract: Performance-based vulnerability assessment of buildings requires dynamic inelastic analysis in the non-linear range of deformations. PERFORM-3D, with hysteretic response of structural elements, was employed to develop fragility curves for Canadian seismicity. The analytical models of two reinforced concrete frame structures, designed based on the recent Canadian practice, were generated. Incremental inelastic dynamic analysis was used to identify maximum inter-storey drift capacities as a damage parameter for fragility response. Suitability of the analytical model developed was verified against SAP2000 and SeismoStruct software. Fragility responses obtained from modelling with rotational limits specified in ASCE 41-13 and ACI 369R-11, as well as those computed based on the ductility limits specified in the National Building Code of Canada and the effective stiffnesses outlined in CSA A23.3-04 were compared. The results show similar fragilities at lower performance levels, whereas the fragilities at the collapse performance level were under-estimated for moderately ductile structures when modeled according to the Canadian practice. When the same building was modelled to be fully ductile, the Canadian practice resulted in lower fragility at the collapse prevention level.

3.1 Introduction

The emphasis in seismic vulnerability assessment of buildings in recent years has shifted from capacity-based to performance-based evaluation, where structural members are assessed for pre-determined performance objectives. The performance objectives are defined on the basis of selected hazard levels and target structural and non-structural performance levels. Building elements show different levels of performance under different levels of hazard, covering the entire spectrum of elastic and inelastic structural response. Performance-based seismic assessment of buildings requires dynamic inelastic response history analysis under different levels of seismic hazard. Alternatively, seismic vulnerability of buildings can be assessed by

using fragility curves that have been developed using Incremental Dynamic Analysis (IDA), as described later in the paper.

The objective of this paper is to illustrate the application of IDA as an analysis method in establishing fragility relationships for a 2-storey and a 5-storey building designed for the city of Ottawa in eastern Canada. The objective also includes the investigation of the parameters that define hysteretic relationships of individual elements with an emphasis on strength, while considering moderately ductile and fully ductile behaviours. The global performance of a structure depends on performance of individual structural elements and it is anticipated that during seismic response some structural members may go beyond their inelastic capacities prior to developing global collapse. Therefore, it is essential to model strength degradation to account for gradual reduction of element contribution to overall structural resistance, as the members progressively experience failure.

The modelling of strength decay can be implemented by following a number of different approaches. ACI 369R-11 (ACI 2011) provided rotational capacities for concrete components of existing buildings, as well as for new concrete components added to existing buildings. These rotational limits can be used to model the onset of strength decay. ASCE 41-13 (ASCE 2014) adopted the same rotational capacities with variations in residual strengths, and can also be used for the purpose of modelling strength decay. Furthermore, the National Building Code of Canada (NBCC) categorizes seismic force resisting systems on the basis of ductility demands where moderately ductile and fully ductile reinforced concrete frame structures are assigned a ductility demand of 2.5 and 4.0, respectively. A moderately ductile frame building designed to fulfill the requirements of CSA A23.3-04 (CSA 2004) for the city of Ottawa, also conforming to the ductility demand specified in 2010 NBCC can be modelled using the ductility ratio of 2.5 as the deformation level, beyond which strength decay can be introduced. Similarly, a ductile frame building can be modelled using the ductility ratio of 4.0. For the 5-storey building selected, these three approaches were used to model strength decay in hysteretic response, along with other stiffness degrading features of reinforced concrete as implemented in PERFORM 3-D (CSI 2013) in generating the fragility curves. For the 2-storey building, the descending branch of the hysteretic relationship was modelled twice, to represent moderately ductile and fully ductile buildings. In this case, the ductility factors specified in the 2010 NBCC and the corresponding

detailing requirements given in CSA A23.3-04 were used with a decay rate as defined in ASCE 41-13. IDA was used with 20 seismic records compatible with the uniform hazard spectra (UHS) specified in the 2010 NBCC for Ottawa. Fragility responses obtained by the use of different strength decay options are compared, while the analytical models used are described in detail.

3.2 Description of Selected Structures

The Two reinforced concrete frame buildings with either a 2-storey or a 5-storey height, and a regular floor plan were selected for analysis. The buildings have a square floor plan with 5 bays in each direction with a 7.0 m span length. The floor height is 4.0 m. The buildings were designed and detailed according to the provisions of CSA A23.3-04 as a moderately ductile structure located in Eastern Canada (Ottawa). The live load was 2.4 kPa for all floors, including the roof, and the superimposed dead load was 1.33 kPa over the self-weight. Uniform hazard spectrum for Ottawa was selected from the 2010 NBCC to calculate seismic base shears. The peak ground acceleration (PGA) for the design earthquake was 0.32g. The building was selected for normal importance (I = 1.0) with Site Class of C. The first 12 modes were considered to account for modal effects on seismic behaviour of structures. The elastic base shear,V_e, was reduced by the product $R_d R_o$, where R_d is the ductility related force modification factor and R_O is the over-strength related force modification factor. These correspond to $R_d = 2.5$ and $R_O = 1.4$ for the city of Ottawa. The buildings were analyzed under the equivalent static seismic loads, as well as the accompanying gravity loads as per 2010 NBCC using software ETABS (CSI 2008) and the appropriate load combinations. The design and detailing requirements stated in CSA Standard A23.3-04 for moderately ductile buildings were implemented. The concrete used was 30 MPa or 40 MPa for the 5-storey and 2-storey buildings, respectively with elastic modulus computed as $E_c = 4500\sqrt{\mathrm{f'_c}}$. In the ETABS analysis, cracked section properties with effective moment of inertia I_e were used as for beam $I_e = 0.4\, I_g$ and for column $I_e = \alpha_C\, I_g$ where $\alpha_C = 0.5 + 0.6\frac{P_s}{A_g f'_c} \leq 1.0$; the symbol denoted as I_g = gross moment of inertia, P_s = axial force on members resulting from the earthquake load combination, f'_c = specified compressive strength of concrete and A_g = gross area of section. Reinforcement yield strength was taken as f_y = 400 MPa. The analysis results provided design quantities for proportioning members. For the 5-storey building, modelled using ASCE 41-13 and ACI 369R-11, the effective moment of inertia

was computed as $I_e = 0.3\, I_g$ for beam, $I_e = 0.7\, I_g$ for columns with axial compression due to design gravity loads$\geq 0.5\, f_c' A_g$, and $I_e = 0.3\, I_g$ for columns with axial compression due to design gravity loads $\leq 0.1\, f_c' A_g$. Linear interpolation was made for columns with axial compression between the above limits.

The difference in effective rigidities resulted in differences in the fundamental period. The period computed based on the CSA A23.3-04 approach resulted in a shorter value than that computed on the basis of ASCE41-13 / ACI 369R-11. As an example, the 5-storey building period was 2.04 sec when the CSA A23.3-04 rigidities were used, and it was equal to 2.23 when the ASCE41-13 / ACI 369R-11 rigidities were used. All the buildings were designed using ETABS Software for the appropriate load and material resistance factors specified in the 2010 NBCC and CSA A23.3-04.

3.3 Development of Analytical Models

Computer software PERFORM-3D was selected to conduct nonlinear dynamic analysis that forms part of the IDA. PERFORM-3D is specialized software for damage assessment, specifically intended for performance-based seismic assessment of structures. The software permits monitoring of inelastic behaviour of structural components with different levels of deformability. It was used by other researchers in the past to perform nonlinear dynamic analysis (Reyes and Chopra 2012, Ghodsi and Ruiz 2010, Zeynep Tuna 2012, Wen-Cheng Liao 2010, Michael W. Hopper 2009).

The two buildings selected were modelled as bare frame buildings, neglecting possible contributions from non-structural elements. The beams were modeled as concrete type FEMA beam-frame elements, consisting of chord-rotation based models as defined in FEMA 356 (FEMA 2000.a). The FEMA beam employed has symmetrical sections at the ends, with equal and opposite end moments with a point of inflection in the middle of the span. No member load is permitted along the beam length. Consequently, the beams rotate in double curvature consisting of two segments between the beam ends with the point of inflection in the middle. Each segment is modelled with an elastic beam element and a plastic hinge, as illustrated in Fig 3.1. The effective slab width in the beam model was included as beam flange width, as defined in CSA A23.3-04. The slab concrete and reinforcement were taken into account when the beam

flange was in compression, and the longitudinal reinforcement of slab was taken into account when the beam flange was in tension. The finite width of beam, integral with the attached column was modelled as a rigid segment, having 10 times the rigidity of the beam element. This implies that the beam-column joints were assumed to be rigid. The columns were modeled as FEMA column elements with axial force-flexure interaction accounted for in the two orthogonal directions. Similar to the beam element, FEMA column comprised of two elastic segments and two plastic hinges with rigid end zones.

The plastic hinges in PERFORM-3D are assigned a hysteretic model that reflects the flexural stiffness of each member during loading, unloading and reloading under seismic excitations. The user specified data includes the flexural yield strength (M_y), the ultimate strength (M_U) prior to strength degradation and the percentage of post-yield stiffness relative to the elastic stiffness. The stiffness degradation that occurs during unloading and reloading, typically observed in reinforced concrete response, is modelled through the use of cyclic energy degradation factor (EDF). EDF is the ratio of area under a degraded hysteresis loop to the area under a non-degraded loop (fully plastic hysteresis loop). In this study, the EDF was calculated from the column tests performed by Ozcebec and Saatcioglu (1987). Accordingly, the hysteretic force-displacement behaviour of specimen U6 was adopted for hysteretic modelling as representative of column behaviour. Because the axial load applied on this specimen was only 12% of the nominal capacity, EDF derived from the specimen was also used for beam elements. Figure 3.2 shows the stiffness degraded hysteresis loop and non-degraded elastic-perfectly-plastic loop. Loading and unloading braches of non-degraded loop was parallel to the effective elastic stiffness of the backbone curve. The effective elastic stiffness was taken as 40% of initial stiffness. The slope of the post-yield branch (strain hardening slope) of the non-degraded parallelogram was considered to be equal to 3% of the effective elastic stiffness. The same procedure was followed to calculate the EDF under increasing levels of inelastic deformation. The resulting factors were found to be 0.62 up to the yield point and 0.56 thereafter. A sensitivity analysis was conducted on the effect of EDF on structural response, as presented later in the paper.

FEMA beam and column elements have rigid-plastic rotational hinges to simulate moment-rotation relationships. When a beam or a column exceeds yield capacity, additional rotations of

elements develop as plastic rotations, which are then assigned to the hinges provided at the ends. The moment-rotation backbone curve of a beam or a column element was developed according to the guideline provided in ASCE 41-13. The yield moment (M_y) of the beam was calculated from sectional analysis using computer software SAP2000 (CSI 2013.a) and the yield chord-rotation (Θ_y) was calculated by the software as $\frac{M_y L}{6E_c I_e}$ where L is the clear span/height. Similarly, for the columns, SAP2000 was used to conduct sectional analysis in presence of constant axial load. Hardening stiffness (post-yield slope) of moment-rotation curve was 3% and 4% of the effective elastic stiffness for beams and columns, respectively. For a moderately ductile structural element based on the ductility limit of CSA A23.3-04, the onset of strength degradation starts at 2.5 times the yield rotation and the corresponding moment was considered as ultimate moment capacity. Similarly, for a ductile element, 4.0 times the yield rotation was used to find the ultimate point (Θ_U) on the hysteretic model. This approach was used when the structure was modelled following the requirements of NBCC and CSA. However, when the moment-rotation relationships of structural elements were modelled according to ASCE 41-13 and ACI 369R-11, plastic chord rotation values provided in respective documents were used. In order to define the strength loss, the moment capacity degraded linearly from the ultimate capacity to a point beyond which the element capacity dropped to zero at constant rotation. Strength degradation slope of the elements modeled according to CSA A23.3-04 was taken as parallel to that modelled using ASCE 41-13. Two different levels were used to model the onset of strength decay depending on the assumed ductility capacity. Both structures were designed and detailed as moderately ductile buildings for Ottawa, which is a medium seismic zone. In this case the strength decay started to occur at 2.5 times the yield rotation. The effect of higher available ductility was also investigated by considering increased level of ductility in the 2-storey building. In this case the strength onset point was modelled to occur at 4.0 times the yield rotation. Figure 3.3 shows the typical moment-rotation envelops for buildings with rotational values (Θ_a, Θ_b and $2.5\Theta_y$) based on different standards and two different levels of ductility based on CSA A23.3.

The behaviour in shear was considered to be elastic. This was assumed to be true even after flexural yielding. In this study E_c remained unchanged and poisson's ratio was taken as 0.2,

which resulted in a constant shear rigidity of $0.4E_cA_w$,where A_w is the gross area of web as specified by ASCE 41-13 and ACI 369R-11.

The damping ratio was taken as 5% of critical damping for all modes of vibration. A small amount (0.2%) of Rayleigh damping was applied to ensure that higher modes would not dominate the response. The effect of Rayleigh damping increases exponentially after the period (T) reduces to 5% of the fundamental period (T_1). Rayleigh damping becomes 0.05% when T increases to a value greater than 50% of T_1. The mass associated with self-weight of the structure, superimposed dead load and live load were applied at each node.

3.4 Non-linear model Validation

The analytical model and the dynamic analysis results obtained by PERFORM-3D for the 5-storey building discussed in the preceding section were verified against those obtained by the use of two general purpose dynamic analysis software; SAP2000 and SeismoStruct (Seismosoft 2013). The validation and comparisons of results are presented in the following sub-sections.

SAP 2000

SAP 2000 is structural analysis software that is commonly used for static and dynamic analysis of structures, developed by Computers and Structures Inc. The same 5-storey bare frame building was also modeled for SAP 2000. The same sectional analyses conducted earlier for columns and T-beams were used for modelling the structure in SAP2000. The same seismic masses were assigned to each node. Beam/column elements were modeled as consisting of elastic elements and member-end hinges. Non-linear moment-rotation properties were assigned to the hinges at the ends of beam/column elements. For the purpose of verification of the models in both PERFORM-3D and SAP 2000 models, the beam effective flexural rigidity (E_cI_e) was taken as constant and was equal to 50% of the gross (uncracked) flexural rigidity. For the columns, the effective flexural rigidity was taken as 70% of the gross column rigidity. The same rotational properties, as recommended by ACI 369R-11 were used in plastic hinges of both PERFORM-3D and SAP 2000 models. The descending branch of the moment-rotation envelop curve was also specified based on the ACI 369R-11 recommendations. Appropriate hysteretic models were used with degrading stiffness characteristics to model the nonlinear hysteretic behaviour of structural elements. Rayleigh damping was applied as 5% of critical damping.

SeismoStruct

SeismoStruct is software which was developed to perform non-linear dynamic analysis of structures. This software was also used to validate the PERFORM-3D model and the analysis results. In SeismoStruct, beam/column elements were defined as inelastic frame elements (infrmFB), which consisted of fibres with non-linear stress-strain relationships specified for concrete and reinforcing steel. The integration of individual fibre behaviour resulted in the overall element performance. InfrmFB provided chord rotations which were compared with those computed by PERFORM-3D. Simplified uniaxial trilinear concrete model "con_tl" was used to define non-linear concrete properties. In con_tl the initial modulus of concrete is linear and can be changed to incorporate the effects of member cracking. Hence, the initial elastic modulus of concrete was reduced to 50% when used to model beam elements, and 70% to model column elements. This resulted in the same $E_c I_e$ properties of elements defined in PERFORM-3D. The degradation of element stiffness was modelled by reducing the slope of the stress-strain relationship of concrete beyond its peak strength. This was done by reducing the slope of the descending branch of the concrete model such that it resulted in the descending branch of elements to 10% of cracked element stiffness for both the beams and columns. The material strengths used to compute the flexural capacities of elements in PERFORM-3D were kept the same to attain the same element strength values in the SeismoStruct model. Damping in SeismoStruct is computed through hysteretic damping, which is included in the nonlinear fibre model formulation of infrmFB. To achieve similar damping as that used in PERFORM-3D analysis, 4% Rayleigh damping was applied to simulate the friction mechanism along the concrete cracks and friction between structural and non-structural members. Seismic masses were assigned to the nodes, as before.

Comparison of Analysis Results

All three analytical models had the same fundamental period and were subjected to the same earthquake record. The results shown in Figure 3.4 indicate that the structural response obtained from SAP 2000 and PERFORM-3D was similar. This observation was expected because the member properties were defined using the same envelop curve in both the PERFORM-3D and

SAP 2000 models. On the other hand, member properties in SeismoStruct were defined using concrete and steel constitutive models. Hence the envelope curve was computed using the material constitutive models rather than being specified by the user. Although the structural response within the elastic range showed very good correlation with PERFORM-3D response, the non-linear range of deformations obtained by SeismoStruct did not show as good correlation as that obtained by SAP 2000. However, the onset of plastification and the response wave form showed reasonably good agreement even within the inelastic range of deformations. This is shown in Figure 3.4. Hysteretic responses of elements are also compared. Figure 3.5 illustrates the hysteretic behaviour of a (a) ground floor column and (b) exterior beam at the 2nd floor level. Figure shows the total chord rotation responses, consisting of elastic plus plastic rotations obtained from PERFORM-3D, SeismoStruct and SAP2000 analyses. The comparison shows very good correlation in column for all three software whereas in beam for PERFORM-3D and SAP2000. It can be concluded from the foregoing discussion that PERFORM-3D modelling and analysis techniques are verified against two commonly accepted, industry standard software, and hence can be used in further developments.

3.5 Sensitivity Analysis of Energy Degradation Factor (EDF) used in PERFORM-3D

EDF is a parameter that affects the overall shape of hysteresis loops in PERFORM-3D; in particular the slopes of unloading and reloading branches of the hysteretic model. The shape of hysteresis loops may potentially affect inter-storey drift, which is used in the current investigation as a damage parameter. Since the main goal of analyses was to find seismic damage state of structures, the effect of EDF on structural drift was studied. Zeynep Tuna (2012) suggested value of EDF for shear critical coupling beam elements to be between 0.5 and 0.35 in the post-yield region, up to the development of residual capacity. Wen-Cheng Liao (2010) used pinching material model to calculate EDF and suggested a value between 0.25 and 0.15 depending on the section properties. Ghodsi and Ruiz (2010) used 0.24 to 0.2 as EDF for frame beam elements. Higher values were found to be suitable for confined ductile flexure-dominant elements, and lower values were found to be suitable for shear controlled elements.

A parametric study was performed by varying EDF for both columns and beams, with EDF values ranging between 0.1 and 0.7. Figure 3.6 shows the change of hysteresis loops and the resulting changes in hysteresis areas (energy dissipations) due to the variation in EDF. A total 80

analyses were conducted using 20 earthquake records and two sets of EDF values for columns and beams. The records were synthetic seismic records compatible with the UHS of Ottawa given in the 2010 NBCC. They were adjusted as suggested by Gail Atkinson (2009). The adjusted records were then amplified and applied in such a way to form hinges in beams and columns, while the structure was approaching collapse. This would amplify the effect of beam/column EDF in the non-linear state of structure. Results are shown in Figure 3.7(a) and (b) for the variation of EDF in beams under a single earthquake record for a predominantly elastic response with limited yielding and a non-linear response with extensive yielding, respectively. It is evident in the Figure 3.7(a) that for constant column EDF, structural drift was not sensitive to changes in beam EDF when the structure behaved essentially elastic with inelastic hinges forming in only few structural members without the collapse of any element. On the other hand in the Figure 3.7(b), when inelastic hinges formed in most structural members, with collapse experienced in some members, the maximum variation of inter-storey (ISD) and full height drift (FHD) was found to be 19% and 17%, respectively.

When the variation in EDF was introduced to the column, as shown in Figure 3.7(c), the effect was negligible even for high levels of inelasticity. Table 3.1 lists the details of all the records and the beam EDF variation, along with the results obtained. It is evident that beam EDF had a minor effect on structural drift. For a wide range of Beam EDF, changing between 0.1 and 0.7, resulted in an average change in FHD and ISD of 6.7% and 6.8%, respectively when the column EDF was kept constant. The maximum variation was found to be 29% for the FHD and 25% for ISD. Dissipated inelastic energy of the structure increased on average 25% with a maximum variation of 51% in beam EDF. At the end of the sensitivity analysis it was decided to adopt the experimentally observed values of EDF for beams and columns, as 0.62 up to the full yield of element (including the curved portion beyond the initial yield point) and 0.56 thereafter.

3.6 Incremental Dynamic Analysis (IDA)

Having established the validity of the analytical model, the dynamic analysis tool selected, and the characteristics of the hysteretic model, the fragility analyses of buildings were carried out using incremental dynamic analysis (IDA). IDA was used extensively by previous researchers, including Erberik and Elnashai (2004), Rajeev and Tesfamariam (2012) and Kircil and Polat (2006). It was adopted by FEMA 350 (FEMA 2000) as a method for performance evaluation of

buildings. IDA is a comprehensive dynamic analysis method where the structure moves progressively from elastic to inelastic state by incrementally increasing the hazard level. The accuracy of IDA depends on the number of single point analysis for each seismic record, which requires high speed computer processing and suitable software for appropriate modelling of structural elements. PERFORM-3D was used to conduct dynamic inelastic response history analyses to establish relationships between spectral acceleration as an intensity measure and inter-storey drift as a seismic demand parameter for selected earthquake records. The resulting relationship is referred to as "IDA curve," facilitating the derivation of fragility curves.

The same UHS compatible 20 seismic records chosen earlier were used for the IDA. All the records had 2% probability of exceedance in 50 years of return period with 5% damping to match with uniform hazard spectra (UHS) in 2010 NBCC. The selected records included near and far field effects (fault distance 15 km to 100 km) for different magnitude earthquakes (Magnitudes 6 to 7). As the structures were designed for site soil class C, all the seismic records were for the same soil class. Spectral acceleration (S_a) at the design code period (T_d), computed on the basis of the 2010 NBCC empirical expression, was used as Intensity Measure (IM). Each record was scaled by using hunt and fill algorithm to minimize the number of required analysis to cover the entire range of structural response (Vamvatsikos and Cornell 2004). Analyses were performed by increasing IM level until the structure became numerically unstable. Additional analyses were performed to limit the gap between successive runs. Maximum inter-storey drift ratio, Θ_{max}, was suggested as a strong indicator for global and local structural damage measure (DM) by Vamvatsikos and Cornell (2002). The same damage measure (Θ_{max}) was selected as seismic deformation demand, D. It was assumed that at a specific spectral acceleration (S_a), D followed lognormal probability distribution, and the median value of D was obtained by linear regression using least squares method of 'cloud' response (Jeong et al. 2012). IDA was then employed to generate deformation demands D at different limit states, corresponding to different performance levels. Figure 3.8 illustrates the IDA curve generated with earthquake record 6C1-3 for the 5-storey building selected.

3.7 Performance Levels

The ACI 374.2R-13 (ACI 2013) provides maximum inter-storey drift ratio, Θ_{max} for different seismic performance levels. In the current study $\Theta_{max}$was adopted as a performance

indicator. Three performance levels were considered. Immediate Occupancy (IO) performance level describes the damage state where structure is safe to be re-occupied having suffered minor damage to the structural elements with minor spalling and flexural cracking. Life Safety (LS) performance level describes the damage state where significant damage has occurred to the structure with extensive cracking and hinge formation in primary structural elements. Collapse Prevention (CP) performance level describes the damage state where structure is at the onset of partial or total collapse with extensive cracking, hinge formation and reinforcement buckling in structural elements. 1% and 2% inter-storey drift ratios were considered as the limits for IO and LS performance levels. The median value of maximum inter-storey drift demands for all records was considered as CP performance level (Ellingwood et al. 2007). The maximum inter-storey drift was obtained as the smaller of the drift at which either dynamic instability is attained or the tangential slope of the IDA curve dropped to 20% of the initial slope (FEMA 350).

3.8 Development of Fragility Relationships

The relationship between ground motion intensities (spectral accelerations) and the probability of attaining a certain damage level in terms of maximum inter-storey drift ratios was used to develop fragility curves. The conditional probability of exceeding a certain limit state (LS) at a given spectral acceleration ($S_a(T_d)$) can be expressed according to Jeong et al. (2011) as equation 1.

$$P\,(D/IM) \;=\; 1 - \Phi\left(\frac{lnD_C - lnD_M}{\sqrt{\left(\beta^2_{\frac{D}{M}} + \beta^2_C + \beta^2_M\right)}}\right) \qquad (1)$$

Where, D_C is median drift capacity specified for a certain limit state. $\beta_{D/M}$ denotes standard deviation of log of deformation demand and assumed to be constant over the spectral acceleration range; β_C denotes standard deviation of log of deformation capacity and is taken as 0.3 (Jeong and Elnashai 2007) for all limit states and β_M denotes uncertainty in analytical modeling and is taken as 0.2 on the assumption that modelling process yields frame response with 90% confidence and within 30% of actual value (Ellingwood et al. 2007); D_M is median drift demand and is defined as $D_M = a.S_a(T_d)^b$ where a and b are regression coefficients that are found from the 'cloud' analysis, as shown in Figure 3.9 for the 5-storey building.

3.9 Fragility Curves for Seismic Performance Evaluation

The fragility curves developed from IDA are shown in Figure 3.10 for seismic performance evaluation of the two buildings considered. The curves show probability of exceedance for each performance level. The fragility analysis indicates that the 5-storey frame building in Ottawa modelled according to CSA A23.3-04, ASCE 41-13 and ACI 369R-11 behaved similarly at IO and LS performance levels. This was expected as yield moments of structural members were specified to be the same, and the element yield rotations, based on CSA A23.3-04 were close to the other two structures. At the design spectral acceleration level, all three structures experienced 28% and 3% probabilities of exceeding IO and LS performance levels, respectively. The building modelled based on CSA A23.3-04 showed higher probability of exceeding CP performance level in comparison with those modelled using ASCE 41-13 and ACI 369R-11. At ultimate capacity, the elements modelled using CSA A23.3-04 had considerably less rotational capacities in comparison with those modelled using ASCE41-13 and ACI 369R-11. Hence, in the former case the elements entered into the strength degradation zone of moment-rotation relationships at a lower rotational capacity. Therefore, this analysis exhibited higher probability of exceedance at the CP performance level. At a higher level of seismic event with S_a = 0.54g (4 times the design S_a), the structure modelled using CSA A23.3-04 had 94%, 51% and 23% for probabilities of exceeding IO, LS and CP performance levels, whereas when the structures were modelled using ASCE 41-13 and ACI 369R-11, probabilities of exceedances were 92%, 49% and 12% for the same levels of performance, respectively. It was also anticipated that the maximum inter-storey drift demand of the building modelled using CSA A23.3-04 would be less than those obtained using ASCE41-13 and ACI 369R-11, because of early strength decay and lower level of rotation at collapse associated with CSA A23.3-04. The differences in the moment-rotation envelope curves computed by using different standards are shown in Figure 3.3 as previously discussed. CP performance level drift capacity, which was considered as median value of maximum inter-storey drift demands, was found to be 2.85% for CSA A23.3-04 and 3.19% for ASCE41-13 and ACI 369R-11 structures. There was virtually no difference between the structures modelled using ASCE41-13 and ACI 369R-11, except for residual strength, the fragility performance at IO and LS levels were the same. Negligible difference occurred at CP performance level because of the difference in the residual strength. However, the difference was small enough to suggest that variation in the residual strength capacity can be neglected. The

fragility responses also indicated that the rotational capacities specified in ASCE 41-13 and ACI 369R-11 for different categories, as dictated by the level of axial compression (for columns), confinement of concrete, longitudinal reinforcement ratio (for beams) and shear strength, can be used to model structural members conforming to CSA A23.3-04. In this case, the results would be similar for IO and LS performance levels, whereas CP performance level would be under-estimated for moderately ductile structures when the CSA A23.3-04 approach is employed.

The fragility curves for the 2-storey building show that both moderate and fully ductile designs resulted in similar fragilities for IO and LS performance levels. This was expected since the building had the same yield strength and rotation when designed as a moderately ductile or fully ductile structure. At design level spectral acceleration, the probabilities of exceeding IO and LS performance levels were 50% and 2%, respectively for both moderately ductile and fully ductile designs. The rotational capacity specified at the onset of strength decay was lower for moderately ductile structure as compared to that for ductile structure. Hence, structural members of moderately ductile structure reached ultimate capacity prior to ductile structure. The same behaviour was observed in the fragility response where probability of exceeding CP performance level was higher for moderately ductile structure in comparison to the ductile structure. At high level of seismic event, when S_a = 1.2g (4 times stronger seismic event as compared to the spectral acceleration at design period), it was observed that both structures would exceed IO performance level, and the probability of exceeding LS performance level was 57%. At CP performance level the moderately ductile and fully ductile structures had 11% and 7% probabilities of exceedances. Also, moderately ductile structure had lower maximum inter-storey drift as the members developed strength decay at lower rotations, as compared to the ductile structure. The maximum inter-storey drift found for moderately ductile and fully ductile structures were 4.03% and 4.75%, respectively. From the fragility analysis of the 2-storey structure it can be concluded that the seismic safety margin in the ductile building, in terms of probability of exceeding the CP performance level, is higher. This conclusion reaffirms the importance of ductile detailing in increasing safety against structural collapse.

3.2.10 Summary and Conclusions

Modeling techniques for dynamic inelastic analysis of reinforced concrete frame structures for PERFORM-3D software are explained with sensitivity analyses conducted for selected

modelling parameters. The effect of EDF, which defines the degree of stiffness degradation in the hysteretic model, is discussed. It was found that a wide range of variation in this parameter for beam hysteretic modelling between 0.1 and 0.7 resulted in an average change in the inter-storey and full height drift ratios of up to 7%. The same level of variation in the column hysteretic models showed negligible effects on drift ratios. Further investigation of the hysteretic model features was conducted by varying the strength decay properties of elements. The provisions of ASCE 41-13, ACI369R-11 and CSA A23.3-04 were used to model the onset and rate of strength decay in members. It was concluded that the variation in these parameters, within the range covered in the three standards, did not have an effect on drift levels within IO and LS performance ranges. Some difference was observed for drift demands at or near collapse level, as this is the deformation range within which some members developed strength degradation. However, the variation was only 12% between the use of CSAA23.3-04 and the other two standards, with the former being smaller than the latter. One may conclude from this observation that the use of these different standards do not translate into a significant difference in seismic assessment of reinforced concrete frame structures.

The PERFORM-3D model and the resulting dynamic inelastic time history analysis were verified against additional analytical results obtained by SAP2000 and Seismostruct software. The same 5-storey frame building, modelled and analyzed using PERFORM-3D, was also modelled and analyzed under the same earthquake record using these software. The results indicated good correlation, with some differences in maximum deformations computed.

Fragility curves were developed for the two frame buildings considered, using 20 seismic records compatible with the UHS specified in the 2010 NBCC for the city of Ottawa. Three sets of fragility curves were developed for the 5-storey building, using the deformation limits as per CSA A23.3-04, ASCE41-13 and ACI 369R-11. The fragility curves showed the same structural vulnerabilities at IO and LS performance levels, with a minor variation at the CP level, suggesting that any one of these standards can be implemented for fragility analysis. The same observation was also made when the fragility analysis was conducted for the 2-storey building, having two levels of ductility. An increase of 60% in the ductility of structural members resulted in an 18% increase in maximum inter-storey drift capacity at the collapse level of protection. It

was also observed that higher safety margin can be attained in structures by incorporating ductility in structural elements as expected.

3.10 References for Chapter 3

American Concrete Institute (ACI), 2011. *Guide for seismic rehabilitation of existing concrete frame buildings and commentary. ACI 369R-11*. ACI committee 369.

American Concrete Institute (ACI), 2013. *Guide for testing reinforced concrete structural elements under slowly applied simulated seismic loads. ACI 374.2R-13.* ACI committee 374.

American Society of Civil Engineers (ASCE), 2007. *Seismic rehabilitation of existing buildings". American Society of Civil Engineers. ASCE/SEI 41-06.* Reston, VA.

American Society of Civil Engineers (ASCE), 2014. *Seismic evaluation and retrofit of existing buildings. ASCE/SEI 41-13*. Reston, VA.

Atkinson, G.M., 2009. Earthquake time histories compatible with the 2005 National building code of Canada uniform hard spectrum. *Canadian Journal of Civil Engineering*. Volume 36, Number 6, June 2009.

Canadian Standards Association (CSA), 2004. *Design of concrete structures. CSA A23.3-04.* CSA standards update service.

Computers and Structures, Inc (CSI), 2008. *ETABS. Nonlinear Version 9.5.0.* Berkeley, CA.

Computers and Structures, Inc (CSI), 2013. *PERFORM-3D. Version 5.0.1*. Berkeley, CA.

Computers and Structures, Inc (CSI), 2013a. *SAP2000. Ultimate 16.0.0*. Berkeley, CA.

Ellingwood, B.R., Celik, O.C., and Kinali, K., 2007. Fragility assessment of building structural systems in Mid-America. *Earthquake Engineering and Structural Dynamics*. Volume 36, Issue 13, Pages 1935-1952, October 2007.

Erberik, M.A., and Elnashai, A.S., 2004. Fragility analysis of flat-slab structures. *Engineering Structures*. Volume 26, Issue 7, Pages 937-948, June 2004.

Federal Emergency Management Agency (FEMA), 2000. *Recommended seismic design criteria for new steel moment-frame buildings. FEMA 350.* SAC Joint Venture. Washington, D.C.

Federal Emergency Management Agency (FEMA), 2000a. *Prestandard and commentary for the seismic rehabilitation of buildings. FEMA 356*. Washington, D.C.

Ghodsi, T., and Ruiz, J.A.F., 2010. Pacific earthquake engineering research/seismic safety commission tall building design case study 2. *The Structural Design of Tall and Special Buildings*. Volume 19, Issue 1-2, pages 197–256, 2010

Hopper, M. W., 2009. Analytical models for the nonlinear seismic response of reinforced concrete frames. M.Sc. Thesis. Pennsylvania State University.

Jeong, S.H. and Elnashai, A.S., 2007. Probabilistic fragility analysis parameterized by fundamental response quantities. *Engineering Structures*. Volume 29, Issue 6, Pages 11238-1251, June 2007.

Jeong, S.H., Mwafy, A.M., and Elnashai, A.S., 2012. Probabilistic seismic performance assessment of code-compliant multi-storey RC buildings. *Engineering Structures*. Volume 34, January 2012, Pages 527-537.

Kircil, M.S., and Polat, Z., 2006. Fragility analysis of mid-rise R/C frame buildings. *Engineering Structures*. Volume 28, Issue 9, July 2006, Pages 1335-1345. July 2006

Liao, W. C., 2010. Performance-based plastic design of earthquake resistant reinforced concrete moment frames. Ph.D. Thesis. University of Michigan.

National building code of Canada (NBCC). 2010. *National Research Council of Canada*. Ottawa, Canada.

Ozcebe, G., Saatcioglu, M. 1987. Confinement of concrete columns for seismic loading. *ACI Structural Journal*. Volume 84, Issue 4, Pages 308-315.

Rajeev, P., and Tesfamariam, S., 2012. Seismic fragilities for reinforced concrete buildings with consideration of irregularities. *Structural Safety*. Volume 39, Pages 1-13, November 2012.

Reyes, J.C., and Chopra, A.K., 2012. Modal pushover-based scaling of two components of ground motion records for nonlinear RHA of structures. *Earthquake Spectra*. August 2012, Vol. 28, No. 3, pp. 1243-1267

Seismosoft., 2013. *SeismoStruct. Version 6.5*. Seismosoft Ltd.

Tuna, Z., 2012. Seismic Performance, Modeling, and Failure Assessment of Reinforced Concrete Shear Wall Buildings. Ph.D. Thesis. University of California. Los Angeles.

Vamvatsikos, D., and Cornell, C.A., 2002. Incremental dynamic analysis. *Earthquake Engineering and Structural Dynamics*. Volume 31, Issue 3, Pages 491-514.

Vamvatsikos, D., and Cornell, C.A., (2004). Applied incremental dynamic analysis. *Earthquake Spectra*. Vol 20, No. 2, Page 523-553.

3.11 Tables and Figures

Table 3.1 Effect of beam EDF on drift and energy dissipation within the non-linear range for various seismic records

Seismic Record	Duration (Sec.)	PGA (g)	Accln. Scale Factor	Full Height Drift		Inter-storey Drift		Dissipated Inelastic Energy (% of Total Energy)	
				Beam EDF 0.1	Beam EDF 0.7	Beam EDF 0.1	Beam EDF 0.7	Beam EDF 0.1	Beam EDF 0.7
6C1-3	5	0.904	5	0.015	0.015	0.026	0.025	35	41
6C1-7	5	0.327	5	0.011	0.011	0.019	0.019	35	40
6C1-12	5	0.645	5	0.015	0.015	0.023	0.023	38	43
6C1-30	5	0.474	5	0.012	0.011	0.026	0.026	33	38
6C1-42	5	0.431	5	0.010	0.009	0.015	0.015	36	43
6C2-3	7	0.438	5	0.018	0.018	0.030	0.030	44	46
6C2-9	7	0.438	6	0.011	0.009	0.018	0.018	27	36
6C2-13	7	0.531	5	0.008	0.007	0.016	0.016	29	38
6C2-15	7	0.298	5	0.014	0.014	0.024	0.024	41	46
6C2-17	7	0.545	5	0.014	0.014	0.019	0.019	28	36
7C1-6	17	0.484	3	0.012	0.012	0.020	0.020	34	39
7C1-18	17	0.270	4	0.010	0.011	0.020	0.016	34	39
7C1-28	17	0.351	4	0.014	0.010	0.024	0.019	34	44
7C1-32	17	0.326	5	0.013	0.013	0.021	0.021	34	45
7C1-36	17	0.393	3	0.015	0.016	0.027	0.027	42	44
7C2-1	20	0.258	4	0.013	0.014	0.020	0.021	31	43
7C2-3	20	0.257	4	0.010	0.009	0.016	0.017	31	42
7C2-7	20	0.203	6	0.015	0.014	0.022	0.017	32	46
7C2-11	20	0.202	6	0.017	0.015	0.034	0.028	32	46
7C2-36	20	0.157	6	0.019	0.014	0.013	0.016	32	49

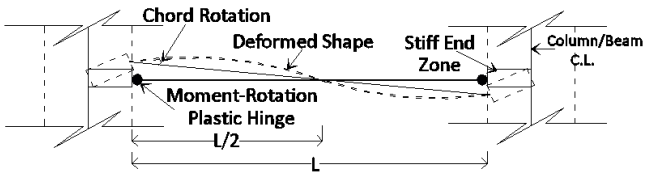

Fig 3.1 Analytical model of beam/column element used to develop frame structure in PERFORM-3D

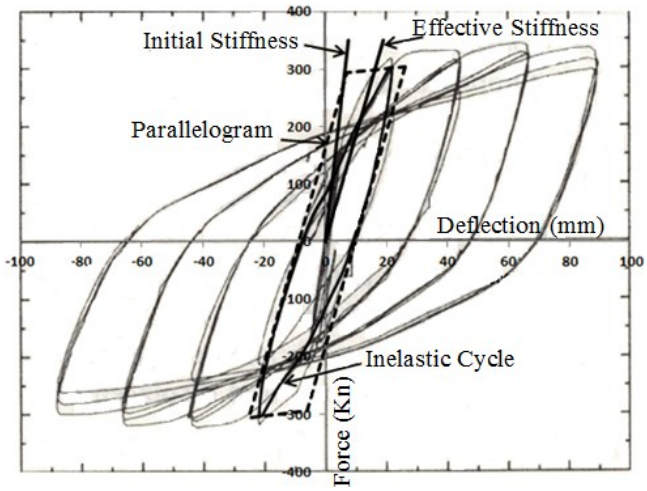

Fig 3.2 Evaluation of Energy Degradation Factor (EDF) for PERFORM-3D from tests performed by Ozcebe and Saatcioglu (1987)

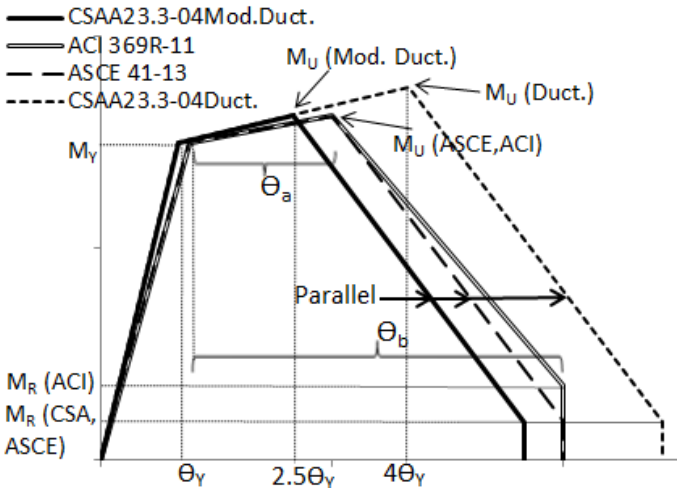

Fig 3.3 Typical moment rotation envelopes used to develop analytical models in PERFORM-3D.

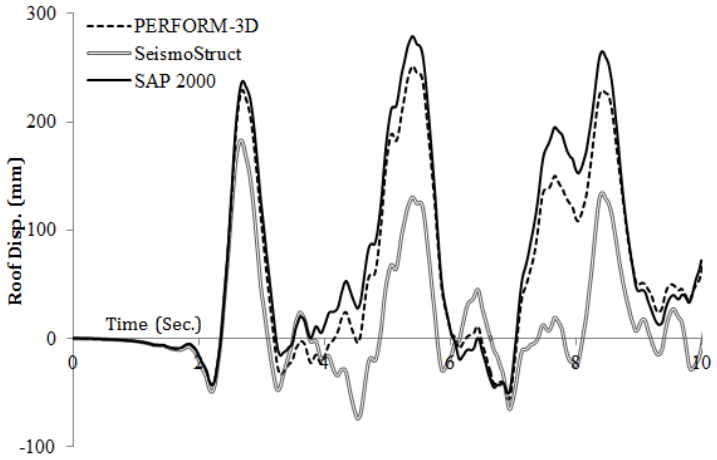

Fig 3.4 Comparison of time-history responses of 5-storey analytical models

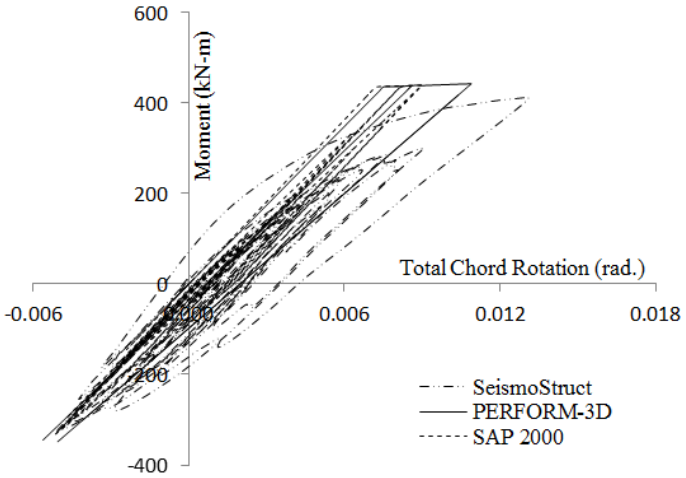

(a)

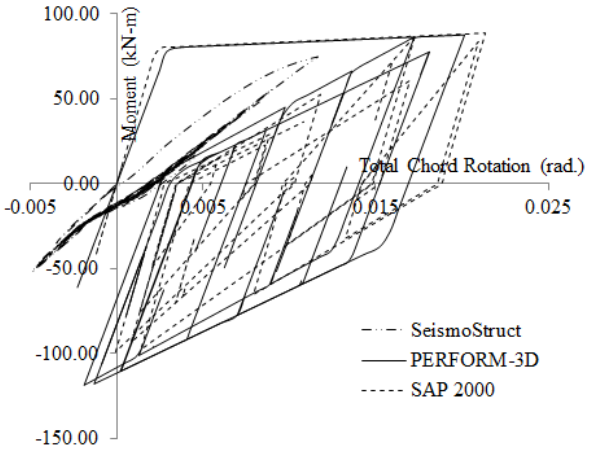

(b)

Fig 3.5 Moment - Total Chord Rotation response for (a) Ground floor column and (b) 2nd floor exterior beam in SeismoStruct, PERFORM-3D and SAP2000

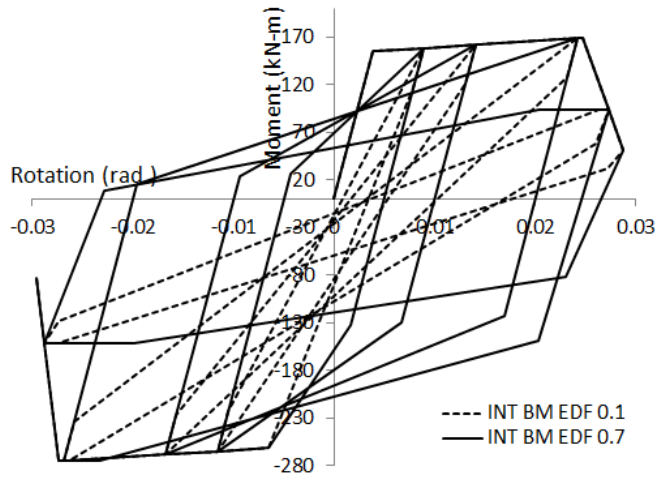

Fig 3.6 Effect of EDF on Interior beam Moment vs Total Chord Rotation hysteresis loop area in PERFORM-3D

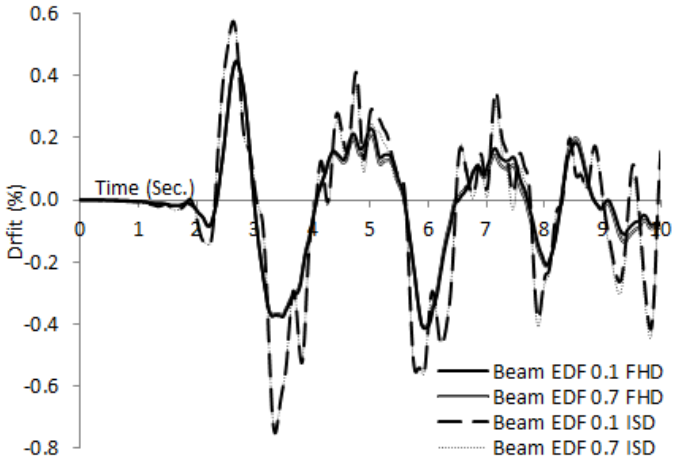

(a)

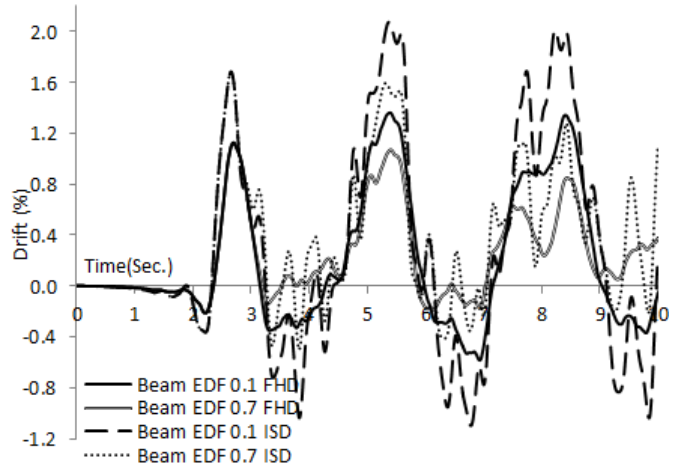

(b)

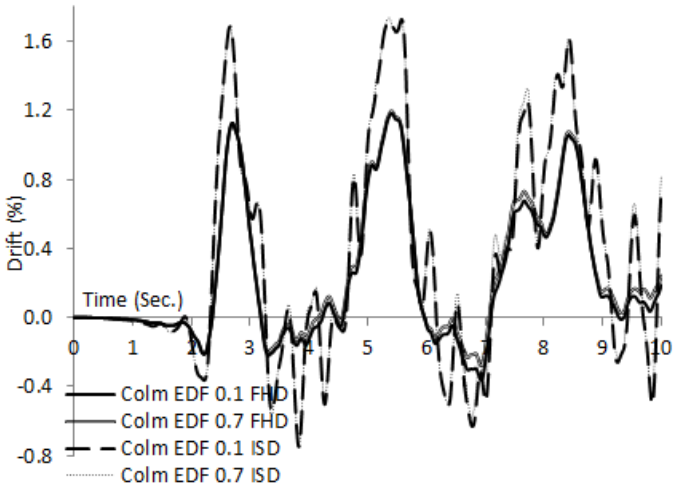

(c)

Fig 3.7 Effect of beam EDF on full-height (FHD) and inter-storey drift (ISD) at second floor level in (a) predominantly linear, (b) non-linear stage and (c) column EDF on full-height (FHD) and inter-storey drift (ISD) in non-linear stage of structure

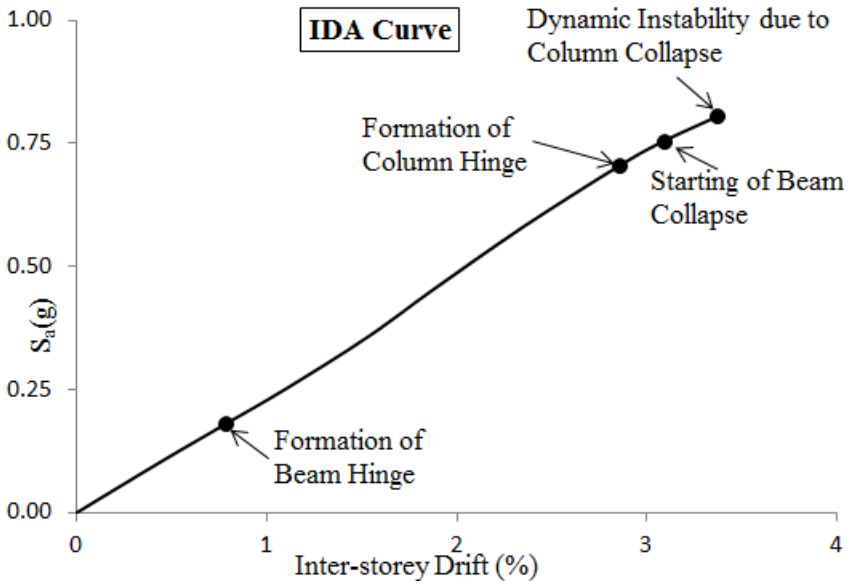

Fig 3.8 IDA Curve and performance of the 5-storey frame building with moderate ductility

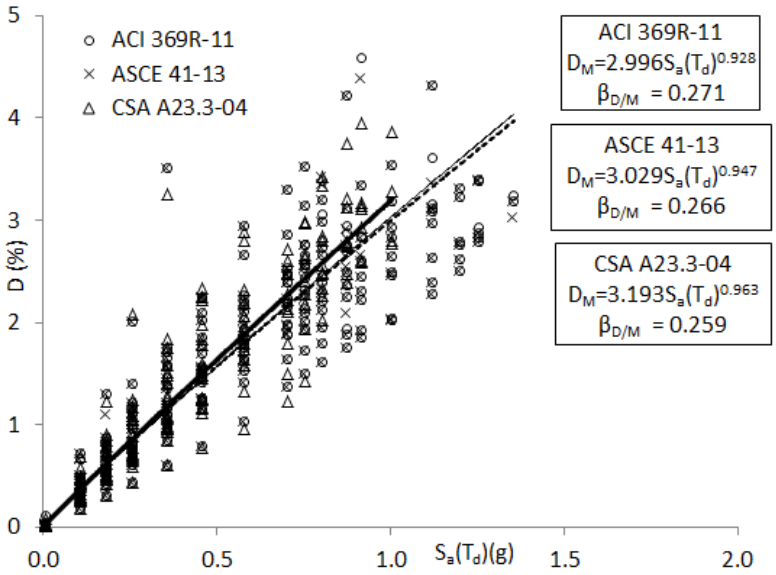

Fig 3.9 Maximum inter-storey drift ratio (%) of 5-storey building designed using elemental rotational values provided in ACI 369R-11, ASCE 41-13 and moderate ductility in CSA A23.3-04 with regression coefficients.

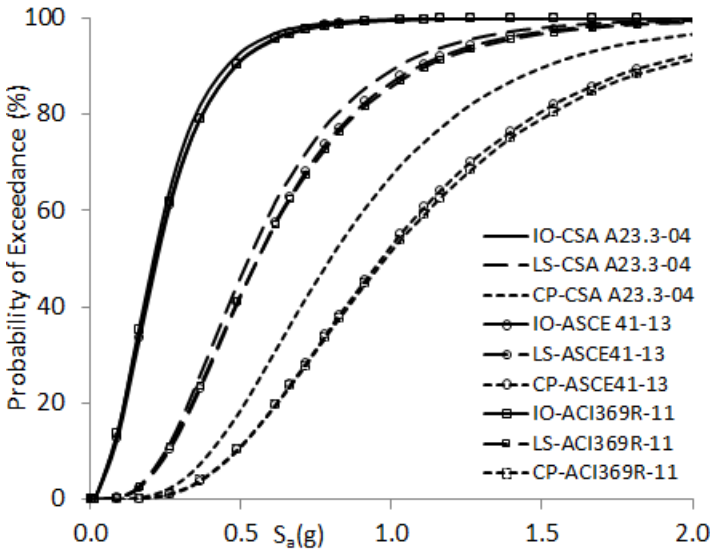

(a)

Fig 3.10 (Cont'd)

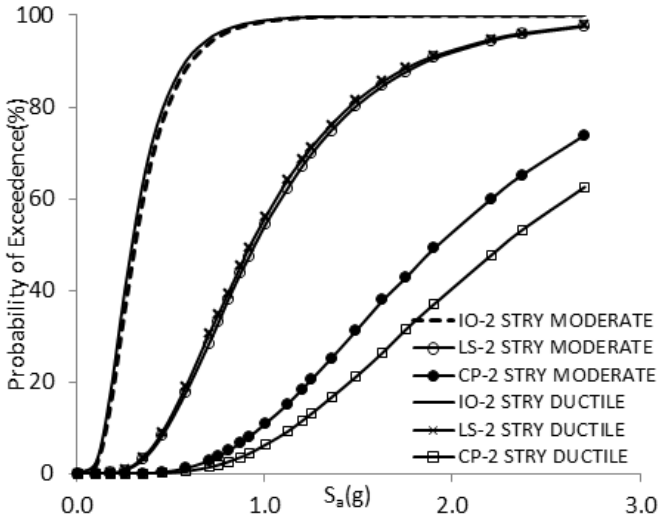

(b)

Fig 3.10 Seismic fragility curves of (a) 5 storey and (b) 2 storey RC frame structures

CHAPTER 4

4. SEISMIC FRAGILITY CURVES FOR REINFORCED CONCRETE FRAME BUILDINGS IN CANADA DESIGNED AFTER 1985

Abstract: Performance of reinforced concrete frame buildings depends on seismic hazard of the region and vulnerability of the structure. Performance-based evaluation of buildings may be conducted through fragility curves developed for different levels of performance. Reinforced concrete frame buildings with 2, 5 and 10-stories, designed as moderately ductile buildings for Ottawa in Eastern Canada and fully ductile buildings for Vancouver in Western Canada were used to generate seismic fragility curves. The buildings were analyzed using PERFORM-3D software to assess seismic vulnerabilities. Incremental Dynamic Analysis was employed to generate fragility curves. Two sets of earthquake records compatible with Uniform Hazard Spectra of 2010 NBCC were selected, where each set contained 20 records for each city. The fragility curves depict probabilities of exceedances for different damage states, and can be used for seismic vulnerability assessment of reinforced concrete frame buildings in Canada designed and built after 1985.

4.1 Introduction

Earthquakes occur frequently in Canada with historic damage. The seismic hazard in Canada can be characterized by the seismicity of two distinct regions; eastern Canada and western Canada; with a relatively stable continental shelf between the two. Significant seismic activities occur in western Canada because of the presences of active faults along the Pacific Rim. Geological Survey of Canada records more than 1000 earthquakes in western Canada with more than 100 earthquakes of magnitude 5 or greater. Seismic activity in eastern Canada occurs with reduced frequency of approximately 500 earthquakes per year, with about three magnitude 5

earthquakes taking place in each decade (GSC 2016). Eastern Canada does not have active faults. The earthquakes in this region are believed to be related to the regional stress fields with earthquakes concentrated in regions of crustal weakness. Stronger earthquakes are expected in the west, though damaging earthquakes have also occurred in the east. Eastern earthquakes tend to be less frequent and of moderate magnitude (GSC 2016). This difference in seismic regions is reflected in building design practices that follow the requirements of the National Building Code of Canada (NBCC).

It is preferable to conduct seismic vulnerability assessment of buildings through dynamic inelastic response history analysis. However, this may not be feasible for the majority of buildings. An alternative is to conduct fragility analysis using fragility curves that incorporate design characteristics of the building being assessed. Fragility analysis provides a probabilistic methodology for assessing seismic vulnerability of existing buildings. It can be conducted using fragility curves that provide probability of exceeding pre-determined performance levels as a function of earthquake intensity for a given region and for a building type with certain characteristics (Vamvatsikos and Cornell 2002). It is best suited to earthquake investigations, with capabilities for providing support to decision makers.

The objective of this paper is to present seismic fragility curves for reinforced concrete frame buildings in Canada. It forms part of a comprehensive research program currently underway at the University of Ottawa involving reinforced concrete frame and shear wall buildings, as well as masonry buildings, with or without irregularities, designed during different periods of building code development.

The building inventory in Canada can be viewed in two broad groups; those designed prior to the enactment of modern seismic codes, and those designed using the more recent seismic hazard values and building design and detailing practices. The design base shear equation in NBCC has changed since the inception of seismic provisions in 1941 (1941 NBCC). Earlier equations defined seismic base shear as a percentage of seismic weight of building as seismic coefficient. In the 1953 NBCC, the building height was introduced as a design parameter, crudely reflecting the effect of building period on seismic coefficient. The hazard values were introduced in 1953 through seismic maps with seismic zones for different regions. In the 1965 NBCC, the differences in construction type and associated level of ductility was introduced through

coefficient C, reducing base shear for reinforced concrete frame and shear wall buildings with detailing for ductile response, while increasing the base shear for other non-ductile buildings. In the 1970 NBCC the hazard values were revised. The effect of construction type was treated more extensively through coefficient K, reflecting the associated level of ductility. Empirical expressions were also introduced for the computation of fundamental period. This was followed by the 1975 NBCC Commentary with ductility factors for different building types for use in dynamic analysis. The requirements remained essentially the same in the 1980 NBCC with refinements made to seismic response coefficient S as affected by fundamental period. New seismic zoning maps were introduced in the 1985 NBCC with seismic velocity and acceleration ratios specified for each zone, refining hazard values significantly based on 10% probability of exceedance in 50 years. Further refinements were introduced to the seismic response coefficient S with a new empirical period equation provided for shear wall buildings. The ductility related construction type factor K was replaced by force modification factor R in 1990 (1990 NBCC), with a calibration factor U, which introduced a reduction in base shear to account for structural over-strength and to bring the force level to the same level of safety implied in earlier codes. The same base shear expression remained essentially the same until 2005 with a revised empirical equation introduced for fundamental period of shear wall buildings. Significant changes were introduced in 2005 (2005 NBCC) with new site specific uniform hazard spectra having 2% in 50 year probability of exceedance. The approach was kept the same in the 2010 NBCC with new hazard values introduced in the 2015 NBCC. The hazard values in the 2015 NBCC are 17% to 28% higher for Vancouver and 24% to 15% lower for Ottawa relative to those in the 2010 NBCC within the 0.5 sec to 1.0 sec building period range.

The design and detailing requirements for reinforcement concrete buildings in CSA A23.3 went through a similar evolution. There were no seismic design requirements prior to CSA A23.3-1973 (CSA 1973), which was referenced in the 1975 NBCC. Ductile design and detailing requirements for seismic resistance were introduced for the first time in 1973, which remained the same until 1984. Significant improvements were made to the standard in 1984 (CSA 1984) with the introduction of capacity design requirements, protecting critical elements and preventing non-ductile failures. Three levels of seismic detailing were specified for the first time for: i) ductile response, ii) moderately ductile response, and iii) frame members that are not part of the seismic resisting system but “go for the ride” during seismic response. Critical elements in

ductile buildings were protected and non-ductile failure modes were prevented by increasing design to levels that are associated with the development of probable moment resistances in plastic hinges at 125% of the steel yield strength. The same capacity design concept was implemented in nominally ductile buildings using nominal capacities. The stringency of design depended on the design ductility demand selected in the 1985 NBCC, which made reference to CSA A23.3-1984. Hence, 1985 was taken as the "benchmark" year for significant improvements in seismic design of reinforced concrete buildings in Canada. The same year was adopted as the bench mark year in the Canadian Seismic Screening Manual (NRC 1992).

An extensive comparison of seismic demands and capacities of reinforced concrete frame buildings was performed as part of the current investigation to assess the significance of variations in building designs between 1985 and 2010. Static seismic base shears for the 2, 5 and 10-storey buildings used in the current investigation were calculated using Equivalent Static Force Procedure (ESFP). Figure 4.1 shows the evolution of seismic design base shear ratio (design base shear V / building weight used for base shear calculations W) assuming buildings in Vancouver have full ductility and those in Ottawa have moderate ductility. It was observed that the change in equivalent seismic base shear (based on the empirical code period) between 1985 and 2010 varied between 0.8 and 1.3 of the 1985 values for 10-storey and 2-storey moderately ductile buildings in Ottawa, respectively. The range was 1.2 and 1.8 of the 1985 values for 10-storey and 2-storey ductile buildings in Vancouver. However, this change in seismic shear demand did not translate into equivalent levels of change in member capacities in final building designs. The seismic load combinations changed from 1.25D+0.7(1.5L+1.5E) in 1985 to 1D+0.5L+1E starting in 1990, implying that the contribution of gravity loads to member design would be higher in 1985 and lower in the post 1990 codes. The changes in load factors may offset the effects of changes in seismic base shear on final designs. Where they don't, as in the case of the 10-storey building in Ottawa, they create higher design capacity with reduced seismic vulnerability. Furthermore, the concrete resistance factor, ϕ_c was 0.6 in CSA A23.3-1984, whereas it was increased to 0.65 in CSA A23.3-2004 (CSA 2004). This results in a nominal capacity that is closer to design resistance in newer buildings. The comparison implies that there is more reserve capacity in older buildings, even though the seismic design force levels at the time were generally lower. Therefore, the final structural designs of the three buildings considered are not expected to show significant variations between 1985 and 2010. Hence,

reinforced concrete frame buildings designed between 1985 and 2010 can be grouped together for the purpose of seismic vulnerability assessment within the ductility ranges considered in design.

4.2 Selection and Design of Buildings

Three regular frame buildings with 2-storey, 5-storey and 10-storey heights were selected for Ottawa, representing eastern Canadian seismicity, and for Vancouver, representing western Canadian seismicity. All the buildings consisted of moment resisting frames in both orthogonal directions with 5 bays in each direction, having a 7.0 m span length, resulting in a 35m by 35m square floor plan. Typical floor height of 4.0 m was used for each floor including the ground level. Figure 4.2 shows elevation view of the buildings. The design dead load included a superimposed dead load of 1.33 kPa consisting of floor finish, partition walls and mechanical/electrical fixtures, in addition to member self-weight. The live load was 2.4 kPa.

The buildings were designed based on the 2010 NBCC seismic requirements with the accompanying CSA Standard A23.3-04 "Design of Concrete Structures" used for proportioning and detailing of members. The equivalent static load approach was used to compute elastic seismic base shear (V_e). The buildings were designed for residential occupancy with an importance factor of I =1.0, on firm soil (Soil Class C). The fundamental period was computed by performing Eigen Value analysis through the use of SAP 2000 (CSI 2013a.) software with reduced section properties according to CSA A23.3-04. These dynamic fundamental periods were longer than those computed by the code-recommended empirical values by more than 150%. Therefore, the period values were taken as 1.5 times the values computed based on the empirical code equations for design. Uniform Hazard Spectra (UHS) values were used for design as prescribed in the 2010 NBCC. These corresponded to spectral accelerations (S_a) of 0.298g, 0.134g and 0.066g for 2-storey, 5-storey and 10-storey building in Ottawa and 0.618g, 0.320g and 0.204g for the buildings in Vancouver, respectively. The buildings in Ottawa consisted of moderately ductile frames designed with ductility related force modification factor R_d and over-strength related force modification factor R_o as 2.5 and 1.4, respectively. The buildings in Vancouver consisted of fully ductile frames, designed with R_d = 4.0 and R_o = 1.7. Concrete compressive strength, f'_c , was taken as 40 MPa for 2-storey and 10-storey buildings and 30 MPa for 5-storey building. The analyses were conducted in two stages. The initial buildings analyzed

had 30 MPa concrete. The buildings subsequently analyzed had 40 MPa. The variation of concrete strength in this rage did not affect building performance as member strength was the primary consideration in the analytical models. Rebar with 400 MPa yield strength was used as reinforcement for all members. The buildings were analysed and designed by using software ETABS (CSI 2008) with the load cases defined in NBCC (2010). Reinforcement obtained from the software was used along with seismic detailing implemented manually for complete member design. Table 4.1 provides the design details for each member. The buildings in Vancouver and Ottawa had the same member dimensions because of similar ratios of seismic demand to inelastic capacity in each city. This resulted in the same fundamental period for the same height buildings. Accordingly, the design fundamental periods for the two, five and ten-storey buildings were computed to be 0.54 sec, 1.06 sec and 1.79 sec, respectively. The effective fundamental periods computed using the Eigen Value solution were 1.08 sec, 2.04 sec, and 2,84 sec for the two, five and ten storey buildings, respectively.

4.3 Incremental dynamic analysis (IDA)

The present study focuses on developing fragility response of reinforced concrete frame structures in Canada with regular structural layout through incremental dynamic analysis (IDA). A set of 20 earthquake records were selected and IDA was employed to generate fragility curves. IDA was conducted for each seismic record with incrementally varying intensity levels, resulting in an IDA curve providing a relationship between earthquake intensity and a structural deformation quantity. In the current investigation the maximum inter-storey drift ratio, Θ_{max} , was used as a damage measure (DM) and 5% damped spectral acceleration was used as an intensity measure (IM) either at design period T_d or at effective period T_e obtained from dynamic analysis. Each earthquake record was scaled in such a way that the successive run would always be within 10% of the previous IM level. Hunt and fill algorithm was used to limit the number of runs while covering the entire range of structural performance (Vamvatsikos and Cornell 2004). Accordingly, the dynamic analysis was first conducted under a reduced earthquake intensity to correspond to a relatively low spectral acceleration of 0.005g to ensure elastic response. In the second analysis, when the spectral accelerations corresponded to T_e, the seismic record was amplified such that the increase in spectral increment was 0.05g with a step increment of 0.025g up to failure. The same approach was used for the IDA when seismic records were amplified

based on $S_a(T_d)$, except for the increase in increments, which was twice the incremental increase used earlier for $S_a(T_e)$. The structural failure was defined either by side-sway collapse (structural instability) or when the rate of change in deformations (the slope of the IDA curve) reached 20% of the initial effective elastic slope as also defined in FEMA 350 (FEMA 2000a). Side-sway collapse was defined as the point of dynamic instability when inter-storey drift increased without bound (Goulet et al. 2007). Figure 4.3 illustrates the definition of maximum drift capacity used in the current study. IDA was used to develop fragility response for different performance levels with associated limit states.

4.4 Modelling for Dynamic Analysis

IDA was conducted using software PERFORM-3D (CSI 2013) to perform nonlinear dynamic analysis and evaluate the inelastic performance of structural components. PERFORM-3D is specialized software for damage assessment, and is used by other researchers (Reyes and Chopra 2012, Ghodsi and Ruiz 2010; Zeynep Tuna 2012; Wen-Cheng Liao 2010; Michael W. Hopper 2009). Three-dimensional analytical models of the bare frame structures designed earlier were developed for dynamic analysis. The frame elements (beam and columns) were modeled to deform in double curvature with two symmetrical segments. Each segment consisted of an elastic beam element and a plastic hinge. Chord rotations were used to define the member end rotations. All beam and column elements had stiff end zones at the joints that represented the end portions built integrally with the adjoining members. The stiffness of these end zones was assigned a value equal to 10 times the member stiffness. Potential softening in beam-column joints was neglected in the analytical models as this was believed to be insignificant for the buildings considered.

Element stiffness was specified as per the requirements of CSA A23.3-04. Both beam and column rigidities were reduced to account for concrete cracking; and effective inertia, I_e, were assigned to the members. Hysteretic behaviour of potential plastic hinge regions was modelled by assigning a stiffness degrading model in PERFORM-3D. The software uses perfectly elasto-plastic hysteretic relations, modified for stiffness and strength degradation under reversed cyclic loading as illustrated in Fig. 4.4. The stiffness degradation is introduced through the "energy degradation factor (EDF)," which is the ratio of the area under an elasto-plastic to stiffness degrading hysteresis loops. In the current investigation, EDF was computed from experimental

observations. Tests of reinforced concrete elements conducted by Ozcebec and Saatcioglu (1987) were used for this purpose. It was found that well confined flexure-controlled elements showed behaviour that could be modelled with the use of EDF = 0.62 up to the yield point, and 0.56 thereafter. The same EDF values were used for both moderately ductile and fully ductile elements. The sensitivity analysis conducted by authors indicated that minor variations in EDF did not result in significant changes in dynamic response (Al Mamun and Saatcioglu 2016)[1].

The envelope curves for the hysteretic models were defined in terms of nominal moment resistances and corresponding chord rotations. This was done according to the ASCE 41-13 (ASCE 2014) guidelines. The yield moment (M_Y) and chord rotation at yield (Θ_Y) were calculated for each element from sectional analysis. The post yield stiffness was defined as strain hardening stiffness with 3% and 4% of the effective elastic stiffness for beam and column elements, respectively up to ultimate capacity (M_U). The ultimate capacity depended on the ductility ratios adopted for moderately ductile and fully ductile structures. The ductility related force modification factor (R_d) values, specified in the 2010 NBCC were used as 2.5 and 4.0 for moderately ductile and fully ductile buildings. These ductility ratios were also reported to have been observed during previous column tests (Park et al. 1982, Beng Ghee et al. 1981, Zahn et al. 1986, Saatcioglu and Ozcebec 1989), though some researchers showed that well confined concrete column could achieve ductility ratios higher than 4.0 irrespective of the level of axial compression. The ultimate rotational capacity (Θ_U) was defined in the current investigation as 2.5 and 4.0 times the yield rotation (Θ_Y) for nominally and fully ductile elements as the onset of strength decay points. The degradation slope of moment-rotation envelope was computed to be the same as that recommended by ASCE 41-13. The ASCE 41-13 ultimate plastic chord rotation (Θ_U) and the residual moment capacity (M_R) depend on the level of axial compression and the confinement steel area ratio. The linear descending branch of the envelop curve continued until the residual moment capacity (M_R) as defined in ASCE41-13 as a ratio of the ultimate moment capacity (M_U). This ratio for the beams was 0.2 and varied for columns between 0.2 and 0 as a function of axial load. Figure 4.5 shows the details of moment-rotation envelope for members having the yield capacity, but different levels of ductility. Further details of analytical modelling techniques employed are reported elsewhere (Al Mamun and Saatcioglu 2016).

[1] Al Mamun and Saatcioglu. 2016. Seismic performance evaluation of RC frame structures using PERFORM-3D. Submitted for publication in *Earthquake Spectra*, the Journal of EERI.

The members were modelled to behave elastically in shear. This is consistent with CSA A23.3-04, which requires higher shear capacity than that corresponding to flexural capacity to prevent brittle shear failure while promoting ductile flexural response. This is a preferred performance observed by researchers (Priestley et al. 1994). Ozcebec and Saatcioglu (1989) experimentally observed that deflections due to shear in flexure-dominant members accounted for 22% of the total deflection, even though local shear deformations within the plastic hinge could be as high as 83% of the hinging region deformations. The contribution of shear to total member deflection was observed to decrease (forming 8% of total deflection in one column test) as inelastic deformations increased in flexure (Saatcioglu and Ozcebec 1989). Linear elastic shear properties of structural elements were also used by previous researches (Borzi et al. 2008; Inel and Ozmen 2006; Liel et al. 2011).

4.5 Selection of Earthquake Records

Synthetic earthquake records, developed for Ottawa and Vancouver, with 2% probability of exceedance in 50 years were selected for the development of the fragility curves. These records were compatible with the Uniform Hazard Spectra (UHS) specified in NBCC (2010), and were developed by Atkinson (2009). The records were modified as suggested by Atkinson (2009) to match the UHS for the period range of interest. The design period of the buildings considered in the current investigation varied between 0.5 and 2.0 seconds, and this range was used to modify the records. A set of twenty records was selected for buildings in Ottawa, and another set of twenty records was selected for buildings in Vancouver. Each set of records reflected two different magnitudes and two different distances, resulting in four different magnitude-distance combinations. 5 records were selected from each magnitude level and distance category. For Ottawa, M6 earthquakes were selected with epicentral distances of 10-15 km and 20-30 km; and M7 earthquakes were selected with epicentral distances of 15-25km and 50-100 km. The durations of records were 5, 7, 17 and 20 seconds, respectively. For Vancouver, M6.5 earthquake was selected with epicentral distances of 10-15 km and 20-30 km; and M7.5 earthquake was selected with epicentral distances of 15-25 km and 50-100 km. The duration of records was 10, 15, 65 and 57 seconds, respectively. Acceleration response spectrum were generated for 5% of critical damping and for Soil Type C. Figure 4.6 shows the comparison of response spectra for mean seismic records with the UHS of NBCC (2010) for Ottawa and Vancouver.

Fragility analysis required IDA under different intensity of earthquakes. This necessitated the amplification of seismic records. Though it is common to amplify seismic records based on the spectral acceleration at fundamental period (Vamvatsikos and Cornell 2002), researchers used several different approaches to amplify seismic records. Jeong et al. (2012) used effective fundamental period based on pushover analysis. Kircil and Polat (2006) used elastic fundamental period as the reference point. In the present study seismic records were scaled to match the target spectral values obtained by the hunt and fill algorithm discussed earlier to represent different earthquake intensities. This scaling was done using two spectral values as the basis, first using the spectral acceleration that corresponded to the code defined design period (T_d), and secondly using the value corresponded to the effective period computed by dynamic analysis using cracked (effective) moment of inertia, T_e. The use of two sets of scaling resulted in two sets of fragility curves as discussed in the following paragraphs.

For each target spectral acceleration, seismic record was multiplied by a factor equal to $S_{a,Target}/S_a(T_d)$ or $S_{a,Target}/S_a(T_e)$, where $S_{a,Target}$ is the target spectral acceleration, $S_a(T_d)$ is spectral acceleration at design period (T_d) and $S_a(T_e)$ is the spectral acceleration at effective period (T_e). The amplification procedure was validated against the spectra of scaled records, where the spectra were computed using software PRISM (2011). In all cases the amplified record was able to generate spectral values that matched $S_{a,Target}$. This is shown Fig. 4.7. The scaled records were then used to perform incremental dynamic analysis (IDA).

4.6 Limit States

The fragility curves were developed for different levels of performance. Commonly accepted performance levels were selected (ASCE 41 2013; FEMA 356 2000b; ACI 374.2R-13 2013). They consisted of; i) Immediate Occupancy (IO), ii) Life Safety (LS), and iii) Collapse Prevention (CP). Inter-storey drift ratio was used as a damage indicator, defining the limit state for each performance level. The inter-storey drift limits were adopted from previous standards/recommendations as 1% and 2% for IO and LS performance levels (ASCE 41-13, FEMA 356, ACI 374.2R-13). The CP performance limit state depended on the onset of strength decay, which in turn depended on the ductility capacity of structural elements. Jeong et al. (2012) used FEMA 356 limit of 4% inter-storey drift, Akkar et al. (2005) used 75% of the median of maximum inter-storey drifts from the records considered, Erberik (2008) used 75% of the mean

of maximum inter-storey drifts, Kircil and Polat (2006) used 5% probability of attaining collapse with 95% confidence level, and Ellingwood et al. (2007) used the median of maximum inter-storey drift ratio. In the current investigation CP limit state was defined as the median of the maximum inter-storey drift ratio attained on the IDA curve.

The IO limit represents very limited structural damage, where the force resisting system nearly retains the pre-earthquake strength and stiffness. Since the risk of fatal injury is very low, the building can be reoccupied immediately. Various approaches were used by researchers to identify the IO limit state drift. Jeong et al (2012) used the inter-storey drift corresponding to the first yield of a structural member, Akkar et al. (2005) used the global yield drift ratio, and Kircil and Polat (2006) used the maximum inter-storey drift ratio at 5% probability of yielding with 95% confidence level. Erberik (2008) used softening index (SI) proposed by DiPasquale and Cakmak (1987) as serviceability limit state, analogous to IO. SI was defined as:

$$\text{SI} = 1 - \frac{T_e}{T_j} \tag{4.1}$$

where T_j is the effective period at intermediate spectral acceleration. SI = 0.20 was attained at IO limit state when $T_j = 1.25\ T_e$. This measure of performance was believed to be more reliable than using 1% drift, since SI provided inter-storey drift ratio for the IO performance level corresponding to seismic records.

4.7 Development of Fragility Relationships

The probability of drift demand (D) at a given Intensity, $S_a(T_e)$ or $S_a(T_d)$, was calculated with the method adopted by Cornell et al. (2002). The conditional median of drift demand, D_M, was expressed as a power function, $D_M = a[S_a(T_e)]^b\varepsilon$ or $D_M = a[S_a(T_d)]^b\varepsilon$; where a and b were regression coefficients and ε was lognormal random variable (Ramamoorthy et al. 2006). It was assumed that the demand had lognormal probability distribution at a given spectral acceleration with the median lognormal random variable equal to unity (ε = 1). Logarithmic standard deviation of lognormal random variable ($\sigma_{ln\varepsilon}$) was equal to the standard deviation of log of demand (σ_D) (Jeong et al. 2012). The regression coefficient of the power function was calculated by linear regression in logarithmic space of the 'cloud' response using least square method. The standard deviation of log of demand (σ_D) was assumed constant with variation of spectral

acceleration, $S_a(T_e)$ or $S_a(T_d)$. The value of regression coefficient a and b and standard deviation of log of demand (σ_D) are shown in Fig. 4.8 for Ottawa and Vancouver buildings for which the analyses were performed with scaled seismic records based on $S_a(T_e)$ or $S_a(T_d)$. The dispersion for all limit states (σ_{LS}) was considered as 0.3 (Jeong and Elnashai 2007) and the uncertainty in analytical modeling (σ_M) was taken as 0.2 with 90% confidence that the analytical model findings were within 30% of actual value (Ellingwood et al. 2007). The effects of aleatoric and epistemic uncertainty were calculated according to the equation suggested by Zareian and Krawinkler (2007), as shown below:

$$\sigma_{EQU} = \sqrt{\sigma_{LS}^2 + \sigma_M^2} \quad (4.2)$$

where σ_{EQU} is the uncertainty component associated with aleatoric and epistemic effect in demand estimation, which was found to be 0.36 in this study. The total uncertainty in finding the probability of collapse, σ_{TOT} , was:

$$\sigma_{TOT} = \sqrt{\sigma_{EQU}^2 + \sigma_D^2} \quad (4.3)$$

The above computed parameters are then substituted into the equation shown below to find the conditional probability of exceeding a limit state at a given intensity, $S_a(T_e)$ or $S_a(T_d)$.

$$P_{LS} = 1 - \phi\left(\frac{lnD_C - lnD_M}{\sigma_{TOT}}\right) \quad (4.4)$$

where, D_C is median drift capacity specified for a limit state. The fragility curves are then presented as plots of P_{LS} versus $S_a(T_e)$ or $S_a(T_d)$. They are shown in Fig. 4.9 and Fig. 4.10 for 2, 5, and 10-storey frame buildings located in Ottawa and Vancouver.

4.8 Seismic Performance Evaluation

The results of the IDA analysis indicated different levels of inelasticity and sequence of hinging among frame members at different performance levels. The yielding of beams was observed prior to developing the IO performance level. The beam yielding occurred at lower floors first, followed by the yielding of the first-storey columns. Upon the yielding of the columns, inter-storey drift levels increased considerably as buildings approached the LS performance level. At LS performance level, more hinging was observed in buildings located in

Ottawa than those in Vancouver. Almost all the first-storey columns hinged at LS level, with increased plastic hinging in beams at upper floors.

The CP performance level was associated with significant plastification of members, followed by the failure of individual elements. In the 2-storey buildings, initial hinges formed in the 2nd storey beams, followed by the 1st storey columns. The structure reached collapse due to the failure of the 2nd storey beams, all in the direction of seismic loading, followed by the 1st storey columns. In the 5-storey buildings, hinges formed in the exterior and interior beams at the 3rd storey level, which extended to the 4th, 5th and 2nd floors. Column hinging occurred at the 1st storey level, followed by the columns at the 3rd floor. Because the columns of the first 2 floors had higher capacities, the 2nd floor column hinging followed the hinging of columns at the 3rd to 4th floors. The structure reached collapse level performance due to the failure of the first-storey columns at the base, following the failures of beams at the 3rd, 4th, 5th and 2nd floor levels. In the 10-storey buildings, the hinges formed in the 2nd floor interior beams, and extended to the 8th floor interior beams, followed by the exterior beams. Subsequently, the 1st storey columns hinged at their base, followed by the hinging of the columns at the 3rd floor. The same building under high intensity earthquakes showed failure of both interior and exterior beams between the 2nd and 7th floors, followed by the failure of the 3rd storey columns.

The yield rotations (Θ_Y) in members were computed to be similar for the same height buildings in Ottawa and Vancouver. However, the member ductility was different depending on design ductility demands. The buildings in Ottawa were designed and detailed for ultimate chord rotations of $\Theta_U = 2.5\Theta_Y$, whereas those in Vancouver were designed and detailed for $\Theta_U = 4.0\Theta_Y$. This implies that the onset of strength decay in members of the Ottawa buildings started at lower rotational values in comparison to those in Vancouver. Therefore, the maximum inter-storey drift of the Ottawa buildings at the CP performance level were lower than those for Vancouver buildings. This is shown in Table 4.2 for both sets of analyses based on the two approaches used for scaling, i.e., $S_a(T_e)$ and $S_a(T_d)$.

The fragility response of structures shown in Fig. 4.9 and Fig. 4.10 indicate a similar trend among the buildings in Ottawa and Vancouver, i.e., 10-storey buildings reached the CP level of performance at lower levels of spectral accelerations because these buildings, with longer periods, were designed for lower spectral accelerations. The 2-storey buildings showed CP level

of performance at higher spectral values. Limit state probabilities at effective period and design period are given in Table 4.2 for two sets of fragility analysis, developed either with $S_a(T_e)$ established based on the building periods obtained from dynamic analysis, which incorporate the effect of structural softening and period elongation during response, or $S_a(T_d)$ established based on the NBCC-recommended building periods. The fragility curves developed based on $S_a(T_e)$ indicated that, on average, the probability of exceeding the IO performance level was 17% for buildings in Ottawa at the design earthquake intensity, whereas the buildings in Vancouver had 93% probability of exceeding the same level of performance. At the same intensity, the buildings in Ottawa developed no probability of exceeding the LS performance level, while those in Vancouver showed 43% of exceeding the same level of performance. The probability of exceeding the CP performance level at design intensity in Ottawa was 0%, whereas in Vancouver it was 6%. The fragility curves depict a trend of increasing probabilities of exceeding performance limits with increasing number of stories; except for 5-storey building in Ottawa at IO performance level, which was slightly lower than that for 2-storey building. Table 4.1 also shows inter-storey drift ratios (Θ_{max}) at the CP performance level. It is noteworthy that the margin between the LS and CP performance levels is higher for buildings in Vancouver, relative to those in Ottawa. Similar response of building performance was obtained from the fragility curves for $S_a(T_d)$; buildings in Ottawa had less probability of exceeding limit states in comparison with buildings in Vancouver. The comparison of building performance as obtained from the fragility curves for $S_a(T_e)$ and $S_a(T_d)$ indicate similar probabilities of exceeding LS performance level in Ottawa. The same is true for the CP performance level for cities. The code specified T_d incorporates potential stiffening effects of non-structural members that may be present in the building. In reality, the structural period falls between the code specified value of T_d and the dynamic period computed based on a model that consists of structural elements only (T_e). However, the probabilities obtained from the fragility curves developed on the basis of $S_a(T_e)$ and $S_a(T_d)$ yield similar probabilities of exceedance for the collapse performance level.

To observe the effect of ductility, additional fragility curves were developed for 2-storey and 5-storey frame buildings in Ottawa when the buildings were designed for the same seismic force level associated with moderate ductility but having full ductility (ductility=4.0). This resulted in higher inter-storey drift ratios at the CP performance level. This set of curves is shown in Fig. 4.11, indicating the same probabilities for the IO and LS performance levels, but lower

probabilities of exceedance at the CP performance level as compared to those for the moderately ductile buildings.

The effect of using softening index (SI) on inter-storey drift ratio for IO performance level was also investigated. The results showed that, using SI resulted in an average of 0.40% and 1.25% inter-storey drift ratios for buildings in Ottawa and Vancouver, respectively, in comparison with the 1% drift ratio recommended by the existing standards (ASCE 41-13, FEMA 356, ACI 374.2R-13). This observation implies that the Ottawa structures yielded at a lower rotation than those in Vancouver.

4.9 Summary and Conclusions

Fragility curves were developed for 2-storey, 5-storey and 10-storey buildings in Ottawa and Vancouver for vulnerability assessment of reinforced concrete frame buildings with regular structural layouts. The earthquake records were scaled based on spectral accelerations at effective period (T_e) and design period (T_d) of structures. It was found that at design period spectral acceleration, the Ottawa buildings showed less probability of exceeding limit state performance levels when compared with those for Vancouver. The Buildings in Vancouver, designed after the 1985 threshold year showed on average 43% probability of exceeding the NBCC target performance level of life safety at design earthquake, whereas the same performance level is exceeded with an average probability of 0% in buildings located in Ottawa. The buildings in Vancouver showed higher inter-storey drift at collapse, with 6% probability of exceedance than those in Ottawa, which showed no probability of exceedance. The fragility curves based on $S_a(T_d)$ did not show a significant difference in probabilities of exceeding the CP performance levels when compared with those developed based on $S_a(T_e)$. Because the design period of T_d reflects the as-built conditions of the buildings incorporating the possible stiffening effects of non-structural elements, it may be more appropriate to use them for seismic vulnerability assessment, with the fragility curves based on T_e reflecting possible softening of buildings during response.

The fragility curves developed in this investigation were all generated using buildings with specific heights, designed based on the 2010 NBCC using moderately ductile and fully ductile design requirements for Ottawa and Vancouver, respectively. While the same ductility capacities

may be attained in buildings designed between 1985 and 2010, the design force levels may show some fluctuations during this period. Therefore, the use the same fragility curves for buildings designed by editions of NBCC other than the 2010 version requires judgement with respect to the effects of variations in design force levels.

4.10 References for Chapter 4

Akkar, S., Susuoglu, H., and Yakut, A. 2005. Displacement-Based Fragility Functions for Low- and Mid-rise Ordinary Concrete Buildings. Earthquake Spectra. 21(4):901-927. doi: http://dx.doi.org/10.1193/1.2084232

American Concrete Institute (ACI). 2013. Guide for testing reinforced concrete structural elements under slowly applied simulated seismic loads. ACI committee 374. ACI 374.2R-13. Michigan, United States.

American Society of Civil Engineers (ASCE). 2014. Seismic evaluation and retrofit of existing buildings. ASCE/SEI 41-13. Virginia, United States.

Atkinson, G.M. 2009. Earthquake time histories compatible with the 2005 National building code of Canada uniform hard spectrum. Canadian Journal of Civil Engineering. **36**(6):991-1000. doi: 10.1139/L09-044

Beng Ghee, A., Priestley, M.J.N., and Park, R. 1981. Ductility of reinforced concrete bridge piers under seismic loading. Report 81-3, Department of Civil Engineering, University of Canterbury, New Zealand..

Borzi, B., Pinho, R., and Crowley, H. 2008. Simplified pushover-based vulnerability analysis for large-scale assessment of RC buildings. Engineering Structures. **30**(3):804-820. doi:10.1016/j.engstruct.2007.05.021

Canadian Standards Association (CSA). 1973. Design of concrete structures. CSA standards update service. CSA A23.3-1973. Mississauga, Canada.

Canadian Standards Association (CSA). 1984. Design of concrete structures. CSA standards update service. CSA A23.3-1984. Mississauga, Canada.

Canadian Standards Association (CSA). 2004. Design of concrete structures. CSA standards update service. CSA A23.3-04. Mississauga, Canada.

Computers and Structures, Inc (CSI). 2008. ETABS. Nonlinear Version 9.5.0. Computers and Structures, Inc. Berkeley, CA.

Computers and Structures, Inc. (CSI). 2013. PERFORM-3D. Version 5.0.1. Computers and Structures, Inc. Berkeley, CA.

Computers and Structures, Inc (CSI), 2013a. SAP2000. Ultimate 16.0.0. Computers and Structures, Inc. Berkeley, CA.

Cornell, CA., Jalayer, F., Hamburger, RO., and Foutch, D.A. 2002. Probabilistic basis for 2000 SAC Federal Emergency Management Agency steel moment frame guidelines. Journal of Structural Engineering. Volume 128, Special Issue: Steel moment frames after Northridge-PartII. Pages: 526-533. doi: 10.1061/(ASCE)0733-9445(2002)

DiPasquale, E., and Cakmak A.S. 1987. Detection and assessment of seismic structural damage. Technical Report NCEER-87-0015. National Center for Earthquake Engineering Research. State University of New York.

Ellingwood, B.R., Celik, O.C., and Kinali, K. 2007. Fragility assessment of building structural systems in Mid-America. Earthquake Engineering and Structural Dynamics. **36**(13):1935-1952. doi: 10.1002/eqe.693

Erberik, M.A. 2008. Fragility-based assessment of typical mid-rise and low-rise RC buildings in Turkey. Engineering Structures. **30**(5):1360-1374. doi:10.1016/j.engstruct.2007.07.016

Federal Emergency Management Agency (FEMA). 2000. Prestandard and commentary for the seismic rehabilitation of buildings. FEMA 356. Washington, D.C.

Federal Emergency Management Agency (FEMA). 2000a. Recommended seismic design criteria for new steel moment-frame buildings. SAC Joint Venture. FEMA 350. Washington, D.C.

Geological Survey of Canada (GSC). 2016. Earthquake Zones in Canada. Available from http://www.earthquakescanada.nrcan.gc.ca/zones/index-en.php (Last accessed 12 May 2016)

Ghodsi T., Ruiz J.A.F. 2010. Pacific earthquake engineering research/seismic safety commission tall building design case study 2. The Structural Design of Tall and Special Buildings. 19(1-2):197–256. doi: 10.1002/tal.542

Goulet, C.A., Haselton, C.B., Mitrani-Reiser, J., Beck,, J.L., Deierlein, G.G., Porter, K.A., and Stewart, J.P. 2007. Evaluation of the seismic performance of a code-conforming reinforced-concrete frame building—from seismic hazard to collapse safety and economic losses. Earthquake Engineering & Structural Dynamics. **36**(13):1973–1997. doi: 10.1002/eqe.694

Hopper, M. W. 2009. Analytical models for the nonlinear seismic response of reinforced concrete frames. M.Sc. Thesis. Department of Architectural Engineering. The Pennsylvania State University. Pennsylvania.

Inel, M., and Ozmen, H.B. 2006. Effects of plastic hinge properties in nonlinear analysis of reinforced concrete buildings. Engineering Structures. 28(11):1494-1502. doi:10.1016/j.engstruct.2006.01.017

Jeong, S.H., and Elnashai, A.S. 2007. Probabilistic fragility analysis parameterized by fundamental response quantities. Engineering Structures. 29(6):11238-1251. doi:10.1016/j.engstruct.2006.06.026

Jeong, S.H., Mwafy, A.M., Elnashai, A.S. 2012. Probabilistic seismic performance assessment of code-compliant multi-storey RC buildings. Engineering Structures. 34:527-537. doi:10.1016/j.engstruct.2011.10.019

Kircil, M.S., Polat, Z. 2006. Fragility analysis of mid-rise R/C frame buildings. Engineering Structures. **28**(9):1335-1345. doi:10.1016/j.engstruct.2006.01.004

Liao, W. C. 2010. Performance-based plastic design of earthquake resistant reinforced concrete moment frames. Ph.D. Thesis. Department of Civil Engineering, The University of Michigan.

Liel, A.B., Haselton C.B., and Deierlein, G.G. 2011. Seismic collapse safety of reinforced concrete buildings. II: Comparative assessment of nonductile and ductile moment frames. Journal of the Structural Engineering. **137**(4):492-502. doi: 10.1061/(ASCE)ST.1943-541X.0000275

Mitchell, D., Paultre, P., Tinawi, R., Saatcioglu, M., Tremblay, R., Elwood, K., Adams, J., and DeVall, R. 2010. Evolution of seismic design provisions in the national building code of Canada. Canadian Journal of Civil Engineering, **37**(9): 1157-1170 (2010). doi:10.1139/L10-054

National building code of Canada (NBCC). 1953. National Research Council of Canada. Ottawa, Canada.

National building code of Canada (NBCC). 1965. National Research Council of Canada. Ottawa, Canada.

National building code of Canada (NBCC). 1970. National Research Council of Canada. Ottawa, Canada.

National building code of Canada (NBCC). 1975. National Research Council of Canada. Ottawa, Canada.

National building code of Canada (NBCC). 1980. National Research Council of Canada. Ottawa, Canada.

National building code of Canada (NBCC). 1985. National Research Council of Canada. Ottawa, Canada.

National building code of Canada (NBCC). 1990. National Research Council of Canada. Ottawa, Canada.

National building code of Canada (NBCC). 2005. National Research Council of Canada. Ottawa, Canada.

National building code of Canada (NBCC). 2010. National Research Council of Canada. Ottawa, Canada.

National building code of Canada (NBCC). 2010. National Research Council of Canada. Ottawa, Canada.

National Research Council of Canada (NRCC). 1993. Manual for Screening of Buildings for Seismic Investigation. ISBN 0-660-15381-5. NRCC 36943. Ottawa, Canada.

Ozcebe, G., and Saatcioglu, M. (1987). Confinement of concrete columns for seismic loading. ACI Structural Journal. **84**(4):308-315.

Ozcebe, G., and Saatcioglu, M. (1989). Hysteretic shear model for reinforced concrete members. Journal of the Structural Engineering, ASCE. **115**(1):132-148. doi: 10.1061/(ASCE)0733-9445(1989)115:1(132)

Park, R., Priestley, M.J.N., and Gill, W.D. (1982). Ductility of square-confined concrete columns. Journal of the Structural Engineering, ASCE. **108**(4):929-950.

Priestley, M., Verma, R., and Xiao, Y. (1994). Seismic Shear Strength of Reinforced Concrete Columns. Journal of the Structural Engineering, ASCE. **120**(8):2310–2329. doi: 10.1061/(ASCE)0733-9445(1994)120:8(2310)

PRISM (2011). Version 1.1. Earthquake Engineering Research Group. Department of Architectural engineering, INHA University, South Korea.

Ramamoorthy, S., Gardoni, P., and Bracc, J. (2006). Probabilistic Demand Models and Fragility Curves for Reinforced Concrete Frames. Journal of the Structural Engineering, ASCE. **132**(10):1563–1572. doi:10.1061/(ASCE)0733-9445(2006)

Reyes, JC., and Chopra, AK. 2012. Modal pushover-based scaling of two components of ground motion records for nonlinear RHA of structures. Earthquake Spectra. August 2012. 28(3):1243-1267. doi: http://dx.doi.org/10.1193/1.4000069

Saatcioglu, M., and Ozcebe, G. 1989. Response of reinforced concrete columns to simulated seismic loading. ACI Structural Journal. 86(1):3-12.

Tuna Z. 2012. Seismic Performance, Modeling, and Failure Assessment of Reinforced Concrete Shear Wall Buildings. Ph.D. Thesis. Department of Civil Engineering, University of California. Los Angeles.

Vamvatsikos, D., and Cornell, CA. 2002. Incremental dynamic analysis. Earthquake Engineering & Structural Dynamics. 31(3):491-514. doi: 10.1002/eqe.141

Vamvatsikos, D., and Cornell, C.A. 2004. Applied incremental dynamic analysis. Earthquake Spectra. **20**(2):523-553. doi: 10.1193/1.1737737

Zahn, F.A., Park, R., and Priestley, M.J.N. 1986. Design of reinforced concrete bridge columns for strength and ductility, Report 86-7, Department of Civil Engineering, University of Canterbury, New Zealand.

Zareian, F., and Krawinkler, H. 2007. Assessment of probability of collapse and design for collapse safety. Earthquake Engineering and Structural Dynamics. **36**(13):1901-1914. doi: 10.1002/eqe.702

4.11 Tables and Figures

Table 4.1 Structural member details of 2, 5, 10-storey structures.

	2 Storey			5 Storey		10 Storey		
	Ottawa and Vancouver			Ottawa and Vancouver			Ottawa	Vancouver
	Size	Rebar		Size	Rebar	Size	Rebar	Rebar
Corner Column 1-Top	300X300	8-20M		300X300	8-20M	350X350	4-25M+4-15M	4-25M+4-15M
Ext Column 1-2	300X300	4-30M		300X300	4-30M	350X350	16-20M	4-30M+8-20M
Ext Column 3-Top	-	-		300X300	4-25M	350X350	4-25M+4-15M	8-25M
Int-1 Column 1-2	325X325	4-20M+4-15M		450X450	12-25M	500X500	12-30M+8-20M	12-30M+8-25M
Int-1 Column 3-5	-	-		450X450	4-25M+4-20M	500X500	8-25M+8-20M	8-30M+8-25M
Int-1 Column 6-10	-	-			-	500X500	4-25M+4-15M	4-25M+4-20M
Int-2 Column 1-2	325X325	4-20M+4-15M		450X450	4-30M+8-20M	500X500	12-30M+8-20M	12-30M+8-20M
Int-2 Column 3-5	-	-		450X450	4-30M	500X500	8-25M+8-15M	12-25M+8-20M
Int-2 Column 6-10	-	-			-	500X500	4-25M+4-15M	4-25M+4-20M
Int-3 Column 1-2	325X325	4-20M+4-15M		450X450	4-25M+8-20M	500X500	8-30M+8-25M	12-30M+8-20M
Int-3 Column 3-5	-	-		450X450	8-20M	500X500	4-25M+8-20M	12-25M+4-20M
Int-3 Column 6-10	-	-			-	500X500	4-25M+4-15M	4-25M+4-20M
Ext Beam Top	300X500	3-20M		300X500	3-20M	350X500	3-20M	3-20M
Ext Beam Bottom	300X500	2-20M		300X500	2-20M	350X500	2-20M	2-20M
		Ottawa	Vancouver					
Int Beam 1-5 Top	300X500	4-20M	4-20M	300X500	3-25M	350X500	4-25M	4-25M
Int Beam 1-5 Bottom	300X500	3-20M	4-20M	300X500	2-25M	350X500	2-25M	4-25M
Int Beam 6-10 Top	-	-	-	-	-	350X500	3-25M	3-25M
Int Beam 6-10 Bottom	-	-	-	-	-	350X500	3-20M	3-25M

Table 4.2 Comparison of limit state probabilities of 2, 5, 10-storey structures.

							Fragility Based on $S_a(T_d)$			Fragility Based on $S_a(T_e)$		
							Prob. of Exceedance at $S_a(T_d)$			Prob. of Exceedance at $S_a(T_e)$		
Building Height	**City**	**T_d, sec**	**T_e, sec**	**$S_a(T_d)$, g**	**$S_a(T_e)$, g**	**Θ_{max} (%)**	**IO (%)**	**LS (%)**	**CP (%)**	**IO (%)**	**LS (%)**	**CP (%)**
10-Storey	Ottawa	1.79	2.84	0.07	0.05	2.44	68	2	0	26	1	0
5-Storey	Ottawa	1.06	2.04	0.13	0.05	2.94	58	0	0	10	0	0
2-Storey	Ottawa	0.54	1.08	0.30	0.13	3.92	47	2	0	14	0	0
10-Storey	Vancouver	1.79	2.84	0.20	0.17	3.07	52	15	7	95	48	14
5-Storey	Vancouver	1.06	2.04	0.32	0.17	3.91	67	15	2	93	42	3
2-Storey	Vancouver	0.54	1.08	0.62	0.32	3.99	87	36	9	92	38	2

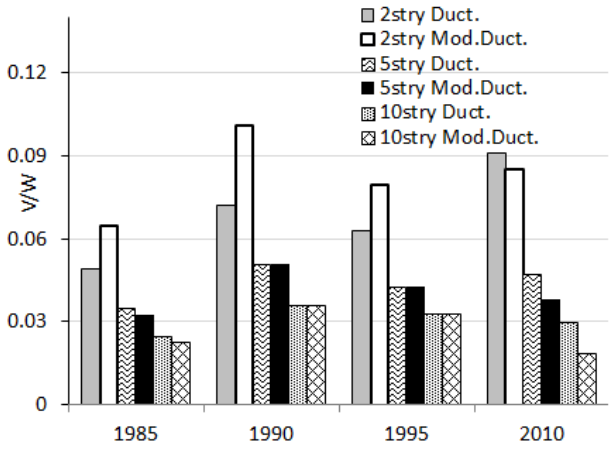

Fig 4.1 Evolution of seismic design base shear ratio of 2, 5, 10-storey structures

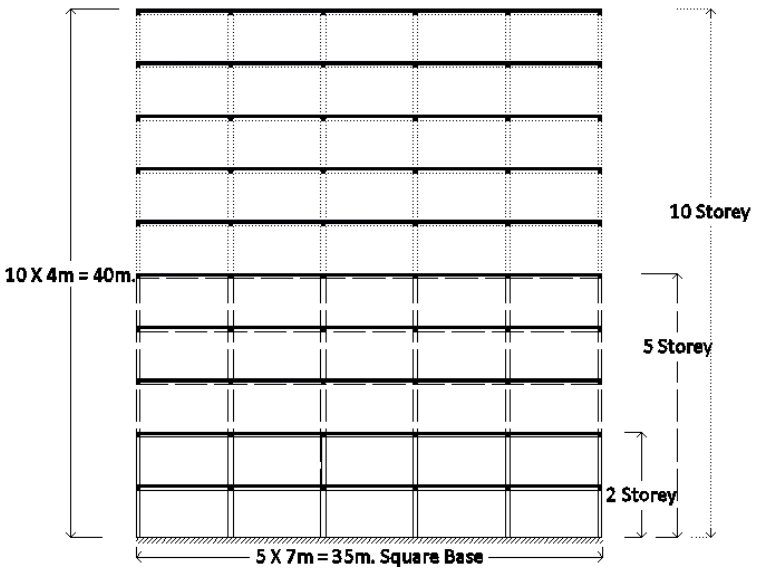

Fig 4.2 Elevation view of the buildings

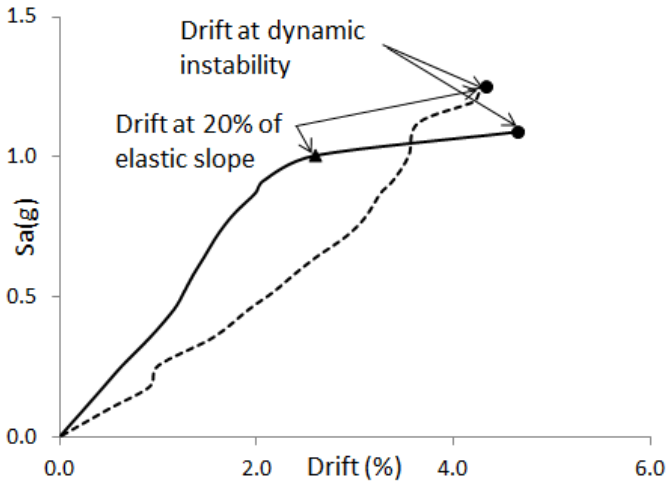

Fig 4.3 Maximum drift capacity on IDA Curve

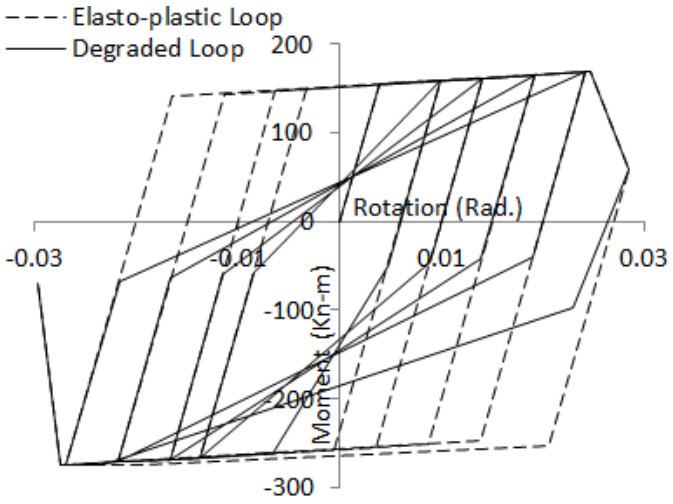

Fig 4.4 Effect of EDF on a Moment vs Total Chord Rotation hysteresis loop area in PERFORM-3D

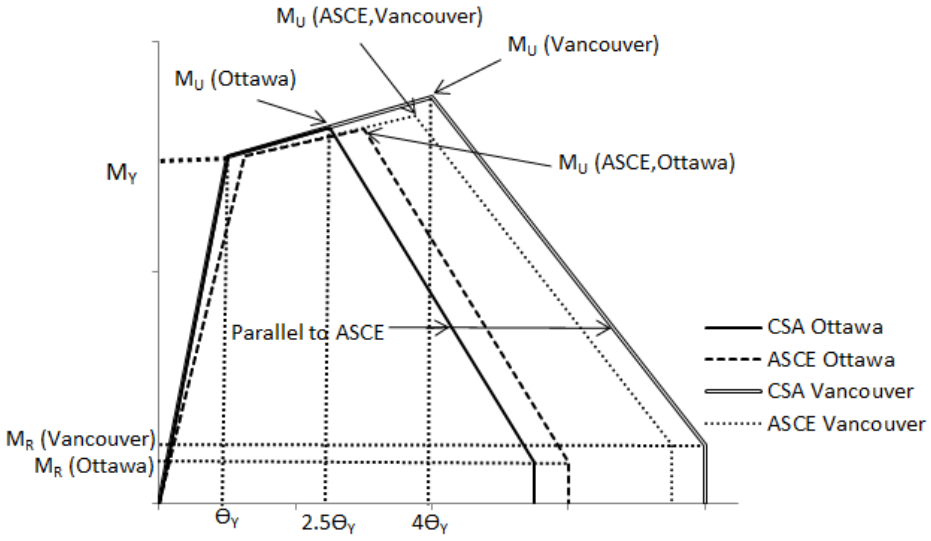

Fig 4.5 Typical moment-rotation envelope curve for same yield capacity member

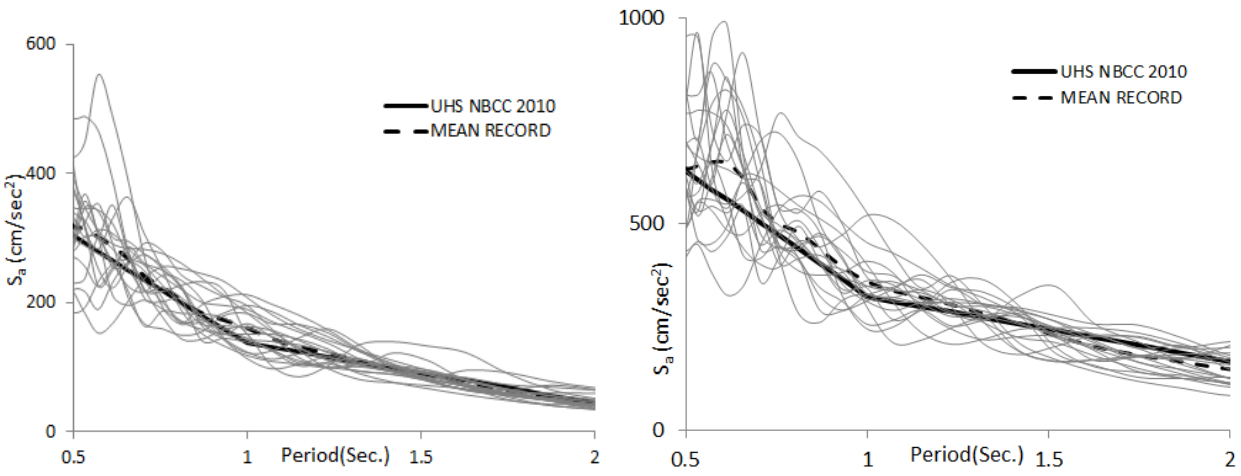

(a) (b)

Fig 4.6 Comparison of mean spectral acceleration of seismic records with NBCC (2010) UHS for (a) Eastern Canada (Ottawa) and (b) Western Canada (Vancouver)

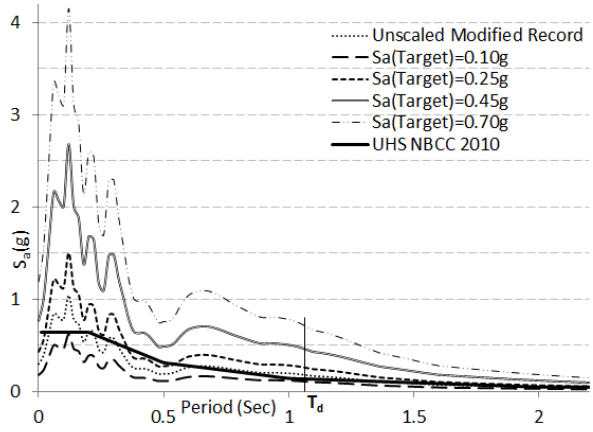

Fig 4.7 Spectral acceleration for single record amplified based on $S_a(T_d)$

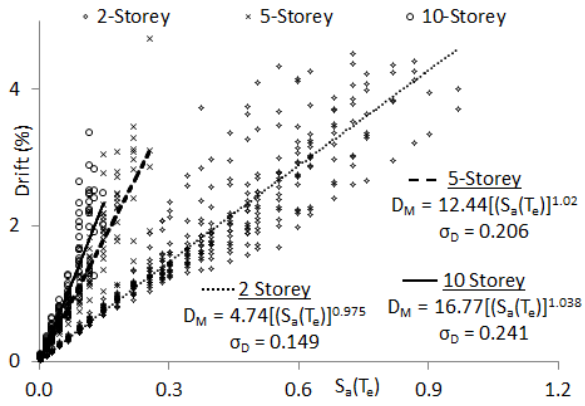

(a) Eastern Canada (Ottawa) with amplification seismic records based on $S_a(T_e)$

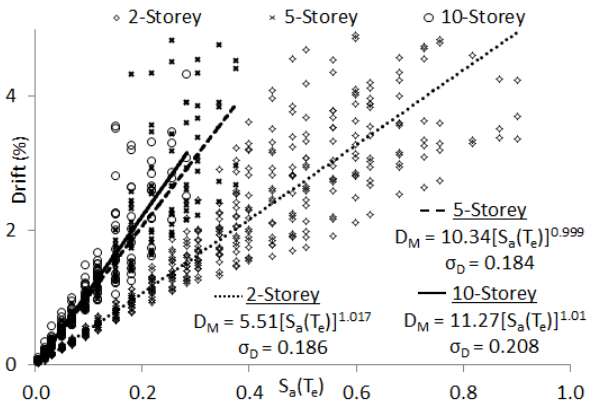

(b) Western Canada (Vancouver) with amplification seismic records based on $S_a(T_e)$

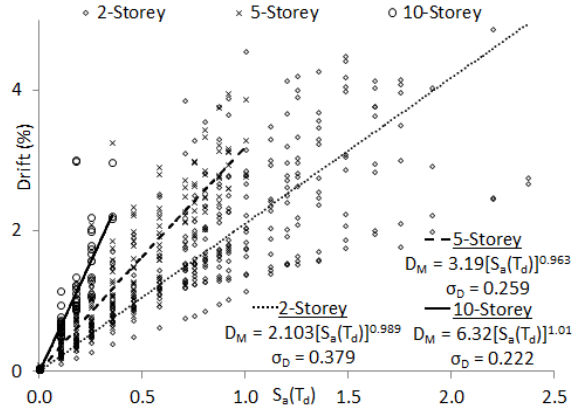

(c) Eastern Canada (Ottawa) with amplification seismic records based on $S_a(T_d)$

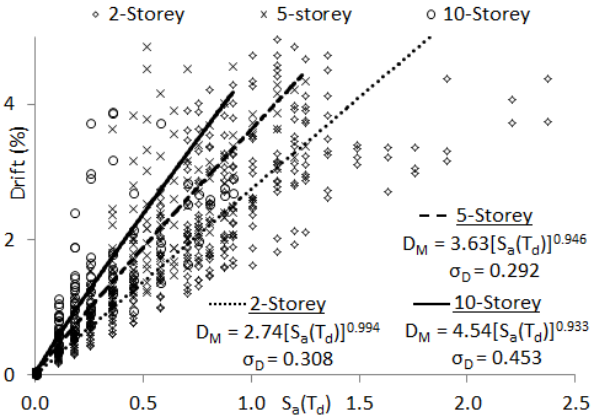

(b) Western Canada (Vancouver) with amplification seismic records based on $S_a(T_d)$

Fig 4.8 Regression analysis of 2, 5, 10-storey structures

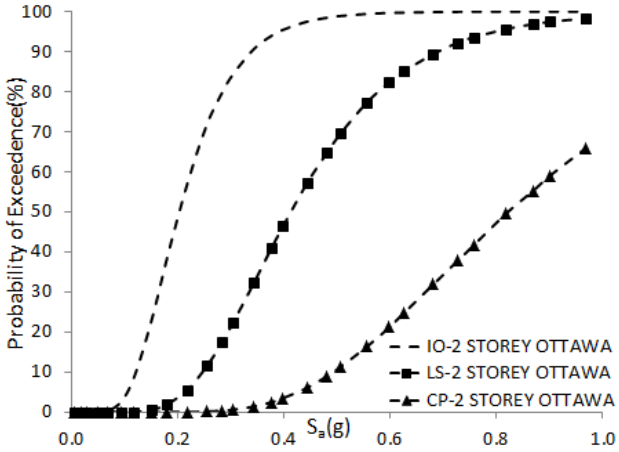

(a) 2- storey structures in Ottawa

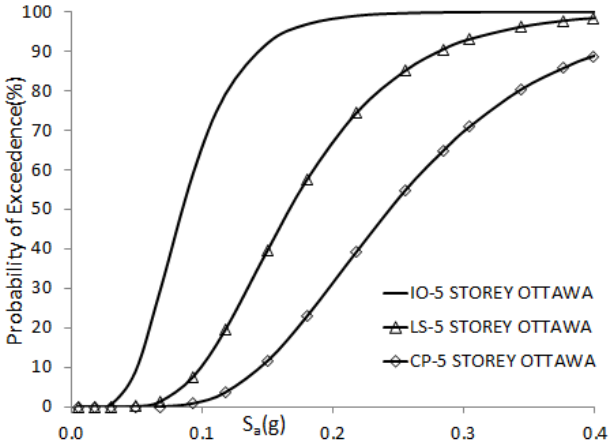

(b) 5- storey structures in Ottawa

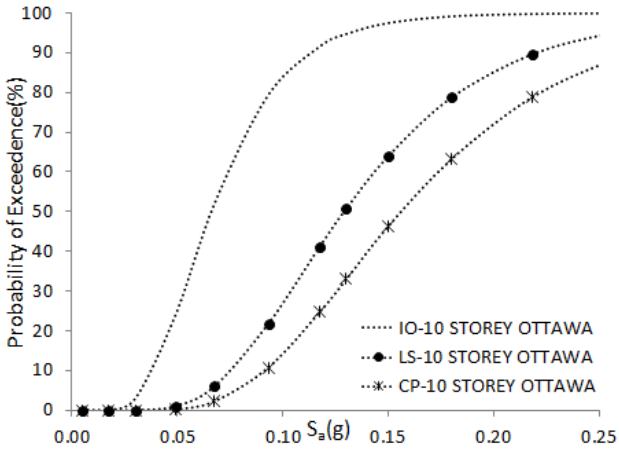

(c) 10- storey structures in Ottawa

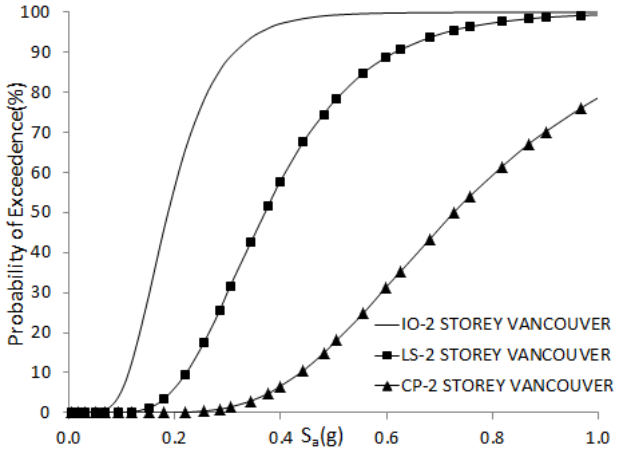

(d) 2- storey structures in Vancouver

Fig. 4.9 (Con't)

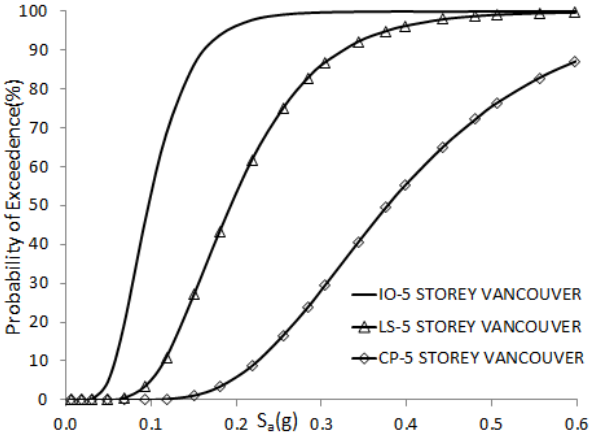

(e) 5- storey structures in Vancouver

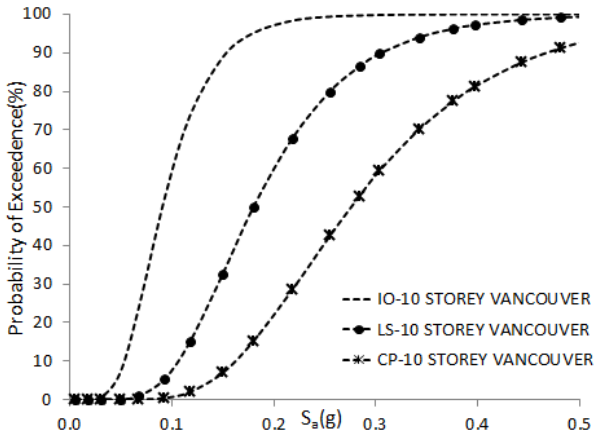

(f) 10- storey structures in Vancouver

Fig 4.9 Fragility response developed with amplified seismic records based on $S_a(T_e)$.

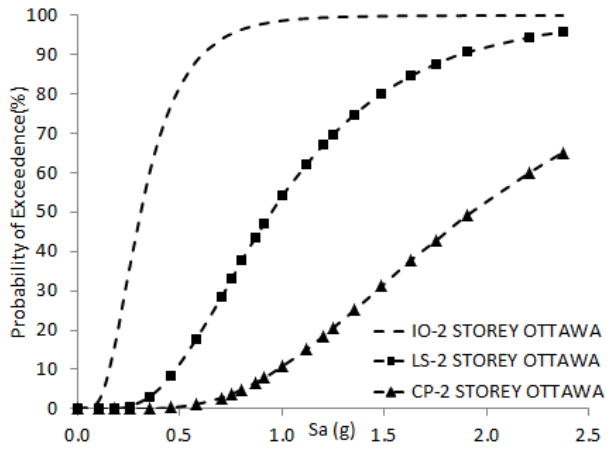

(a) 2- storey structures in Ottawa

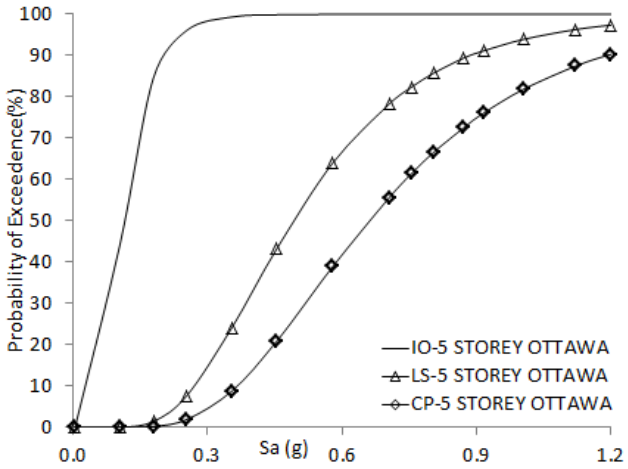

(b) 5- storey structures in Ottawa

Fig. 4.10 (Cont'd)

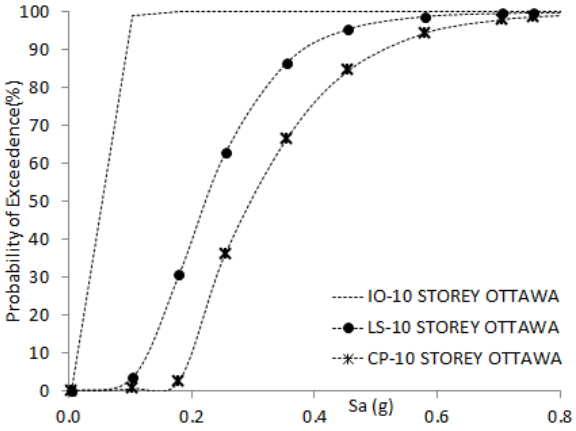

(c) 10- storey structures in Ottawa

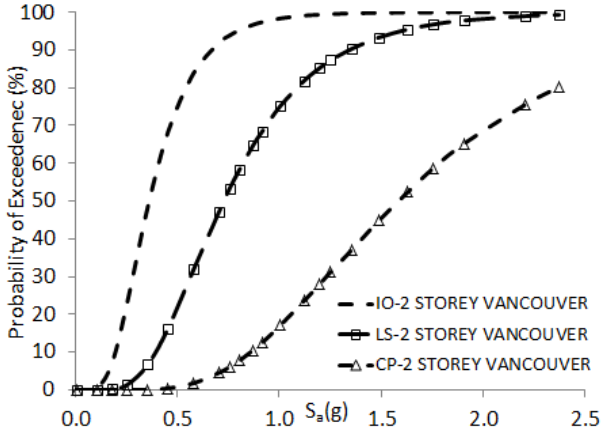

(d) 2- storey structures in Vancouver

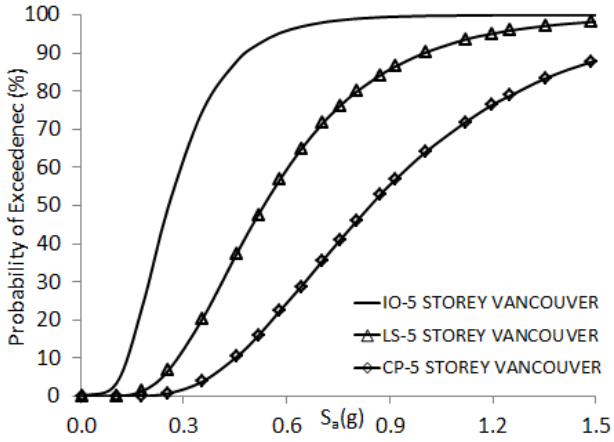

(e) 5- storey structures in Vancouver

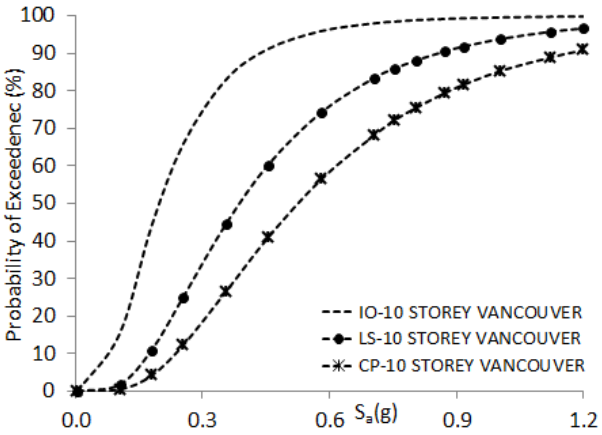

(f) 10- storey structures in Vancouver

Fig 4.10 Fragility response developed with amplified seismic records based on $S_a(T_d)$.

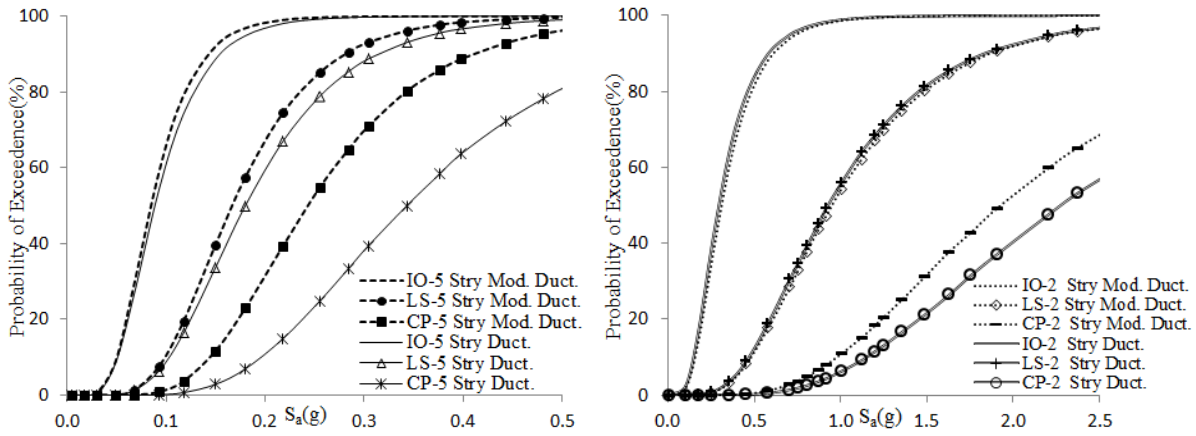

(a) (b)

Fig 4.11 Comparison of (a) 5-storey and (b) 2-storey structures fragility responses developed with Eastern Canada (Ottawa) seismic records.

CHAPTER 5

5. SEISMIC FRAGILTY ANALYSIS OF PRE-1975 CONVENTIONAL CONCRETE FRAME BUILDINGS IN CANADA

Abstract: Fragility analysis was conducted for reinforced concrete frame buildings in Canada designed based on the 1965 National Building Code of Canada as representative of pre-1975 era of seismic design practice. The buildings with three different heights, consisting of 2-, 5- and 10-stories, were designed for Vancouver and Ottawa, representing buildings in high and medium seismic regions with respective site-specific hazards. They were modelled for inelastic response time history analysis, with respective inelastic hysteretic models for flexure and shear. Computer software PERFORM-3D was used to conduct incremental dynamic analysis under incrementally increasing earthquake intensity based on a set of synthetic earthquake records generated for western and eastern Canada. The seismic intensity measure used was the spectral acceleration. Three different performance levels were used to assess building performance, consisting of i) immediate occupancy, ii) life safety, and iii) collapse prevention. Probabilistic analysis of the results of incremental dynamic analysis led to the development of fragility functions, which can be used as seismic vulnerability assessment tools for pre-1975 concrete frame buildings in Canada. The results are compared with those generated earlier by the authors for frame buildings designed on the basis of the 2010 NBCC as representative of post-1975 buildings. The comparison indicates that the probability of exceeding performance levels are significantly higher for older buildings in both locations relative to those for more recently designed fully ductile and moderately ductile buildings in Vancouver and Ottawa, respectively. The vulnerability assessment extended to include mean annual frequency of collapse for the 2-storey building, as well as the push-over analysis of the same building, illustrating increased vulnerability of older buildings relative to those design using ductile practices of more recent codes.

5.1 Introduction

Seismic design requirements in the National Building Code of Canada (NBCC) have evolved over the years. The procedure for determining seismic shear forces improved since its inception in 1941. The effects of dynamic characteristics of structures, ductility demands for energy dissipation, and improved seismic hazard values were implemented as the knowledge on earthquake engineering has advanced. Older buildings designed prior to the enactment of modern seismic codes remain vulnerable to earthquakes. The current research project addresses seismic assessment of reinforced concrete frame buildings designed and built prior to the implementation of ductile design provisions using a probabilistic approach. More specifically, fragility curves have been developed for representative concrete frame buildings designed by the 1965 NBCC (NRCC 1965) for Vancouver, located in a high seismic region and Ottawa, located in a moderate seismic region. The fragility curves and the results of seismic vulnerability assessment are presented in this paper. The results are compared with earlier fragility analysis conducted by the authors (Al Mamun and Saatcioglu, 2017)[2] for ductile and moderately ductile buildings in Canada conforming to the more recent 2010 NBCC (NRCC 2010) seismic provisions.

The 1941 National Building Code (NRCC 1941) defined base shear as percentage of building mass, which varied with bearing capacity of soil. The 1953 NBCC (NRCC 1953) was the first edition where seismic hazard was expressed in terms of seismic zones, and zoning map was used to calculate base shear. In the 1965 NBCC (NRCC 1965), ultimate strength design was permitted as an alternative method and capacity reduction factors were introduced. Also, importance factor and foundation factor were introduced as improvements that affect seismic base shear. In the 1970 NBCC (NRCC 1970), the base shear equation was modified to accommodate the effect of fundamental period. Seismic zoning map was revised. The advantage of structural ductility was recognized for the first time and a new structural type factor was introduced to account for the ductility of the structural system selected. In the 1975 NBCC (NRCC 1975), the base shear equation was revised and dynamic analysis was permitted as an alternative method. In 1977 (NRCC 1977) the base shear computed by dynamic analysis was limited not to be lower than the 90% of the value computed using the equivalent static load procedure. The requirements

[2] Al Mamun and Saatcioglu. 2017. Seismic fragility curves for reinforced concrete frame buildings in Canada designed after 1985. Submitted for publication in *Canadian Journal of Civil Engineering*.

remained the same for the 1980 NBCC (NRCC 1980) with a small change in calculating seismic response factor, S. New seismic zoning maps were introduced in the 1985 NBCC (NRCC 1985). The base shear computed through dynamic analysis was limited not to be less than 100% of the value computed by the equivalent static load procedure. In the 1990 NBCC (NRCC 1990), force modification factor based on ductility demand was considered in base shear with revised equations for fundamental period of frame structures introduced in 1995. Major revisions were introduced to the NBCC in the 2005 edition (NRCC 2005). New hazard values were introduced in the form of site-specific uniform hazard spectra (UHS). The equation for fundamental period of frame structures was revised. Factors for higher mode effects as well as coefficients for acceleration and velocity based foundation effects were introduced. A new set of force modification factors for over-strength and ductility were included with refined classification of seismic force resisting systems. Dynamic analysis was made the preferred method of analysis, with restrictions for the equivalent static force procedure. The 2010 NBCC (NRCC 2010) and 2015 NBCC (NRCC 2015) requirements remained essentially the same with improved hazard values and some minor changes.

In addition to the evolution of seismic base shear calculations outlined in the NBCC, the requirements for design and detailing of reinforcement in concrete buildings, specified in CSA A23.3 (CSA), also evolved over the years. These requirements were first introduced in CSA A23.3-1973 (CSA 1973), which was referenced in the 1975 NBCC. Though ductile design and detailing requirements were first introduced in 1973, the ductility based K factor to account for different types of construction had been introduced in the 1970 NBCC. Hence, buildings constructed prior to 1975 were considered in the current investigation as old conventional buildings. Significant improvements were introduced in CSA A23.3 (CSA 1984) after 1984 with the introduction of capacity design requirements, protecting critical elements and preventing non-ductile failures.

Considering the evolution of seismic design practices in Canada, summarized above, the concrete frame building inventory may be viewed in two categories; buildings designed prior to 1975, and those designed using the ductile design requirements of the post-1975 era. The current paper focuses on buildings in the former category.

Figure 5.1 illustrates the variation of seismic base shear over the years for six reinforced concrete frame buildings, three in Vancouver, and the other three in Ottawa. The buildings have 2, 5 and 10 storey heights. Because there was no distinction in seismic zones between Ottawa and Vancouver at the time of the design NBCC, and there was no ductile design and detailing requirements prior to 1975, the design base shear in both cities were the same, and the buildings were designed to have conventional, non-ductile frame systems. The 1970 NBCC was the exception, which made a distinction between non-ductile and ductile structural systems though ductile design and detailing were not implemented. Figure 5.1 also includes design base shears after 1975 with two levels of ductility, fully ductile for Vancouver and moderately ductile for Ottawa.

The current investigation focuses on seismic assessment of non-ductile frame buildings built between 1953 and 1975. The design base shear remained approximately the same in this period, with lowest values given by the 1965 NBCC. The 1965 design was taken as the representative design for the era. This would result in somewhat conservative assessment of buildings designed for higher base shears. Comparing the 1965 base shear values with those computed based on the 2010 NBCC, it can be observed that the base shear of moderately ductile and fully ductile structures increased by 25% and 33% for the 2-storey structures, decreased by 29% and 12% for the 5-storey structures and decreased by 52% and 24% for the 10-storey structures relative to the conventional base shears calculated according to the 1965 NBCC. Though design seismic base shear showed this variation, final designs of buildings did not vary as much. This can be explained by the changes in seismic load combinations and strength reduction factors. Table 5.1 compares the design details for columns and beams, designed based on the 1965 and 2010 NBCC.

The non-ductile frame buildings designed for the 1965 NBBC were modelled for non-linear dynamic analysis. The structural models were then used to conduct non-linear time history analysis using computer software PERFORM-3D. The analysis was repeated under different earthquake intensities to implement the incremental dynamic analysis procedure from which fragility curves were obtained through probabilistic evaluation of results. These fragility curves were then compared with those developed earlier for the 2010 NBCC buildings to illustrate the differences in seismic vulnerabilities of older and newer frame buildings in Canada.

In addition to the comparison of the fragility curves, two other comparisons were made to assess the significance of the change in building design practices between 1965 and 2010. First, the mean annual frequency of collapse was computed for each set of structures, and compared. Secondly, push-over analyses were performed to assess the performance under incrementally increasing static forces. The results are presented and discussed in the paper.

5.2 Building Details and Analysis Approach

2-, 5- and 10-storey reinforced concrete frame buildings with 8 m, 20 m and 40 m heights, respectively, were considered as representative structures for design and analysis. All the buildings had identical 5 bays, each having a 7 m span, resulting in a 35 m by 35 m square plan. Figure 5.2(a) shows a three dimensional view of the 5-storey building modeled in ETABS software (CSI 2008). The buildings were designed for 1.33 kPa superimposed dead load in addition to their self-weight, and 2.44 kPa live load. The lateral seismic base shear of 1965 NBCC structures were calculated according to the equations provided in the respective code, which resulted in the same design for both buildings in Vancouver and Ottawa, as there was no distinction between the two regions at the time. The buildings were analyzed for the load combinations specified in code. The compressive strength of concrete (f_c') used was 30 MPa for 2- and 5-storey buildings and 40 MPa for the 10-storey building. Yield strength of reinforcement was 400 MPa for all designs.

Seismic records selected for the non-linear dynamic analysis required for the development of fragility curves were those that are compatible with the UHS specified in the 2010 NBCC. They consisted of 20 code compatible earthquake records (Gail Atkinson 2009) for each of the two regions considered, i.e., eastern and western Canada, adapted to the UHS for Ottawa and Vancouver, respectively. The algorithm proposed by Vamvatsikos and Cornell (2004) was used to increase or decrease the intensity of records to perform incremental dynamic analysis (IDA). Further details of the implementation of the IDA are provided by the authors relative to the fragility analysis of newer buildings that conform to the 2010 NBCC (Al Mamun and Saatcioglu 2017).

The fragility analysis required a seismic intensity measure and damage indices for performance limits. The intensity measure used in the IDA was the spectral acceleration. The

inter-storey drift ratio was adopted as a damage indicator. Three damage states were considered, corresponding to three performance levels as commonly accepted performance limits; i)Immediate Occupancy (IO), ii) Life Safety (LS), and iii) Collapse prevention (CP) (ASCE41, 2013, FEMA 356, 2000, ACI 374.2R, 2013). Immediate Occupancy (IO) performance level describes the damage state where structure is safe to be re-occupied having suffered minor damage to the structural elements with minor spalling and flexural cracking. The inter-storey drift of 1% was considered for this limit state. Life Safety (LS) performance level describes the damage state where significant damage has occurred to the structure with extensive cracking and hinge formation in primary structural elements. The inter-storey drift of 2% was adopted for this limit state. Collapse Prevention (CP) performance level describes the damage state where structure is at the onset of partial or total collapse with extensive cracking, hinge formation and reinforcement buckling in structural elements. The median value of maximum inter-storey drift demands for all records was considered as CP performance level. This approach was also used by Ellingwood et al. (2007). The maximum inter-storey drift for CP limit was obtained as the smaller of the drift at which either dynamic instability is attained or the tangential slope of the IDA curve dropped to 20% of the initial slope (FEMA 350).

In addition to the fragility curves, the outcome of fragility analysis was used to establish mean annual frequency of collapse (λ_c). λ_c was calculated for each structure by integrating collapse fragility curve with site specific seismic hazard. The same approach was also used by previous researchers to assess seismic collapse performance of buildings (Bradley and Dhakal 2008, Goulet et al. 2007, Haselton 2006). The following equation specified by Ibarra and Krawinkler (2005) was used to calculate λ_c:

$$\lambda_c = \int_0^\infty F_{C,S_{a,C}}(x).\nu.f_{S_a}(x).dx \quad (1)$$

where $F_{C,S_{a,C}}(x)$ represents probability of exceeding certain spectral acceleration, x, corresponding to the collapse fragility curve, ν represented annual probability of exceedance of certain rate of seismicity, x and $f_{S_a}(x)$ represented the probability density function at certain spectral acceleration value, x. Return periods associated with 2% and 10% probability in 50-year hazard values for spectral accelerations for Ottawa and Vancouver were obtained from

Geological Survey of Canada (Adams and Halchuk 2003), and were used to calculate annual probability of exceedance (ν).

Pushover analysis was also performed to determine the static lateral seismic resistance capacity of structures. Yield base shear capacity was determined through idealized bilinear force deformation relationship according to FEMA 356 (FEMA 2000). Since the cracked stiffness was used to model structural members, linear cracked slope of the load deformation curve was found as effective stiffness of the structure. Yield shear force (V_y) and yield roof drift (δ_y) in idealized bilinear curve was calculated by using site specific UHS in the 2010 NBCC. From push-over analysis, over-strength factor (R_o) for each building was calculated as the ratio of yield shear capacity (V_y) to design base shear (V_d). Displacement ductility (μ) of a building was calculated as the ratio of maximum roof drift (δ_u) corresponding to 0.8 times the maximum shear strength (V_{max}) to yield roof drift (δ_y).

5.3 Analytical Models

The buildings were modeled using software PERFORM-3D (CSI 2013). Beams and columns were modeled using two segments, each consisting of an elastic frame element with an inelastic hinge at the end, connected together at the point of inflection. Figure 5.2(b) shows the schematic diagram for a concrete frame in the analytical model. Elastic frame elements were assigned linear elastic properties with plastic deformations lumped at the hinges. Both flexural and shear hinges were provided. A rigid end zone was specified at the end of each structural element to eliminate deformations within the adjoining member, ensuring that potential plastic hinges form at the face of the adjoining member, rather than at their centrelines. Energy degradation factor (EDF) was used to introduce stiffness degrading hysteretic behaviour in flexure and shear, as typically observed in reinforced concrete elements.

A tri-linear envelop curve was used for modelling moment-rotation hysteretic relationship. The initial linear segment represented the effective cracked stiffness based on 35% and 70% of uncracked flexural rigidities for beams and columns, respectively. The yield moment was calculated from sectional analysis with the corresponding chord rotation at yield calculated as $\frac{ML}{6EI}$, where M represents yield moment, L represents member length, E represents the elastic modulus of concrete, and I represents the effective moment of inertia of the section. The second

linear segment in the post yield range was established by assuming post-yield slopes of 8.5% and 4% of effective elastic slopes for beams and columns, respectively. The post yield segment continued up to an ultimate rotation of 1.5 times the yield rotation prior to the onset of strength decay. The descending branch, which ended at the residual strength, was based on the ASCE41-13 (ASCE 2014) recommendation. The strength decay slope for both beams and columns was adopted from ASCE41 for flexure-controlled response with nonconforming transverse reinforcement. The residual strength for beams was specified as 20% of maximum capacity. It varied between 0% and 20% of maximum capacity for columns depending on the accompanying level of axial load.

Once the primary curve was defined, the next step involved the computation of energy degradation factor (EDF), which introduced stiffness degradation characteristics of reinforced-concrete elements under reversed cyclic loading. EDF is the ratio of area under degraded cycle to fully elastoplastic non-degraded cycle. This factor changes the hysteretic behaviour from perfectly elasto-plastic behaviour to stiffness degrading behaviour that is typically observed in reinforced concrete elements. The value for EDF was established by examining experimental data. Column tests conducted by Ozcebec and Saatcioglu (1989) were used for this purpose. The force-displacement hysteretic response of test column U1 was used to define flexural EDF as shown in Figure 5.3(a). Accordingly the EDF values of 0.62 up to the yield point and 0.50 thereafter were found to match the experimental data. The same EDF values were used for both beams and columns.

The shear behaviour was also modelled with a tri-linear envelop curve for both beams and columns. A linear variation was considered for shear force-shear distortion relationship up to concrete shear capacity (V_c) and corresponding shear strain (γ_c), where $\gamma_c = \frac{V_c}{GA_v}$, A_v is shear area and G is shear rigidity. The second linear segment continued with a positive slope, but with a reduced shear rigidity $G_E = 0.1G$. This branch continued up to total shear capacity ($V = V_c + V_s$), consisting of concrete and transverse steel contributions (V_s). The total shear strain (γ) at this level was calculated as $\gamma = \gamma_c + \gamma_s$ where $\gamma_s = \frac{V_s}{G_E A_v}$. Shear displacement ($\Delta$) was calculated as $\Delta = 0.5\gamma h$ where 0.5h corresponds to hinge length (50% of member depth, h). The third line segment with a descending slope was obtained from the ASCE41-13 (ASCE 2014)

recommendation specified for beam-column joints. The values specified in ASCE 41-13 for elements with nonconforming transverse reinforcement and axial loads of less than 10% of $A_g f_c'$ (where A_g is gross concrete area) were used for both beams and exterior columns. For the interior columns, the value for axial loads greater than 40% $A_g f_c'$ was used. Residual shear capacity was considered to be 20% of beam and exterior column shear capacities, and 0% for interior column capacity. It was found that the degradation slope of shear force-shear displacement backbone curve was between 2 to 3% of initial slope for both beams and columns. The EDF for shear was based on experimental data. The hysteretic shear force-displacement relationship experimentally obtained by Ozcebec and Saatcioglu (1987) was used as shown in Fig 5.3(b). Among the columns tested, the test column U1 was considered as representative of shear behaviour. The same EDF values were used both for beams and columns with values of 0.44 up to the end of the first line segment and 0.29 thereafter.

5.4 Performance Assessment of the Buildings

The results of dynamic analysis of buildings designed based on the 1965 NBCC indicated that beam hinging was observed as early as 1% storey drift, with the first storey columns also experiencing inelasticity. This implies that at the IO performance level inelastic hinging has already started. These buildings never developed the 2% inter-storey drift associated with LS performance and failed prior to reaching this limit state. Indeed, the CP limit state was reached on average at 1.5% storey drift, indicating that the older buildings could collapse prior to developing the assumed life safety performance. In the 2-storey building analysed, flexural hinges formed in the 2nd floor beams, followed by the 1st floor columns. Similar trend was observed in reaching ultimate moment capacities of members. For all cases, the beams developed failure at the 1st floor level first, followed by the 1st floor columns. The shear hinges formed in the 1st floor columns at the same time as flexural hinges. Though column shear demands exceeded concrete shear capacity, no shear failure was observed. The 5-storey building experienced shear hinging first in the 1st floor interior columns, followed by flexural hinging of the 2nd floor exterior beams. Subsequently, flexural hinging extended to the 2nd, 3rd and 4th floor beams, followed by the flexural hinging of the 1st floor columns. The failure was caused by insufficient flexural capacity in the 1st floor columns. A similar trend was observed in the 10-storey building; flexural hinging started forming in the 2nd floor beams and then gradually

propagated up to the 6th floor level. Shear hinging occurred in the ground floor columns, followed by flexural hinging. The failure was due to insufficient shear capacity of these columns under high intensity excitations. The beams were not critical in shear, and there was no beam-shear hinging observed in any of the buildings.

The fragility analysis indicates that the 1965 buildings in Vancouver show 93% to 99% probability of exceeding the IO performance level at the 2010 NBCC hazard levels. The same buildings under the same intensity levels show 68% to 91% probability of exceeding the CP level. The 1965 buildings in Ottawa showed somewhat lower probabilities of exceedances, showing 11% to 30% probability of exceeding the IO limit, and 1% to 9% probability of exceeding the CP limit state. Figure 5.4 shows the fragility curves for all the 1965 buildings, located in Vancouver and Ottawa. The same figure also includes the fragility curves developed by the authors (Al Mamun and Saatcioglu, 2017) for the same buildings designed using the 2010 NBCC requirements. A similar comparison is given in Table 5.2. It was observed from Table 5.2 that at IO performance level, all the 1965 buildings exhibit similar response as those for the 2010 buildings. At the CP limit state, the 1965 buildings in Ottawa and Vancouver showed on the average 6% and 76% higher probabilities of exceedance relative to the 2010 buildings, respectively.

Further comparisons of older and more recent building performances indicate that the maximum inter-storey drift ratio (δ_{max}) attained in 1965 buildings were lower than those for the 2010 buildings. This is shown in Table 5.2, and is expected because of the brittle performance of older buildings. It is noteworthy that all the buildings had approximately the same yield drift capacities. This implies that the ductility levels considered in design are reflected in the analysis results. The ultimate flexural rotations of structural elements in the 1965 buildings developed 1.5 times their yield rotations; whereas the members in the 2010 buildings showed 2.5 and 4.0 times the yield rotation for buildings in Ottawa and Vancouver corresponding to moderately and fully ductile buildings.

The comparisons extended to include annual probability of exceedances. Figure 5.5 shows the graphical representation for calculating annual probability of exceedance (ν) for the 2-storey 2010 building in Vancouver. Figure 5.6 graphically shows the approach for calculating the mean annual frequency of collapse (λ_c) for the same building at design spectral acceleration (x)

corresponding to the empirical code period. In the figure, $f_{S_a}(x)$ is developed from probability distribution function of maximum spectral acceleration (S_a) observed in IDA and $F_{C,S_{a,C}}(x)$ is obtained from fragility response. Table 5.2 indicates that the 2010 Ottawa buildings have the lowest mean annual frequency of collapse (λ_c), whereas the 1965 Vancouver buildings have the highest λ_c .

Push-over analysis was also used to compare the performances of the 1965 and 2010 buildings. Figure 5.7 shows the comparison of push-over responses for 2-storey buildings, and Figure 5.8 shows the bilinear idealization of the push-over response for the 2-storey 2010 building in Vancouver. Table 5.2 compares shear force responses obtained through push-over analyses of buildings. It indicates that the 2010 buildings in Vancouver have higher shear capacities, relative to the 1965 buildings. On average, the maximum shear capacity of 2010 Ottawa and Vancouver buildings are on average 26% and 56% higher than those for 1965 buildings, respectively. Similar trend is observed for the maximum roof drift ratio (δ_u) due to different ductility assigned to the members of the buildings. Ottawa buildings show lower maximum roof displacements relative to the buildings in Vancouver. Over-strength ratio (R_o) obtained from the push-over analysis of 2010 Ottawa and Vancouver buildings are on average 39% and 76% higher than those for 1965 buildings, respectively. For the 5- and 10-storey 1965 buildings, the maximum shear capacity (V_{max}) is less than the design shear strength (V_d), which implies over-strength ratios (R_o) of less than 1.0. Insufficient shear capacity and low ductility of structural elements explain the poor performance of 1965 buildings observed in the comparison. Though structural members were detailed for a ductility-related force modification factors of 1.5 for the 1965 building, and 2.5 and 4.0 for the 2010 buildings in Ottawa and Vancouver, respectively, the average global ductility ratio based on roof displacements are shown to be 1.6 for 1965 buildings, and 2.7 and 2.6 for the 2010 buildings in Ottawa and Vancouver.

Figure 5.9(a) and 5.10(a) shows the effect of global ductility ratio (μ) on mean annual collapse frequency (λ_c) of the buildings. It is observed that for a given building; the mean annual collapse frequency decreases with increasing building ductility. Similarly, the mean annual collapse frequency (λ_c) decreases with increasing over-strength ratio (R_o) as shown in Figure 5.9(b) and 5.10(b). The same trend was observed for all building height considered (2-, 5- and

10-storey). This suggests that the seismic safety margin can be increased with increasing ductility (μ) and over-strength (R_o) ratios.

5.5 Summary and Conclusions

Three reinforced concrete frame buildings were designed based on the 1965 NBCC for seismic vulnerability analysis of buildings in Ottawa and Vancouver, as representative cities located in medium and high seismic regions in Canada. The buildings had 2-, 5- and 10-storey heights, and were designed as conventional buildings without the ductile seismic detailing called for in current seismic codes. Dynamic inelastic response history analyses were conducted using computer software PERFORM-3D under site specific earthquake records. Incremental dynamic analyses were performed under incrementally increasing seismic intensity, based of spectrum intensity as the intensity measure. The results were evaluated for different performance levels as dictated by corresponding damage indices, where inter-storey drift was adopted as the damage indicator. Commonly accepted performance levels, defined as immediate occupancy, life safety and collapse prevention were adopted. It was observed that the collapse prevention limit state was exceeded prior to developing the commonly accepted 2% storey drift as the life safety limit. Probabilistic analysis of the results of incremental dynamic analysis provided data to generate fragility curves that can be used as analytical tools for seismic vulnerability assessment. Fragility curves were developed and presented for six 1965 buildings, three in each location, for immediate occupancy and collapse prevention as performance levels. The fragility curves are compared with those generated in an earlier phase of the same investigation by the authors. The results indicate that the frame buildings in Vancouver showed very high probability of collapse when investigated under the 2010 NBCC hazard, prior to reaching life safety limit of 2% of inter-storey drift. The frame buildings in Ottawa showed very small probabilities (on average 6%) of exceeding the collapse prevention limit under the same level of seismic hazard. All the buildings experienced inelastic shear deformations in their first storey columns, with the 10-storey building experiencing shear failure. The beams remained elastic in shear but developed flexural hinges. The buildings showed poor performance relative to those designed and analysed earlier on the basis of ductile design requirements of the 2010 NBCC. The comparisons and the specific probabilities of exceedances for different levels of performance are indicated in the paper. In addition to the fragility based assessment, two other approaches were employed for

seismic performance assessment of 1965 buildings; annual frequency of collapse and push-over analysis. Both approached showed agreement with the fragility analysis, indicating similar trends, i.e., significantly poor performance of 1965 buildings relative to 2010 buildings, both for western Canada (as represented by Vancouver buildings) and eastern Canada (as represented by Ottawa Buildings). It may be concluded the fragility curve generated provide useful analytical tools for pre-1975 reinforced concrete frame buildings in Canada, with regular structural layouts having a wide range of fundamental periods.

5.6 References for Chapter 5

ACI. 2013. Guide for testing reinforced concrete structural elements under slowly applied simulated seismic loads. ACI committee 374. American Concrete Institute. ACI 374.2R-13

ASCE. 2014. Seismic evaluation and retrofit of existing buildings. American Society of Civil Engineers. ASCE/SEI 41-13.

Adams, J. and Halchuk, S. 2003. Fourth generation seismic hazard maps of Canada: Values for over 650 Canadian localities intended for the 2005 National Building Code of Canada. Geological Survey of Canada. Open file 4459.

Atkinson, G.M. 2009. Earthquake time histories compatible with the 2005 National building code of Canada uniform hard spectrum. Canadian Journal of Civil Engineering. Volume 36, Number 6, June 2009.

Borzi, B., Pinho, R., Crowley, H. 2008. Simplified pushover-based vulnerability analysis for large-scale assessment of RC buildings. Engineering Structures. Volume 30, Issue 3, pp. 804-820.

Bradley, B. and Dhakal, R. 2008. Error estimation of closed-form solution for annual rate of structural collapse. Earthquake Engineering & Structural Dynamics. Volumn 37, Issue 15. Pages 1721-1737.

CSA. 1973. Design of concrete structures. CSA standards update service. Canadian Standards Association. Missisuaga, ON.

CSA. 1984. Design of concrete structures. CSA standards update service. Canadian Standards Association. Missisuaga, ON.

CSA. 2004. Design of concrete structures. CSA standards update service. Canadian Standards Association. Missisuaga, ON.

CSI. 2008. ETABS. Nonlinear Version 9.5.0. Computers and Structures, Inc. Berkeley, CA.

CSI. 2013. PERFORM-3D. Version 5.0.1. Computers and Structures, Inc. Berkeley, CA.

FEMA. 2000. Prestandard and commentary for the seismic rehabilitation of buildings. Federal Emergency Management Agency. FEMA 356.

Goulet, C.A., Haselton,C.B.,Reiser,J.M., Beck, J.L., Deierlein, G.G., Porter, K.A. and Stewart, J.P. 2007. Evaluation of the seismic performance of a code-conforming reinforced-concrete frame building—from seismic hazard to collapse safety and economic losses. Earthquake Engineering & Structural Dynamics. Volume 36, Issue 23. Pages 1973-1997.

Haselton, Curt B. 2006. Assessing seismic collapse safety of modern reinforced concrete moment frame buildings. Stanford University. Ph.D. Thesis.

Ibarra, L.F. and Krawinkler, H. 2005. Global collapse of frame structures under seismic excitations. Department of Civil and Environmental Engineering. Stanford University. Final report on PEER project 3192002. Report no. 152.

Inel, M., Ozmen, H.B. 2006. Effects of plastic hinge properties in nonlinear analysis of reinforced concrete buildings. Engineering Structures. Volume 28, Issue 11, pp. 1494-1502.

Jeong, S.H., Elnashai, A.S. 2007. Probabilistic fragility analysis parameterized by fundamental response quantities". Engineering Structures. Volume 29, Issue 6, Pages 11238-1251.

Liel, A., Haselton, C., and Deierlein, G. 2011. Seismic Collapse Safety of Reinforced Concrete Buildings. II: Comparative Assessment of Nonductile and Ductile Moment Frames. Journal of Structural Engineering, Volume 137, Issue 4, Pages 492-502.

NRCC. 1941. National building code of Canada 1941. Associate Committee on the National Building Code. National Research Council of Canada, Ottawa, ON.

NRCC. 1953. National building code of Canada 1953. Associate Committee on the National Building Code. National Research Council of Canada, Ottawa, ON.

NRCC. 1960. National building code of Canada 1960. Associate Committee on the National Building Code. National Research Council of Canada, Ottawa, ON.

NRCC. 1965. National building code of Canada 1965. Associate Committee on the National Building Code. National Research Council of Canada, Ottawa, ON.

NRCC. 1970. National building code of Canada 1970. Associate Committee on the National Building Code. National Research Council of Canada, Ottawa, ON.

NRCC. 1975. National building code of Canada 1975. Associate Committee on the National Building Code. National Research Council of Canada, Ottawa, ON.

NRCC. 1977. National building code of Canada 1977. Associate Committee on the National Building Code. National Research Council of Canada, Ottawa, ON.

NRCC. 1980. National building code of Canada 1980. Associate Committee on the National Building Code. National Research Council of Canada, Ottawa, ON.

NRCC. 1985. National building code of Canada 1985. Associate Committee on the National Building Code. National Research Council of Canada, Ottawa, ON.

NRCC. 1990. National building code of Canada 1990. Associate Committee on the National Building Code. National Research Council of Canada, Ottawa, ON.

NRCC. 1995. National building code of Canada 1995. Associate Committee on the National Building Code. National Research Council of Canada, Ottawa, ON.

NRCC. 2005. National building code of Canada 2005. Associate Committee on the National Building Code. National Research Council of Canada, Ottawa, ON.

NRCC. 2010. National building code of Canada 2010. Associate Committee on the National Building Code. National Research Council of Canada, Ottawa, ON.

NRCC. 2015. National building code of Canada 2015. Associate Committee on the National Building Code. National Research Council of Canada, Ottawa, ON.

Ozcebe, G., Saatcioglu, M. 1987. Confinement of concrete columns for seismic loading. ACI Structural Journal. Volume 84, Issue 4, Pages 308-315.

Ozcebe, G., Saatcioglu, M. 1989. Hysteretic shear model for reinforced concrete members. Journal of the Structural Engineering, ASCE. Volume 115, Issue 1, pp. 132-148.

Vamvatsikos, D., Cornell, C.A. 2004. Applied incremental dynamic analysis. Earthquake

Spectra. Vol 20, No. 2, Page 523-553, May 2004.

5.7 Tables and Figures

Table 5.1 Structural member flexural yield capacities (Kn-m) of structures designed according to NBCC.

	2 Storey (40Mpa)			2 Storey (30Mpa)		5 Storey (30Mpa)		5 Storey (30Mpa)		10 Storey (40Mpa)			10 Storey (40Mpa)	
	2010			1965		2010		1965			2010 (Ottawa)	2010 (Vanc.)	1965	
	Size	Rebar		Size	Rebar	Size	Rebar	Size	Rebar	Size	Rebar	Rebar	Size	Rebar
Corner Column 1-Top	300X300	8-20M		300X300	4-25M+4-20M	300X300	8-20M	300X300	4-25M+4-15M	350X350	4-25M+4-15M	4-25M+4-15M	350X350	8-20M
Ext Column 1-2	300X300	4-30M		300X300	8-25M	300X300	4-30M	325X325	8-25M	350X350	16-20M	4-30M+8-20M	400X400	8-25M
Ext Column 3-Top	-	-		-	-	300X300	4-25M	325X325	4-25M+4-20M	350X350	4-25M+4-15M	8-25M	400X400	4-25M+4-20M
Int-1 Column 1-2	325X325	4-20M+4-15M		300X300	8-15M	450X450	12-25M	400X400	8-30M	500X500	12-30M+8-20M	12-30M+8-25M	500X500	12-25M+4-20M
Int-1 Column 3-5	-	-		-	-	450X450	4-25M+4-20M	400X400	4-25M+4-15M	500X500	8-25M+8-20M	8-30M+8-25M	500X500	8-25M
Int-1 Column 6-10	-	-		-	-		-		-	500X500	4-25M+4-15M	4-25M+4-20M	500X500	4-25M+4-15M
Int-2 Column 1-2	325X325	4-20M+4-15M		300X300	8-15M	450X450	4-30M+8-20M	400X400	4-30M+4-25M	500X500	12-30M+8-20M	12-30M+8-20M	500X500	8-25M+8-20M
Int-2 Column 3-5	-	-		-	-	450X450	4-30M	400X400	8-20M	500X500	8-25M+8-15M	12-25M+8-20M	500X500	4-25M+8-15M
Int-2 Column 6-10	-	-		-	-		-		-	500X500	4-25M+4-15M	4-25M+4-20M	500X500	4-25M+4-15M
Int-3 Column 1-2	325X325	4-20M+4-15M		300X300	4-20M	450X450	4-25M+8-20M	400X400	8-25M	500X500	8-30M+8-25M	12-30M+8-20M	500X500	12-25M
Int-3 Column 3-5	-	-		-	-	450X450	8-20M	400X400	8-20M	500X500	4-25M+8-20M	12-25M+4-20M	500X500	4-25M+4-15M
Int-3 Column 6-10	-	-		-	-		-		-	500X500	4-25M+4-15M	4-25M+4-20M	500X500	4-25M+4-15M
Ext Beam Top	300X500	3-20M		300X500	4-20M	300X500	3-20M	300X500	4-20M	350X500	3-20M	3-20M	350X500	2-25M
Ext Beam Bottom	300X500	2-20M		300X500	2-20M	300X500	2-20M	300X500	2-20M	350X500	2-20M	2-20M	350X500	2-20M
		Ottawa	Vanc.											
Int Beam 1-5 Top	300X500	4-20M	4-20M	300X500	3-25M	300X500	3-25M	300X500	3-25M	350X500	4-25M	4-25M	350X500	5-25M
Int Beam 1-5 Bottom	300X500	3-20M	4-20M	300X500	3-15M	300X500	2-25M	300X500	3-20M	350X500	2-25M	4-25M	350X500	4-20M
Int Beam 6-10 Top	-	-	-	-	-	-	-	-	-	350X500	3-25M	3-25M	350X500	4-25M
Int Beam 6-10 Bottom	-	-	-	-	-	-	-	-	-	350X500	3-20M	3-25M	350X500	2-25M

Table 5.2 Analytical assessment of 2, 5 and 10-storey structures designed according to NBCC.

Design Code	Building	Region	T_e	$S_a(T_d)$	$S_a(T_e)$	δ_{max} (%)	LS Prob. at $S_a(T_e)$		λ_c at $S_a(T_d)$ x10^{-04}	V_y Kn	δ_y (%)	V_d Kn	δ_u (%)	V_{max} Kn	μ	R_o
							IO	CP								
2010 NBCC	10-Storey	Ottawa	2.84	0.07	0.05	2.44	26	0	0	2438	0.26	1843	0.74	3468	2.8	1.3
	5-Storey	Ottawa	2.04	0.13	0.05	2.94	10	0	3	1983	0.48	1456	0.95	2738	2.0	1.4
	2-Storey	Ottawa	1.08	0.30	0.13	3.92	14	0	0	1667	0.54	1370	1.85	2413	3.4	1.2
	10-Storey	Vanc.	2.84	0.20	0.17	3.07	95	14	18	3790	0.37	2936	0.86	5123	2.3	1.3
	5-Storey	Vanc.	2.04	0.32	0.17	3.91	93	3	54	2424	0.59	1669	1.38	3031	2.4	1.5
	2-Storey	Vanc.	1.08	0.62	0.32	3.99	92	2	32	2296	0.78	1463	2.48	2509	3.2	1.6
1965 NBCC	10-Storey	Ottawa	2.81	0.07	0.05	1.53	30	8	30	2475	0.27	3438	0.35	2925	1.3	0.7
	5-Storey	Ottawa	2.15	0.13	0.05	1.04	11	9	160	1651	0.45	1770	0.60	1986	1.3	0.9
	2-Storey	Ottawa	1.14	0.30	0.13	1.80	18	1	82	1313	0.48	1097	1.15	1909	2.4	1.2
	10-Storey	Vanc.	2.81	0.20	0.17	1.69	99	88	121	2234	0.25	3438	0.35	2925	1.4	0.6
	5-Storey	Vanc.	2.15	0.32	0.17	1.27	97	91	163	1440	0.39	1770	0.60	1986	1.5	0.8
	2-Storey	Vanc.	1.14	0.62	0.31	1.48	93	68	222	1214	0.64	1097	1.15	1909	1.8	1.1

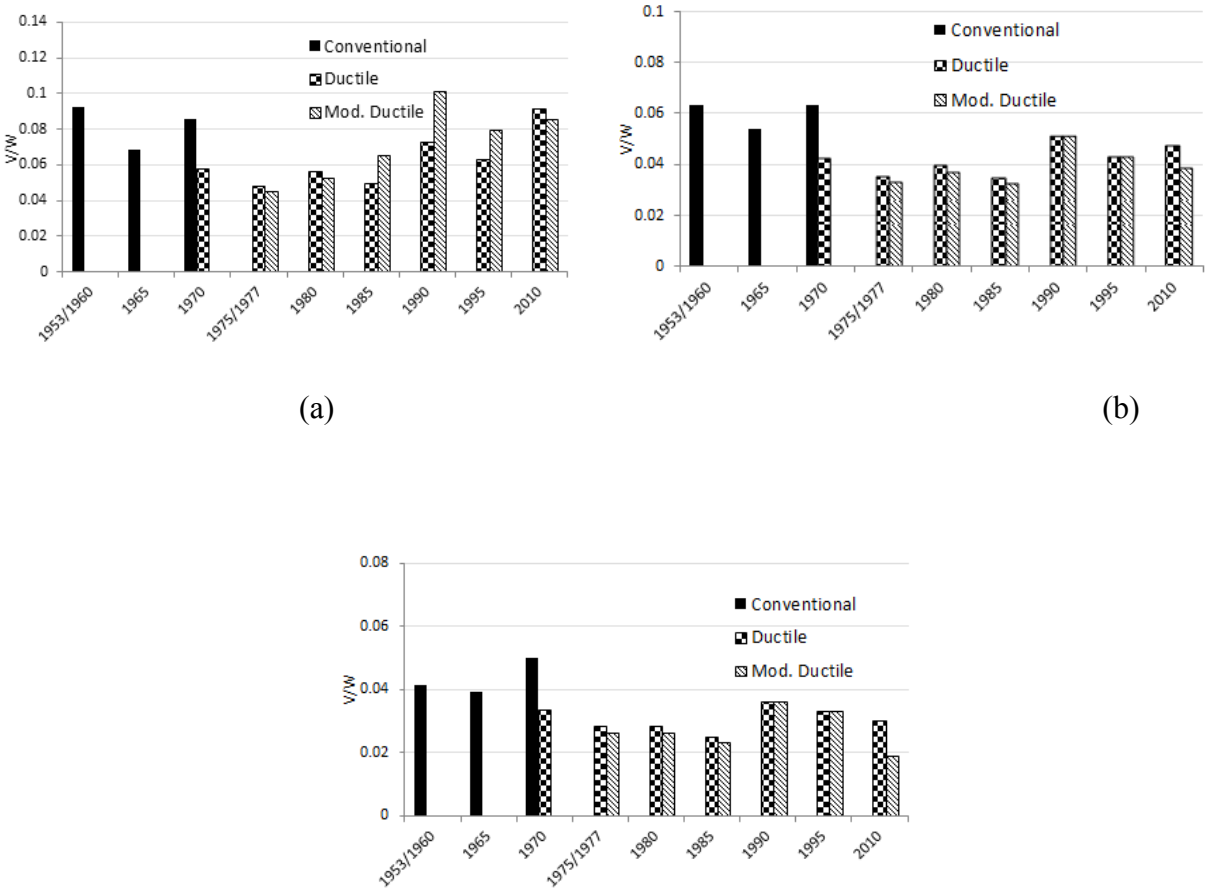

Fig 5.1 Base shear evolution of (a) 2-storey, (b) 5-storey and (c) 10-storey buildings according to NBCC

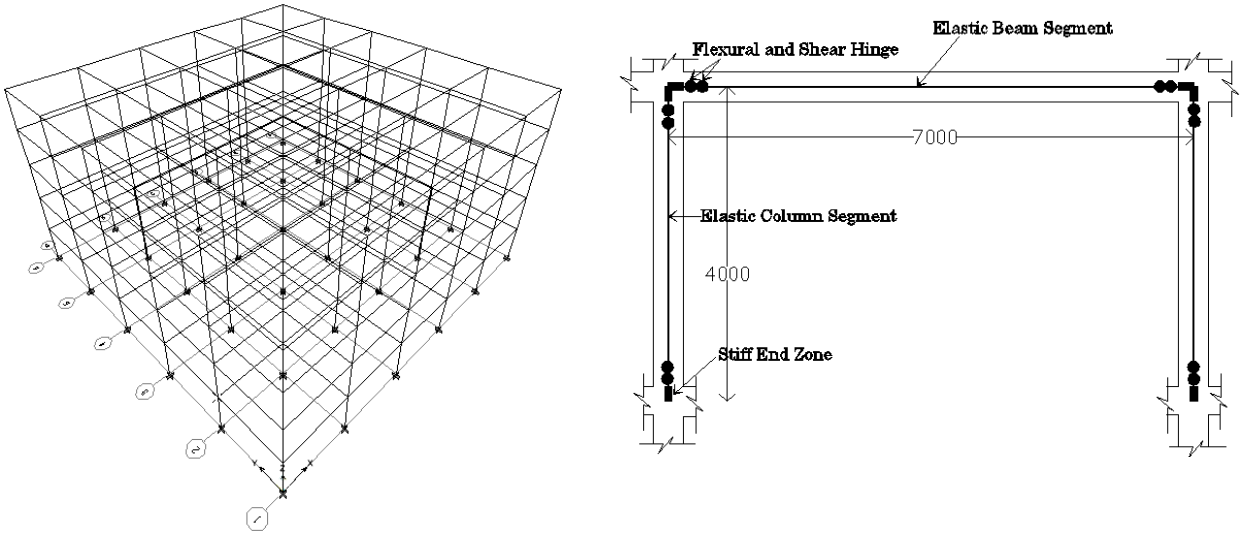

(a) (b)

Fig 5.2 Schematic diagram of (a) 5-storey building modeled in ETABS and (b) concrete frame element in analytical model developed with PERFORM-3D and

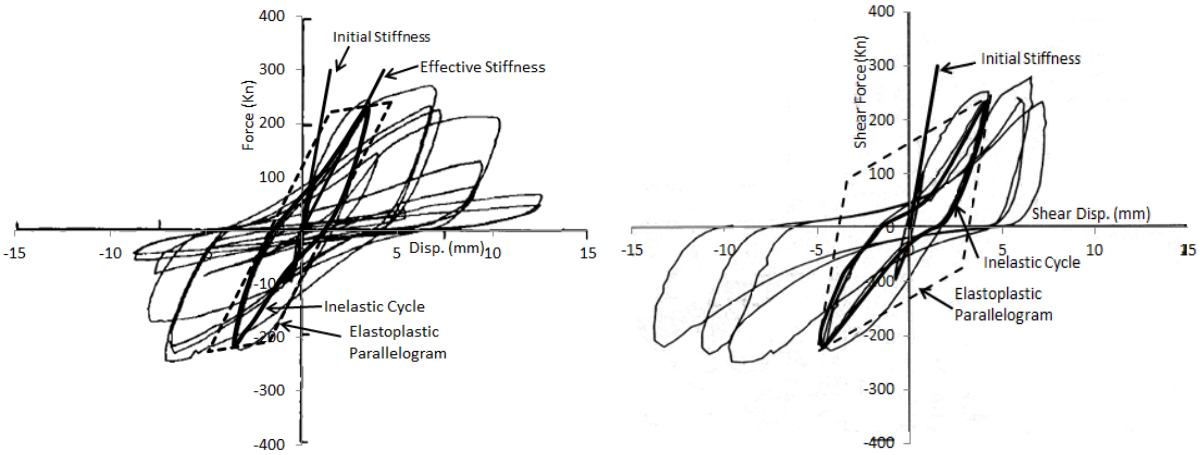

(a) (b)

Fig 5.3 Evaluation of (a) flexural and (b) shear EDF for 1965 NBCC structures from test (specimen U1) performed by Ozcebe and Saatcioglu (1987).

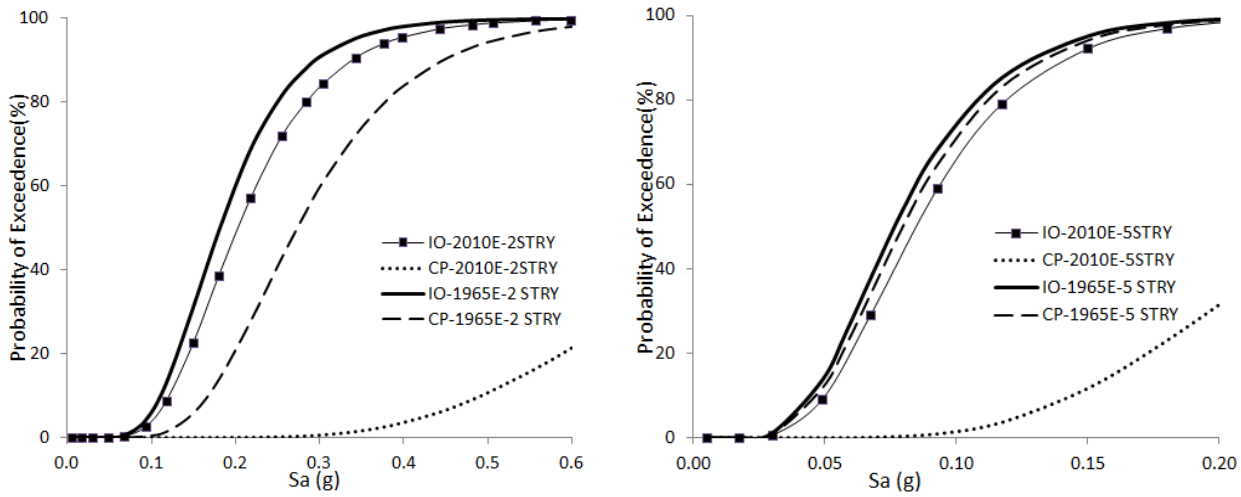

(a)

(b)

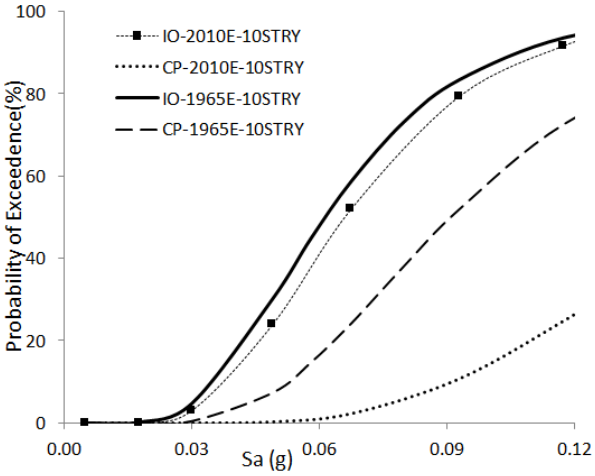

(c)

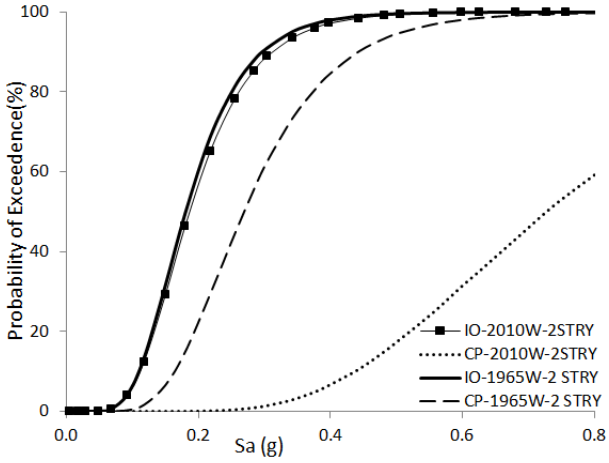

(d)

Fig. 5.4 (Cont'd)

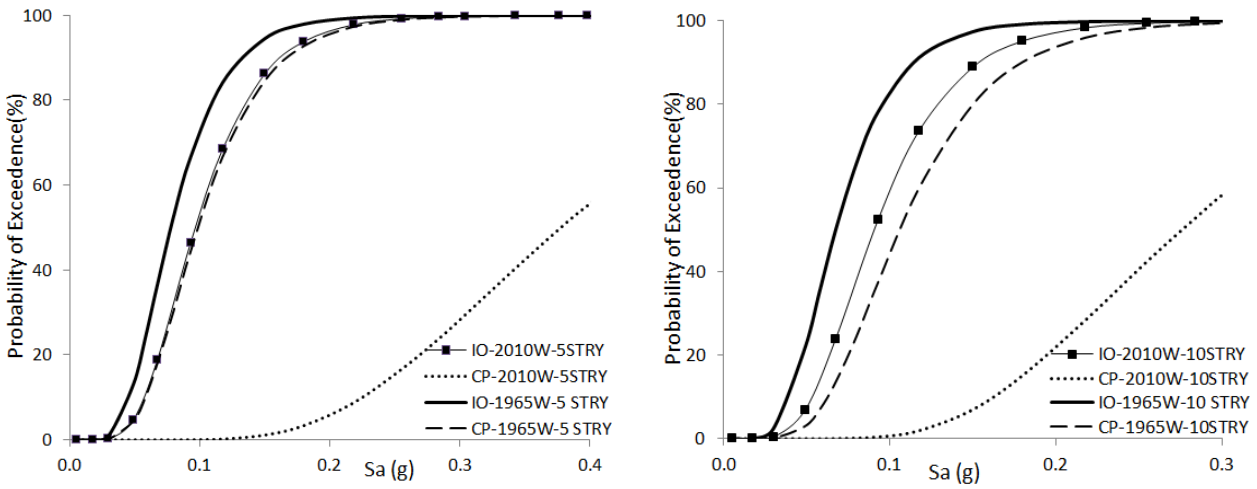

(e) (f)

Fig 5.4 Fragility responses of (a) 2-storey, (b) 5-storey, (c) 10-storey buildings in Ottawa and (c) 2-storey, (d) 5-storey, (e) 10-storey buildings in Vancouver designed according to 2010 and 1965 NBCC.

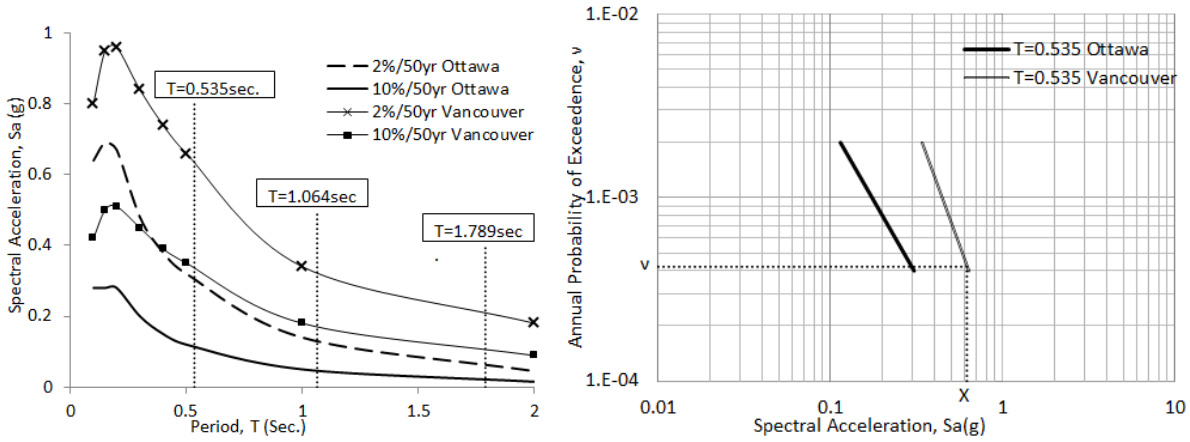

Fig 5.5 Graphical representation to calculate annual probability of exceedance (ν) for 2-storey 2010 NBCC western structure.

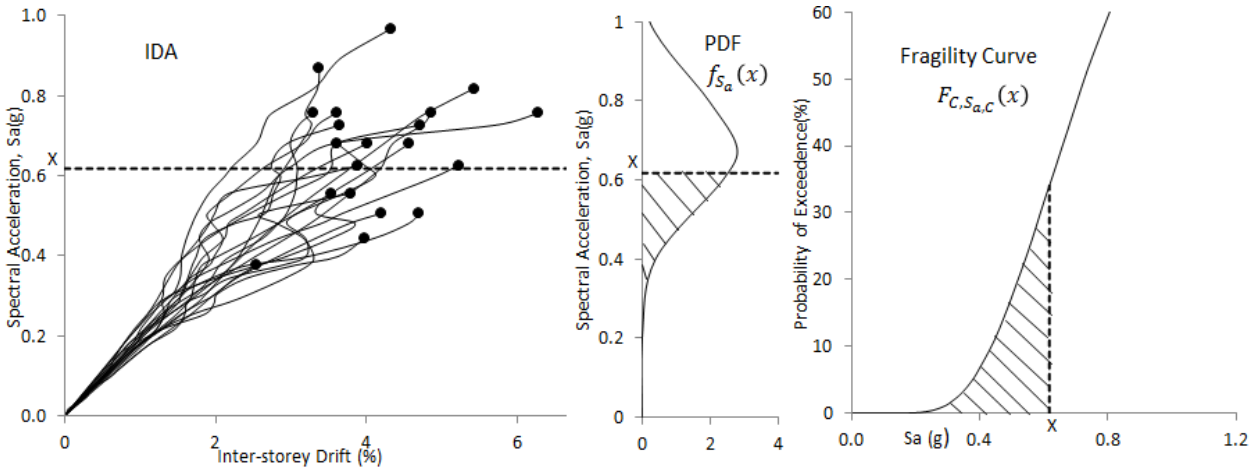

Fig 5.6 Graphical representation of mean annual frequency of collapse (λc) for 2-storey 2010 NBCC Vancouver structure.

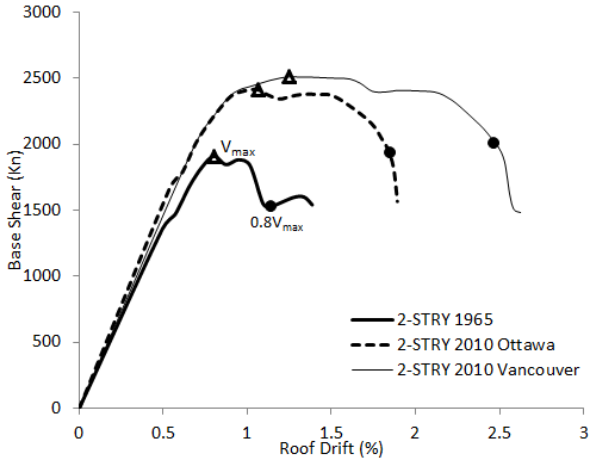

Fig 5.7 Push-over curve for 2-storey structures.

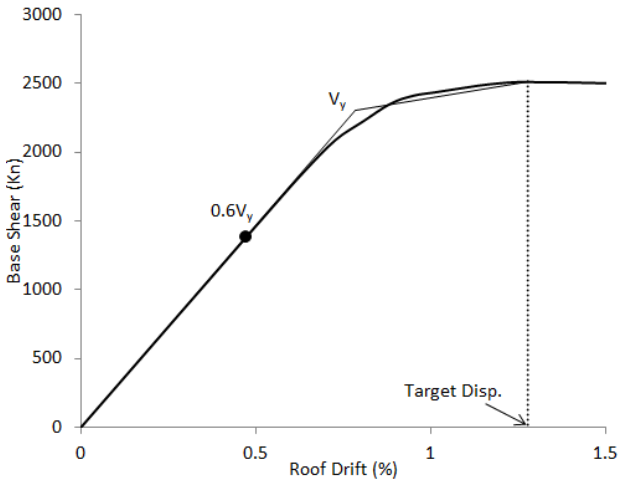

Fig 5.8 FEMA 356 idealized bilinear force-deformation curve to determine yield point of 2-storey 2010 NBCC western structure.

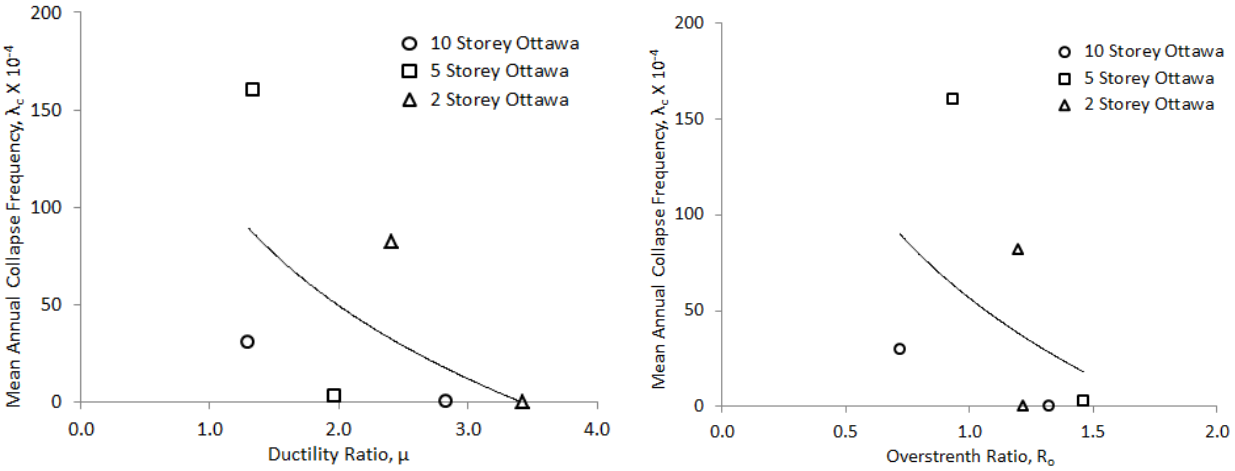

(a) (b)

Fig 5.9 Effect of (a) global ductility ratio and (b) over-strength ratio on mean annual collapse frequency in Ottawa.

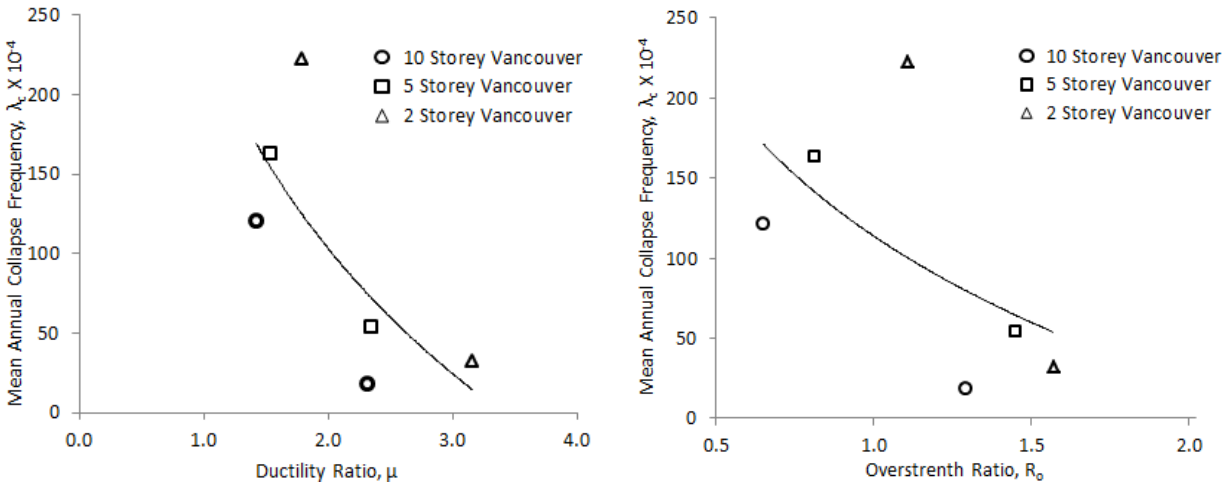

(a) (b)

Fig 5.10 Effect of (a) global ductility ratio and (b) over-strength ratio on mean annual collapse frequency in Vancouver.

CHAPTER 6

6. SEISMIC PERFORMANCE ASSESSMENT OF PRE-1975 IRREGULAR CONCRETE FRAME BUILDINGS IN CANADA

Abstract: Seismic assessment was conducted for reinforced concrete frame buildings with irregularities, designed based on the 1965 National Building Code of Canada as representative of the pre-1975 era of seismic design practice. A 5-storey frame building was designed and investigated under a set of site-specific seismic records for Vancouver and Ottawa, representing high and medium seismic regions in Canada. Four different irregularity types were considered, consisting of vertical irregularities caused by change in storey height, use of setbacks and soft storey created by the use of masonry infill walls above the first storey level, as well as a building with torsional sensitivity. The buildings were modelled for inelastic response time history analysis, with respective inelastic hysteretic models for flexure and shear. Computer software PERFORM-3D was used to conduct incremental dynamic analysis under incrementally increasing earthquake intensity. The seismic intensity measure used was the spectral acceleration. Three different performance levels were used to assess building performance, consisting of i) immediate occupancy, ii) life safety, and iii) collapse prevention. Probabilistic analysis of the results of incremental dynamic analysis led to the development of fragility functions, which can be used as seismic vulnerability assessment tools to illustrate the effects of irregularities on pre-1975 mid-rise concrete frame buildings in Canada. PERFORM-3D was also used to carry out non-linear static analysis of buildings under incrementally increasing lateral loads (push-over analysis). The results indicate that the collapse prevention performance level was exceeded before the life safety limit was reached, indicating brittle response of 1965 buildings. The probability of exceeding performance levels was not affected significantly by the

irregularities considered. However, the distribution of shear and energy dissipation in structural elements were affected significantly, indicating concentration of damage in soft stories and storey levels above setbacks, as well as the columns on the flexible side of torsionally sensitive buildings.

6.1 Introduction

Seismic Older buildings designed and built without the implementation of modern seismic design provisions of more recent building codes pose seismic risk. This is especially true for buildings having structural irregularities. Irregular configurations in buildings increase seismic deformation and force demands, often leading to significant structural damage (Athanassiadou 2008). Several research projects were undertaken in the past to assess the seismic behaviour of irregular buildings worldwide (El Kholy et al. 2012, Stefano and Pintucchi 2008). The detrimental effects of irregularities have been recognized by researchers and structural engineers, resulting in improved design provisions in recent codes to mitigate their effects. Building irregularities are categorized in recent editions of the National Building Code of Canada (NBCC), more systematically since the 2005 NBCC. More stringent seismic provisions have been implemented, and dynamic analysis was specified as the preferred method of analysis, especially for irregular structures. However, irregularities are present in older buildings, which did not benefit from the more enhanced design provisions of more current building codes. Therefore, the objective of the current research project, reported in this paper, has been adopted as the assessment of seismic vulnerability of older irregular reinforced concrete frame buildings in Canada.

Seismic design provisions were first introduced in the 1941 NBCC (NRC 1941) empirically as lateral forces with base shear equal to a percentage of seismic weight. The first seismic zoning map was introduced in the 1953 NBCC, which was updated in 1970 and 1985. Site specific uniform hazard spectrum (UHS) was introduced in the 2005 NBCC with design spectral accelerations specified for each municipality in Canada. While seismic hazard predictions improved over the year, the estimation of design base shears also went through evolution since its inception in 1941. Structural ductility was incorporated in design in the 1975 NBCC with ultimate strength design introduced in the Canadian design standard for reinforced concrete design, i.e., CSA A23.3-1973(CSA 1973), though the 1970 NBCC introduced a factor that

recognizes available ductilities in different structural systems. The evolution of seismic design provisions is summarized by Mitchel et. al. (2010), and Al Mamun and Saatcioglu (2017) in more details. No seismic design and detailing was included in CSA A23.3 prior to 1973 (CSA 1973), which was referenced in the 1975 NBCC. Hence, buildings constructed prior to 1975, before the adoption of ductile design provisions, may be vulnerable against earthquake effects (Rajeev and Tesfamariam 2012). The current investigation has the objective of investigating seismic vulnerabilities in 5-storey reinforced concrete frame buildings with irregularities, located in Vancouver and Ottawa as representatives of buildings subjected to western and eastern Canadian seismicities. Figure 6.1 illustrates the variation of NBCC design base shears over the years for a 5-storey reinforced concrete frame building. It is evident in this figure that, while the seismic base shear for conventional buildings did not vary significantly prior to 1975, the 1965 NBCC produced the lowest seismic base shear of the era. This edition of the code was selected for the design of buildings in the current investigation as representatives of non-ductile buildings built prior to 1975.

Four reinforced concrete frame buildings with three types of irregularities were considered. Dynamic analyses of buildings were conducted to develop fragility function. This necessitated incremental dynamic analysis (IDA) under different earthquake intensities. Damage states of buildings were monitored relative to pre-selected performance levels. Inter-storey drift was used as a damage indicator. The building performance, as affected by irregularities, was investigated in terms of the extent of plastic hinges, sequence of member failures, energy dissipation, and inter-storey drift. Pushover analysis was also conducted to compare structural response under incrementally increasing non-linear static loading. Static and dynamic shear force distributions were compared with the design shear force level.

6.2 Building Information

Five-storey reinforced concrete frame buildings were considered as representative frame structures with different types of irregularity. A total of five frame buildings were designed, one having a regular structural layout and the remaining four having different irregularities for Vancouver and Ottawa. The building details are presented in Table 6.1. All the buildings had a square floor plan, consisting of 5 bays in each direction, each having a 7.0 m long span. The floor height was 4.0 m. Superimposed dead load of 1.33 kPa and a live load of 2.4 kPa was

applied in addition to the self-weight of the structure. The buildings were designed according to the load combinations and guidelines specified in the 1965 NBCC. Seismic base shear was calculated according to the equation specified in code. Since there was no distinction of seismic zones between Vancouver and Ottawa in the seismic zoning map provided in 1953, the seismic base shear as well as the design was the same both for Vancouver and Ottawa buildings. The elevation and plan views are shown in Fig. 6.2(a) and 6.2(b) for the regular building (labelled as "Regular"). The first vertical irregularity consisted of vertical stiffness irregularity, and the building was labelled as "Stiff-Irr." In this building, the first floor was a soft storey with the floor height increased to 6.0 m, while the other floor heights remained as 4.0m. The building was designed according to the NBCC 1965, which required the amplification of design moments for the 6.0 m-high first storey columns due to slenderness. The storey shear was recalculated as the building height changed and the building was designed for increased moments at the first floor level. The first floor stiffness for this building was found to be 72% of the average stiffness of the three floors above (2^{nd}, 3^{rd} and 4^{th} floors). This change in stiffness would qualify the building as having vertical stiffness irregularity based on the irregularity definition specified in the 2010 NBCC.

The second type of vertical irregularity was geometric irregularity, and consisted of a building with a setback (labelled as "Setback-Irr"). Of the 5 bays at the first floor level, only three interior bays continued above the first floor level. The floor heights remained unchanged as 4.0 m. The elevation view of the building is shown in Fig. 6.2(c). This change reduced the horizontal dimension of the plan by 60% above the first-storey level, from 35 m x 35m to 21 m x 21 m. The setback introduced would qualify the building as having a vertical geometric irregularity based on the definition given in the 2010 NBCC. The design base shear, as well as the distribution of forces along the building height was calculated with due considerations given to the reduced seismic mass in the upper floors. The building was designed according to the 1965 NBCC, without any implication of the geometric irregularity in the building.

The third type of vertical irregularity was introduced by using masonry infill walls in the regular building above the first floor level. The resulting building was labelled as "Stiff-Irr-Inf." The infill walls were assumed to be non-structural elements in design, well isolated from the enclosing frame elements. The infill walls were only used in exterior frames above the first floor

as part of the building envelop. The plan and elevation views of Stiff-Irr-Inf building are showing in Fig. 6.2(d) and 6.2(e). The presence of masonry infill walls above the first floor resulted in a soft storey, which only had a stiffness of 9% of the stiffness of the 2nd floor, and 10% of the average stiffness of the 2nd, 3rd and 4th floors.

The plan irregularity considered had a torsionally sensitive building. The plan view of the building is shown in Fig. 6.2(f). The eccentricity of mass in this building was created due to the concentration of masonry infill walls at one end. The building was otherwise the same as the regular building, as was designed as a regular building. The masonry walls started at the ground level and continued up to the roof. This building was labelled as "Torsion-Irr." This orientation of infill walls was selected to simulate old structures with a staircase and/or elevator core at one end of the building, generating the eccentricity of the center of rigidity. The torsional constant B, as defined in the 2010 NBCC, was computed for all the floors as 1.75, 1.77, 1.75, 1.71, 1.65 at the 2nd, 3rd, 4th and 5th floor slab levels and the roof level, respectively. The B value was greater than 1.7 specified in the 2010 NBCC as the limit for torsionally sensitive building.

All the buildings were designed as conventional reinforced concrete frame buildings without any ductile detailing. They were designed with 30 MPa concrete and Grade 400 MPa reinforcement. Table 6.2 illustrates the cross-sectional properties of members, also showing the reinforcement arrangement. All the members had 10M transverse shear reinforcement with a minimum spacing of d/2, where d is the effective depth of the structural member Additional shear reinforcement was provided in structural elements when shear force was greater than that resisted by concrete alone as per the 1965 NBCC.

6.3 Analytical Modelling and Analysis of Buildings

The selected 5-storey buildings, with and without irregularities, were modelled and analysed under site specific earthquake records. Computer software PERFORM-3D (CSI 2013) was employed for non-linear response time history analysis. Analytical models were generated for the frame elements. Beams and columns were modeled using FEMA Beam and FEMA Column elements incorporated in the software. Each element consisted of two elastic segments with a point of inflection in the middle of the member and two flexural hinges, one at each end. A rigid end zone was specified at the end of each structural element to eliminate deformations within the

adjoining member, ensuring that potential plastic hinges form at the face of the adjoining member, rather than at their centrelines. Fig. 6.3 shows the schematic diagram for a concrete frame in the analytical model. Total chord rotation was used to develop the moment-rotation envelope curve assigned to the flexural hinges. A tri-linear relationship was used for this purpose. The initial linear segment represented the effective cracked stiffness, based on 35% and 70% of uncracked flexural rigidities for beams and columns, respectively. The yield moment was calculated from sectional analysis with corresponding chord rotation based on effective elastic rigidity. The second linear segment in the post yield range was established by assuming post-yield slopes of 8.5% and 4% of effective elastic slopes for beams and columns, respectively. Though the members were not designed and detailed for ductility, a minimum ductility ratio of 1.5, inherent to reinforced concrete response and typically used for conventional building, was assigned to each member. This implies that the post yield segment continued up to an ultimate rotation of 1.5 times the yield rotation prior to the onset of strength decay. The descending branch, which ended at the residual strength, was based on the ASCE41-13 (ASCE 2014) recommendations for members having nonconforming transverse reinforcement. The residual strength was specified as per the same requirements with values ranging between 0 and 20% of maximum moment capacity. The basic hysteretic model in the software, assigned to plastic hinges, was perfectly elasto-plastic model modified for use in reinforced concrete elements. This was done through energy degradation factor (EDF), which to introduced stiffness degradation characteristics under reversed cyclic loading. The higher the EDF was the more the reduction in the unloading slopes of hysteretic relationship would be. The EDF values were derived from tests conducted by Ozcebec and Saatcioglu (1989) with values ranging between 0.50 and 0.62. Further details of flexural modelling are discussed by the authors elsewhere (Al Mamun and Saatcioglu 2017).

Inelastic shear springs were introduced to account for shear distress in member under reversed cyclic loading. The shear force-shear distortion hysteretic behaviour followed the same rules as those for flexural. It had a tri-linear envelop curve with linear variation up to the onset of diagonal tension cracks at concrete shear capacity (V_c), based on elastic shear rigidity. The second linear segment continued with a positive slope computed based 10% of elastic shear rigidity up to the ultimate shear capacity when the transverse reinforcement has reached its yield The third line segment with a descending slope was obtained from the ASCE41-13 (ASCE 2014)

recommendation specified for nonconforming transverse reinforcement and under different levels of axial load. The EDF for shear was obtained from experimentally generated hysteretic shear force-shear displacement relationship (Ozcebec and Saatcioglu 1987), and varied between 0.29 and 0.44. Further details of shear modelling are discussed by the authors elsewhere (Al Mamun and Saatcioglu 2017).

The masonry infill walls, creating a soft storey, were modelled using the compression strut analogy. The walls were simulated by diagonal masonry struts, as defined in ASCE 41-13. They were modelled as 1-D strut elements in PERFORM-3D. The masonry walls consisted of 200 mm standard hollow concrete block units with S type mortar. The compressive strength of concrete blocks and of mortar, specified in the 1965 NBCC was used as f'_m = 6.5 MPa, which was defined in CSA S304.1-04 (CSA 2004). The equivalent cross sectional area and the capacity of each strut was calculated based on the recommendations made by Drysdale and Hamid (2005). Modulus of elasticity (E_m) of masonry infill was taken as $E_m = 850\, f'_m$ where f'_m is the compressive strength of concrete block masonry. Bilinear stress-strain relationship of concrete strut was developed according to ASCE 41-13, and is illustrated in Fig. 6.4. The effect of window and door openings in infill walls was neglected in the analytical model.

Synthetic seismic records were used separately for Vancouver and Ottawa. The records were selected from Engineering Seismology Toolbox (EST 2016) and adjusted according to the procedure specified by Atkinson (2009) to match the Uniform Hazard Spectra (UHS) specified in the 2010 NBCC for the two cities considered. They were then amplified or de-amplified according to Hunt and fill algorithm (Vamvatsikos and Cornell 2004) to perform incremental dynamic analysis (IDA). The spectral acceleration (S_a) from UHS at the selected building fundamental period was used as the base point for increasing and decreasing the earthquake intensity for the IDA. The stiffening effects of infill panels were included in period calculations when present.

The buildings were also analyzed under incrementally increasing lateral static loads (push-over analysis) for comparison with dynamic response. They were modelled using the same analytical models used for dynamic analysis, and the push-over analysis was conducted using the same software, i.e., PERFORM-3D. Inelastic hinges were assigned the tri-linear envelop curves described earlier for hysteretic modelling. They were subjected to equivalent static loads with

lateral force distribution along the building height as recommended by the design building code. The loads were increased until structural instability was encountered.

6.4 Generation of Fragility Functions

The IDA discussed in the preceding section was conducted for each building to obtain IDA curves under different earthquake intensities, with spectral acceleration used as the intensity measure. These IDA curves were then used to generate probabilistic assessment of building response at pre-determined performance limits. These performance limits were associated with damage levels. Each damage level was expressed in terms of maximum inter-storey drift ratio, which was used as the damage indicator following the FEMA 356 (FEMA 2000) recommendation. Three damage states were considered; i) Immediate Occupancy (IO), ii) Life Safety (LS), and iii) Collapse prevention (CP). Immediate Occupancy (IO) performance level describes the damage state where structure is safe to be re-occupied, having suffered minor damage to the structural elements, with minor spalling and flexural cracking. The inter-storey drift of 1% was considered for this limit state. Life Safety (LS) performance level describes the damage state where significant damage has occurred to the structure with extensive cracking and hinge formation in primary structural elements. The inter-storey drift of 2% was adopted for this limit state. Collapse Prevention (CP) performance level describes the damage state where structure is at the onset of partial or total collapse with extensive cracking, hinge formation and reinforcement buckling in structural elements. The median value of maximum inter-storey drift demands for all records was considered as CP performance level. This approach was also used by Ellingwood et al. (2007). The maximum inter-storey drift for CP limit was obtained as the smaller of the drift at which either dynamic instability is attained or the tangential slope of the IDA curve dropped to 20% of the initial slope (FEMA 350). In all the dynamic analyses conducted, the 1st storey exhibited highest displacements at failure.

The IDA results indicated that the collapse prevention limit state was exceeded prior to developing the 2% life safety limit under the 2010 NBCC hazard levels. This was attributed to the substandard building designs implemented using the1965 NBCC. Therefore, the fragility functions were generated for the IO and CP limit states only. Figure 6.5 illustrates the fragility curves for all 10 buildings with and without irregularities.

6.5 Performance Evaluation

Observations made from dynamic analysis of buildings indicate that the building failure was governed by flexure in all cases. The regular building showed flexural hinge formation at the 2nd, 3rd, 4th and 5th storey beams followed by the 1st storey columns. The building collapse was triggered by the flexural failure of beams, followed by the first-storey columns. Shear hinging formed only in the 1st-storey columns. However, no shear failure was observed in any member.

Similar response was observed in the building with vertical irregularity resulting from the difference in first-storey height (Stiff-Irr Building). Flexural hinges formed in the 2nd storey beams first, followed by the 3rd and 4th storey beams. Column flexural hinging occurred only at the 1st storey level. The building eventually collapsed due to flexure upon the formation of plastic hinges in the 1st storey columns. No shear hinge has formed and the shear force demands remained below the concrete shear capacity.

The building with the setback (Setback-Irr Building) developed flexural hinges in the 3rd, 4th and 5th storey beams followed by the 2nd storey beams and columns prior to the 1st storey columns. The building collapse was triggered by flexural failure, following the formation of plastic hinges. Plastic shear hinges formed in the 1st and 2nd storey columns, but no shear failure was observed.

The building with a soft first storey, resulting from the use of masonry infill walls in upper stories (Stiff-Irr-Inf Building), developed the first set of flexural hinges in the soft storey exterior columns. This was followed by the hinging of the 2nd, 3rd and 4th storey exterior beams. Subsequently the interior columns of the soft storey and the 2nd, 3rd and 4th storey interior beams have hinged. The structure failed due to collapse of the 1st storey exterior columns. Shear hinges formed only in the first-storey exterior columns, but no shear failure was observed. Infill walls maintained their integrity during the entire structural response without failure.

The building with torsional sensitivity (Torsion-Irr Building) showed higher drift ratios on the flexible side where the frames did not have infill walls, as expected. During response, the first set of flexural hinges formed in the beams of the 2nd, 3rd and 4th stories on the flexible side, followed by the 1st-storey columns of the same frames. The flexural hinging of beams and columns propagated towards the frames with infill walls. At this end of the building, flexural hinges formed only at the 2nd floor beams, followed by the 1st storey columns. Infill walls suffered

damage and failed at the 1st-storey level at about the time as the beams on the flexible side developed hinging. Subsequently the infill walls at the 2nd, 3rd and 4th stories failed. The building eventually collapsed due to the beam failure at the 2nd and 3rd storey levels on the flexible side, followed by the 1st storey column of the frame stiffened by infill walls. No other column failure on the flexible side and beam failure on the rigid side were observed. Columns and beams remained elastic in shear, developing shear demands below the concrete shear capacity.

Table 6.3 shows maximum inter-storey drift capacities at the CP performance level. It is evident from the table that the buildings had low maximum inter-storey drift capacities at the CP performance level. In all cases the CP drift limit was less than the LS drift limit of 2%, except for the buildings with setbacks, which showed almost equal drift limits for CP and LS limit states. The results imply that the buildings developed failure shortly after the IO performance limit of 1% inter-storey drift with very little safety margin.

Fragility curves of Fig. 6.5 and the summary of results in Table 6.3 indicate higher probability of exceeding performance limit states in Vancouver in comparison with Ottawa. At the 2010 hazard levels, the probabilities of exceeding IO and CP performance levels were high for all buildings in Vancouver, with an average probability of exceedance of 96% and 83%, respectively. For the Ottawa buildings, the average probabilities of exceeding the IO and CP limits were found to be 21% and 10%, respectively. All buildings in Vancouver exhibited similar probabilities of exceeding the IO performance level. While the same can be said for buildings in Ottawa, the building with a soft storey associated with the presence of masonry infill walls above the first floor (Stiff-Irr-Inf) showed the highest probability of exceedance. The same irregularity also showed the highest probability of exceeding the CP performance limit in both cities. The regular buildings and buildings with higher first stories (Stiff-Irr) exhibited similar probabilities of exceedances because designs of these two buildings were both governed by the 1965 NBCC guidelines, and their fundamental periods were almost the same, as indicated in Table 6.3. The other irregularities were not address in the 1965 design code. The buildings with setbacks (Setback-Irr) developed higher drift ratios in upper stories. Therefore, the inter-storey drift was higher at collapse, as indicated in Table 6.3. The probability of exceeding a higher drift limit associated with the CP limit was lower than that for regular buildings with smaller drift ratios at CP. Similarly, torsionally sensitive buildings (Torsion-Irr) developed higher drift ratios on the

flexible side of the buildings and the probability of exceeding the CP limit was lower than that for regular buildings.

The effect of irregularities was further assessed by examining the amount of energy dissipated during seismic response by each building. The energy dissipated was calculated as the average of energy dissipated during the 20 seismic events selected for Vancouver. The results are illustrated in Fig. 6.6. Because of the similarities in response between the Regular and Stiff-Irr buildings, the energy dissipation was almost the same for these two buildings. Stiff-Irr had only 8% higher energy dissipation because of the extensive damage incurred in the 1st storey columns. Setback-Irr building also dissipated similar inelastic energy as Regular building. Inelastic energy in this building was dissipated due to extensive plastic hinging mostly at upper floors. Stiff-irr-Inf building exhibited the lowest dissipated energy among all the buildings. The dissipated inelastic energy was only 25% of that for Regular building. This was because inelasticity was limited to the 1st storey elements. Torsion-Irr building showed the highest energy dissipation because of the extensive hinging of the frame elements on the flexible side of the building. Due to the torsional effects, the number of hinges that reached or approached CP performance level was very high resulting in inelastic energy dissipation equal to 2.7 times that for regular building.

The effects of irregularities on building response under static lateral loads were investigated by conducting push-over analyses. Force-displacement relationships under incrementally increasing static loads are shown in Fig. 6.7 as pushover curves in the form of total base shear-roof drift relationships. The figure indicates that both Regular and Stiff-Irr buildings behaved in a similar manner during the initial elastic and subsequent inelastic ranges of displacements. The total shear resistance provided by Stiff-Irr was somewhat higher. When infill walls were placed, shear resistance, as well as the initial stiffness increased markedly. The building with a soft storey (Stiff-Irr-Inf) developed higher drift, as expected. It should be noted that the roof drift plotted for torsionally sensitive building (Torsion-Irr) is the drift on the rigid side of the building. However, the buildings became brittle without displaying any ductility. This was due to the failure of ground floor columns without hinging of structural elements at upper floors. Figure 6.7 showed the roof drift on infill side for Torsion-Irr building. Setback-Irr showed the lowest shear resistance as the design shear force was low. However, the building collapsed at a higher roof drift due to extensive inelastic hinge rotations in upper floors.

Figure 6.8 shows the distribution of inter-storey drift ratios along the building height, obtained from push-over analyses. Maximum inter-storey drifts for both the regular building and the building with higher 1st storey (Stiff-Irr) took place at the 2nd storey level. The 1965 NBCC accounted for the effect of stiffness irregularity associated with column slenderness. Therefore, both Regular and Stiff-Irr buildings had similar deflections. The building with setback (Setback-Irr) showed the highest drift among all the buildings. Since the structural plan dimension was reduced above the 1st storey level, upper floors had lower stiffness and exhibited higher displacements. The maximum inter-storey drift took place at the third storey level. In contrast, the building with soft first-storey, having masonry infill walls above (Stiff-Irr-Inf), showed the highest inter-storey drift at the first-storey level. The inter-storey drift above the soft-storey was negligible. Torsionally sensitive building (Torsion-Irr) showed negligible storey drifts on the infill side, whereas the flexible side showed inter-storey drifts similar to those for the regular building.

The results of push-over analysis were also used to assess shear force distribution at each floor level as affected by irregularities. Figure 6.9 compares static shear distribution as obtained from push-over analysis with design shear forces obtained from the equivalent static design forces specified in the 1965 NBCC. It is evident from the figure that the code design shear forces are always lower than the static shear resistance provided by the buildings during the push-over analysis. Setback-Irr building had the lowest design shear force because of its relatively low seismic mass. It can be observed from the figure that the Regular building had the lowest safety margin, as the difference between the static shear resistance and design shear force was small. Since infill walls were added to the Regular building, design shear forces for Stiff-Irr-Inf and Torsion-Irr buildings were the same as those for the Regular building. However, the shear resisting provided by both Stiff-Irr-Inf and Torsion-Irr was higher in comparison with Regular building due to the added strength by the infill walls.

Because infill walls increased the shear resistance of buildings, the contribution provided by infill walls was calculated. Figure 6.10 shows the amount of shear resisted by infill walls in Stiff-Irr-Inf and Torsion-Inf buildings. In the Stiff-Irr-Inf building, the contribution of infill walls started at the 2nd storey level because of the absence of walls in the 1st storey. On average, 78% of total shear in each storey was resisted by infill walls. In Torsion-Irr building, on average 53%

of total shear in each storey was resisted by infill walls. This observation indicates that infill walls provided significant participation in the lateral force resisting system.

Shear force resistance during dynamic response is compared with that provided during non-linear static load application (pushover analysis) in Figure 6.11. The figure indicates that dynamic base shear resistance was higher than the static base shear resistance. Dynamic shear resistance was calculated as the average of shear forces generated by all the seismic events considered for Vancouver. In general dynamic and static shear force variation is found to be comparable, though some differences are observed in shear force distribution as affected by structural irregularities. Regular and Stiff-Irr buildings showed similar dynamic shear force distributions. Both Stiff-Irr-Inf and Tosion-Irr had similar shear force distribution above the 1st storey level. The dynamic shear resistance continued to increase in the 1st storey for Torsion-Irr building as the infill walls were continuous in this building through the 1st floor. However the dynamic shear resistance of the 1st storey in Stiff-Irr-Inf building with a soft first storey was negligible. Dynamic shear distribution in Setback-Irr was different than that under incremental static force application, as the dynamic shear was resisted mostly by the 1st storey. Dynamic shear was less than static shear at the 2nd storey where the setback was located.

6.6 Summary and Conclusions

Performance of buildings with irregularities, designed according to the 1965 NBCC, was evaluated and compared with that of regular buildings designed using the same code. It was observed that the building with vertical stiffness irregularity associated with having a higher storey height (Stiff-Irr) showed collapse sequence similar to that of the regular building. The building with setback irregularity (Setback-Irr) collapsed at higher storey level because of excessive yielding in upper floors. Soft storey generated by the use of masonry infill walls at upper floors (Stiff-Irr-Inf) created a weak storey, developing failure at the soft first-storey level. Torsionally sensitive building (Torsion-Inf) collapsed due to torsional stresses developed on the flexible side of the building. Fundamental periods of irregular buildings shortened in buildings with setback or infill walls. The irregularity that resulted from the use of a different floor height showed the same fundamental period as the regular building because the more slender columns were designed for higher capacities, with increased column dimensions.

The collapse prevention (CP) storey drift limit was lower in older building designed on the basis of the 1965 NBCC design provision, as they resulted in brittle structural response. Life safety limit of 2% storey drift could not be met in these buildings and the CP limit was reached prior to fulfilling the LS limit. Inter-storey drift of regular and irregular buildings of pre-1975 era were similar, except for the buildings with setbacks where the more flexible portion of the building above the setback level developed higher drift ratios. Irregularity type had an effect on the location of maximum inter-storey drift. The building with a soft-storey developed higher storey drifts at the soft-storey level. Torsionally sensitive buildings having rigidities at one end resulting from the use of masonry infill walls developed maximum storey drift at the bare side.

All buildings in Vancouver developed similar probabilities of exceeding the immediate occupancy (IO) performance level, though irregular buildings exhibited higher probabilities of exceeding the same performance level in Ottawa. Irregular buildings showed lower probability of exceeding the CP performance level in both Vancouver and Ottawa due to higher maximum inter-storey drifts experienced at collapse. These buildings include irregularities associated with setbacks, soft-stories resulting from the use of infill walls at other stories, and torsionally sensitive buildings. In terms of energy dissipation, as indicative of overall damage propagation, the buildings with setbacks showed similar energy dissipation as the regular buildings and building having storey height irregularity, except for the concentration of damage in upper floors. The building with a soft-storey experienced the smallest energy dissipation because of the concentration of damage to only one storey, whereas the building with torsional sensitivity developed the highest energy dissipation because of widespread damage distributed to frame element on the flexible side of the building.

It was revealed that storey shear resistance provided under incrementally increasing lateral static forces (under push-over forces) for regular and irregular buildings were higher than the 1965 NBCC code-based design shear demands. The same trend was followed when dynamic storey shears were compared with the 1965 NBCC code level storey design shears. The behaviour of irregular structures with infill walls indicated that infill walls resisted a major portion of storey shear, which was proportional to the rigidity provided by the walls. It was also observed that static push-over behaviour of the structures resembled the dynamic behaviour of structures. Irregular buildings with infill walls had the highest shear resistance, but showed brittle response,

whereas the building with setback showed lowest shear resistance. Stiffness irregularity due to change in storey height, resulting in more slender columns in a given storey level did not have any significant effect on overall behaviour, including shear resistance.

It can be concluded that, though no substantial difference was observed between regular and irregular frame buildings in terms of probability of exceeding pre-defined performance levels, the irregularity had substantial effect on the inter-storey drift demands, damage conditions, energy dissipation, shear force distribution and overall static and dynamic behaviour of buildings. Hence, all the above mentioned factors need to be accounted for when performing risk assessment of old irregular buildings in Canada. The results suggest that performance limits developed and used for regular buildings may not be sufficiently good indicators for seismic vulnerability of irregular buildings.

6.7 References for Chapter 6

American Concrete Institute (ACI), 2011. Guide for seismic rehabilitation of existing concrete frame buildings and commentary. ACI 369R-11. ACI committee 369.

American Concrete Institute (ACI), 2013. Guide for testing reinforced concrete structural elements under slowly applied simulated seismic loads. ACI 374.2R-13. ACI committee 374.

American Society of Civil Engineers (ASCE), 2014. Seismic evaluation and retrofit of existing buildings. ASCE/SEI 41-13. Reston, VA.

Athanassiadou, C.J., 2008. Seismic performance of R/C plane frames irregular in elevation. Engineering Structures. Volume 30, Issue 5, Pages 1250-1261, May 2008

Atkinson, G.M., 2009. Earthquake time histories compatible with the 2005 National building code of Canada uniform hard spectrum. Canadian Journal of Civil Engineering. Volume 36, Number 6, June 2009.

Canadian Standards Association (CSA), 1973. Design of concrete structures. CSA A23.3-73. CSA standards update service.

Canadian Standards Association (CSA), 2004. Design of masonry structures. CSA S304.1-04. CSA standards update service.

Computers and Structures, Inc (CSI), 2013. PERFORM-3D. Version 5.0.1. Berkeley, CA.

Drysdale, R.G. and Hamid, A.A. (2005): Masonry Structures: Behaviour and Design. Canada Masonry Design Centre, Mississauga, Ontario.

El-Kholy, S.A., El-Assaly, M.S., Maher, M. (2012). "Seismic Vulnerability Assessment of Existing Multi-Storey Reinforced Concrete Buildings in Egypt". Arabian Journal for Science and Engineering. Vol 37, Page 341-355. DOI 10.1007/s13369-012-0170-0

Ellingwood, B.R., Celik, O.C., and Kinali, K., 2007. Fragility assessment of building structural systems in Mid-America. Earthquake Engineering and Structural Dynamics. Volume 36, Issue 13, Pages 1935-1952, October 2007.

Engineering Seismology Toolbox (EST). (2016). Time histories for 2005 National Building Code of Canada. Available at http://www.seismotoolbox.ca/NBCC2005.html (Last accessed 8th December 2016)

Federal Emergency Management Agency (FEMA). 2000. Prestandard and commentary for the seismic rehabilitation of buildings. FEMA 356. Washington, D.C.

Jeong, S.H., Mwafy, A.M., and Elnashai, A.S., 2012. Probabilistic seismic performance assessment of code-compliant multi-storey RC buildings. Engineering Structures. Volume 34, January 2012, Pages 527-537.

National Building Code of Canada (NBCC). National Research Council of Canada. Ottawa, Canada.

Ozcebe, G., Saatcioglu, M. (1987). "Confinement of concrete columns for seismic loading." ACI Structural Journal. Volume 84, Issue 4, Pages 308-315.

Ozcebe, G., Saatcioglu, M. (1989). "Hysteretic shear model for reinforced concrete members". Journal of the Structural Engineering, ASCE. Volume 115, Issue 1, pp. 132-148.

Rajeev, P., and Tesfamariam, S., 2012. Seismic fragilities for reinforced concrete buildings with consideration of irregularities. Structural Safety. Volume 39, Pages 1-13, November 2012.

Stefano, M.D., and Pintucchi, B. (2008). A review of research on seismic behaviour of irregular building structures since 2002. Bulletin of Earthquake Engineering. Volume6, Issue 2, Pages: 285-308, May 2008.

Vamvatsikos, D., and Cornell, C.A., (2004). Applied incremental dynamic analysis. Earthquake Spectra. Vol 20, No. 2, Page 523-553.

6.8 Tables and Figures

Table 6.1 Details of buildings designed according to 1965 NBCC

Building Name	Building Detail	Irregularity Type	Location
Regular	Uniform plan &elevation	Regular	Vancouver & Ottawa
Stiff-Irr	First Floor 6m	Vertical Stiffness	Vancouver & Ottawa
Setback-Irr	4 bay above First Floor	Vertical Geometric	Vancouver & Ottawa
Stiff-Irr-Inf	Exterior Infill wall above First Floor	Vertical Stiffness	Vancouver & Ottawa
Torsion-Irr	Infill wall at side from Ground to roof	Torsional Sensitivity	Vancouver & Ottawa

Table 6.2 Structural member sectional properties of buildings

	Regular Stiff-Irr-Inf Torsion-Irr		**Setback-Irr**		**Stiff-Irr**	
	Member Size (mm)	Member Rebar	Member Size (mm)	Member Rebar	Member Size (mm)	Member Rebar
Corner Column 1-5	300X300	4-25M+4-15M	300X300	4-25M+4-15M	400X400	4-30M
Ext Column 1-2	325X325	8-25M	300X300	4-25M+4-15M	400X400	4-25M+4-20M
Ext Column 3-5	325X325	4-25M+4-20M	-	-	400X400	4-25M+4-20M
Int-1 Column 1-2	400X400	8-30M	350X350	4-25M+4-20M	475X475	4-25M+8-20M
Int-1 Column 3-5	400X400	4-25M+4-15M	350X350	4-25M+4-20M	475X475	4-30M[1]
Int-2 Column 1-2	400X400	4-30M+4-25M	350X350	4-25M+4-20M	475X475	4-25M+4-20M
Int-2 Column 3-5	400X400	8-20M	350X350	4-25M+4-20M	475X475	4-30M[1]
Int-3 Column 1-2	400X400	8-25M	400X400	4-25M	475X475	4-30M
Int-3 Column 3-5	400X400	8-20M	400X400	4-25M	475X475	4-30M
Ext Beam Top	300X500	4-20M	300X500	3-20M	300X500	3-25M
Ext Beam Bottom	300X500	2-20M	300X500	2-20M	300X500	2-20M
Int Beam 1-5 Top	300X500	3-25M	300X500	3-25M	300X500	2-30+1-25M
Int Beam 1-5 Bottom	300X500	3-20M	300X500	3-20M	300X500	2-25M

[1] Rebar from 2nd to 5th Floor

Table 6.3 Performance assessment of buildings

Location	Building Name	Period (Sec.)	Sa(Te)	Drift (%)	IO	CP
Vancouver	Regular	2.15	0.17	1.27	98	91
	Stiff-Irr	2.20	0.17	1.17	94	88
	Setback-Irr	1.85	0.19	1.91	97	69
	Stiff-Irr-Inf	1.40	0.27	1.11	97	95
	Torsion-Irr	1.48	0.25	1.42	93	72
Ottawa	Regular	2.15	0.05	1.04	11	9
	Stiff-Irr	2.20	0.05	1.22	13	6
	Setback-Irr	1.85	0.06	2.1	25	1
	Stiff-Irr-Inf	1.40	0.10	1.11	41	31
	Torsion-Irr	1.48	0.09	1.31	16	5

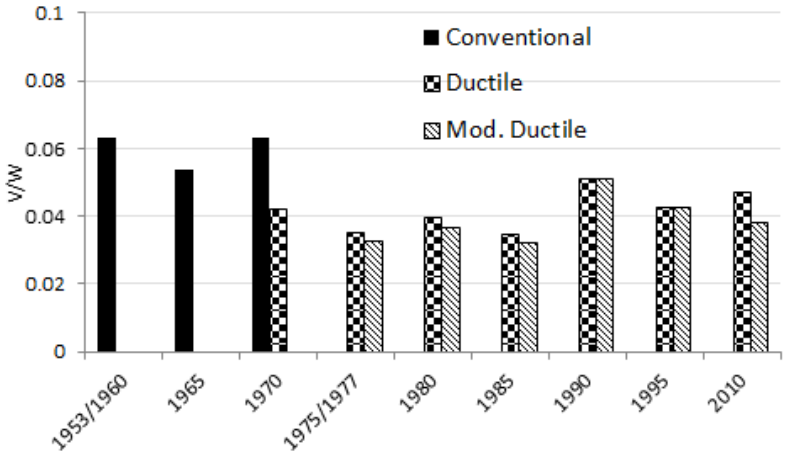

Fig 6.1 Base shear evolution of 5-storey building according to NBCC

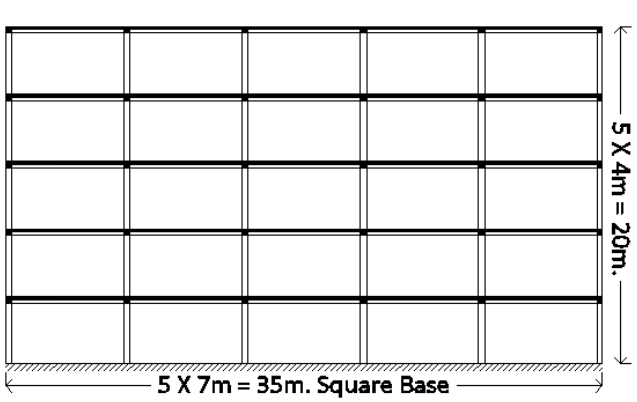

(a) Regular building elevation

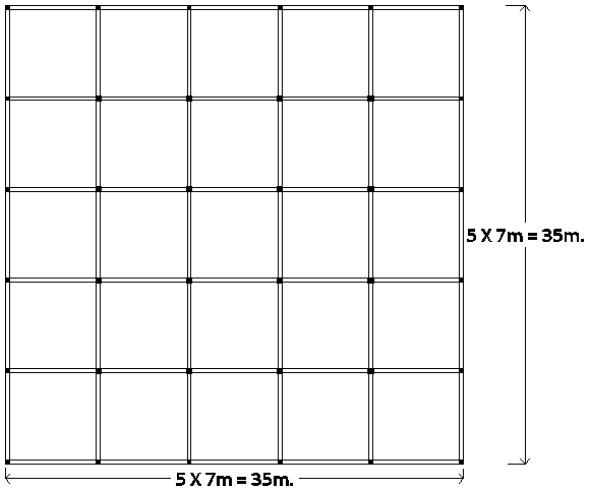

(b) Regular building plan

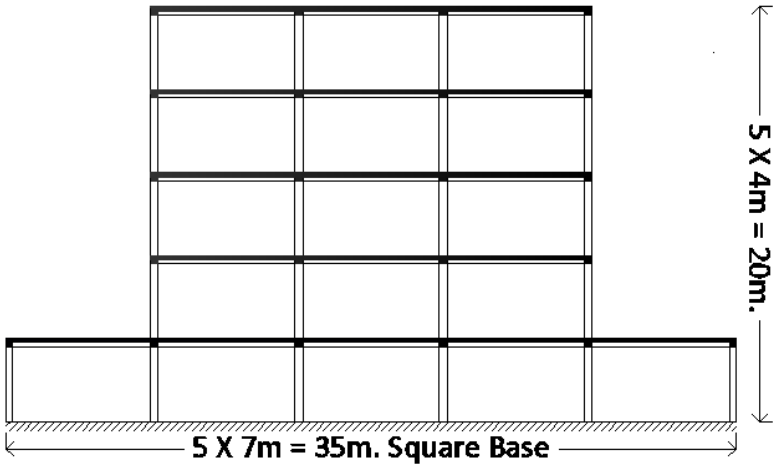

(c) Setback-Irr building elevation

Fig. 6.2 (Cont'd)

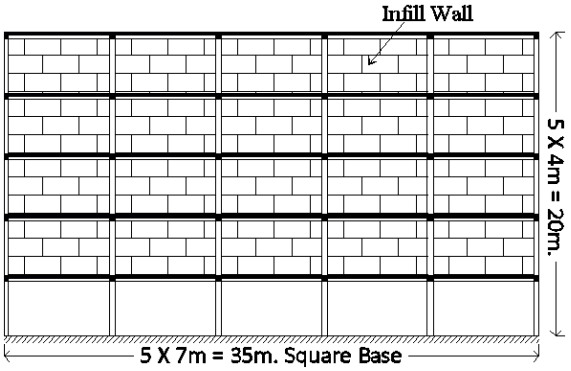

(d) Stiff-Irr-Inf building elevation

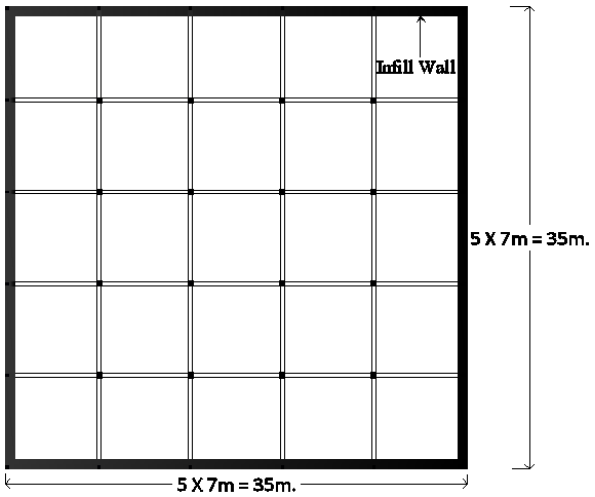

(e) Stiff-Irr-Inf building plan (2nd to 5th Floor)

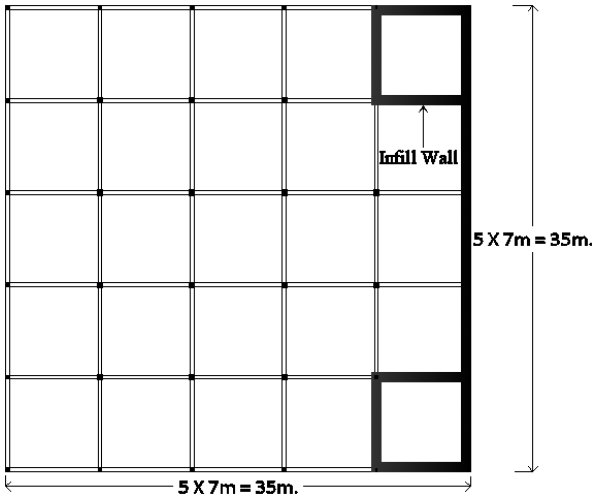

(f) Torsion-Irr building plan (GF to 5th Floor)

Fig 6.2 Plan and elevation of buildings

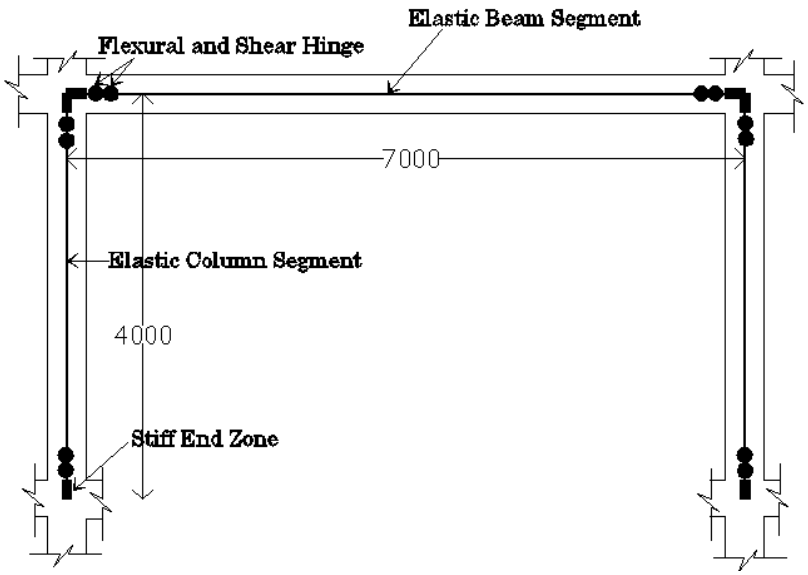

Fig 6.3 Schematic diagram of concrete frame element in analytical model developed with PERFORM-3D

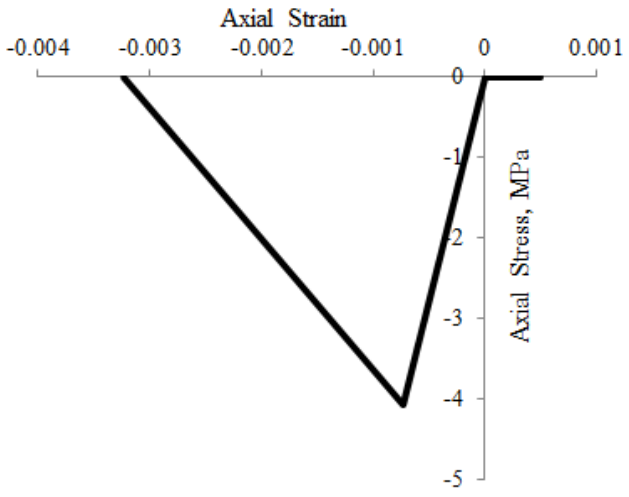

Fig 6.4 Axial Stress-Strain relation of concrete strut

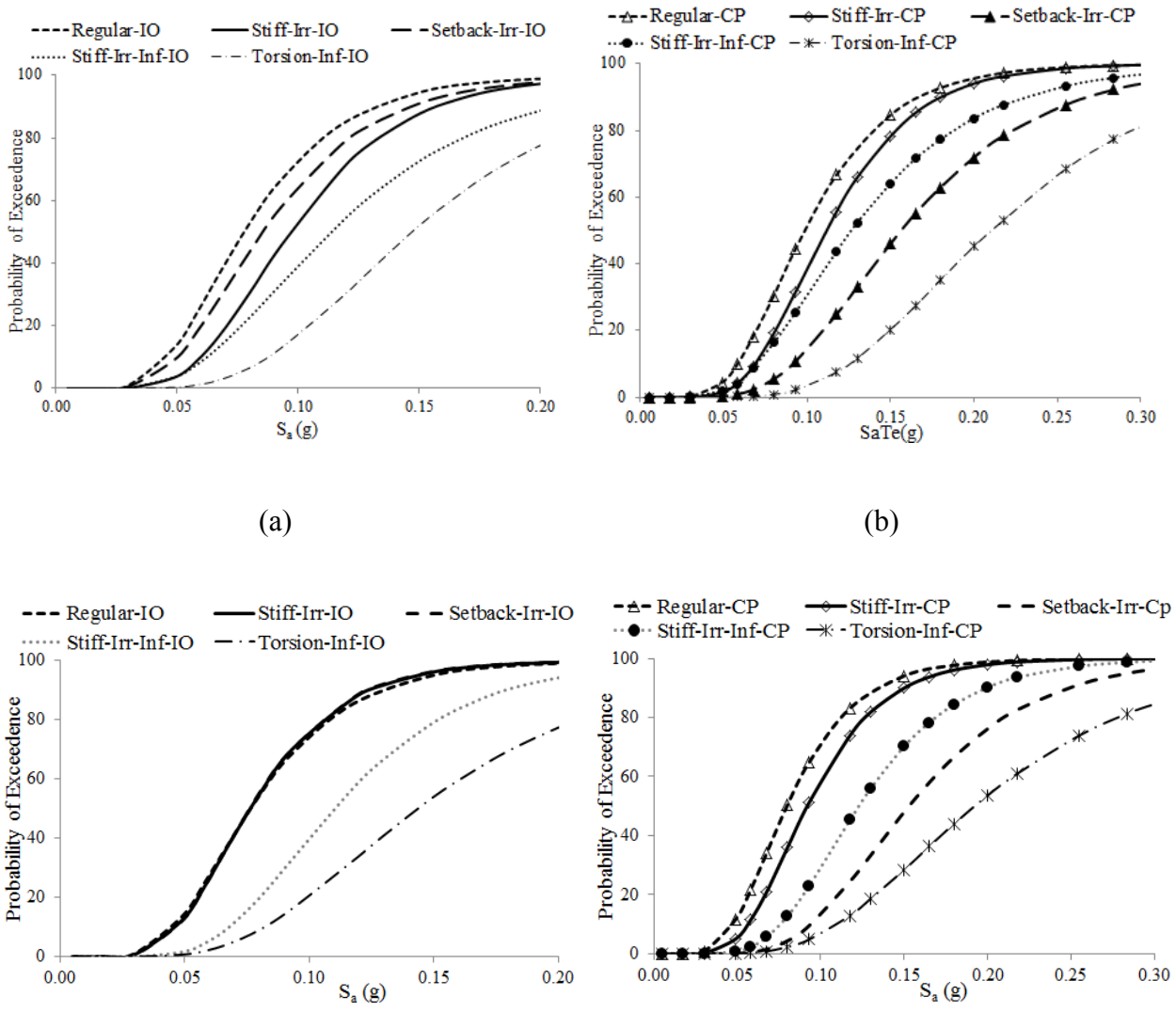

Fig 6.5 Fragility response of the buildings at (a) IO, (b) CP performance level at Vancouver and (c) IO, (d) CP performance level at Ottawa.

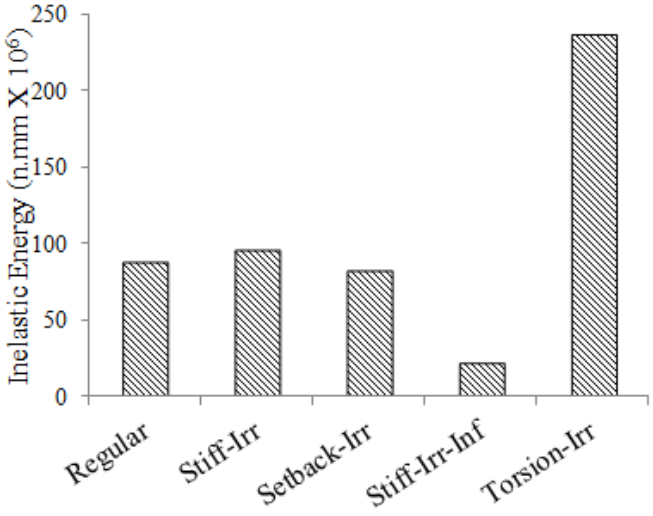

Fig 6.6 Inelastic dissipated energy of buildings

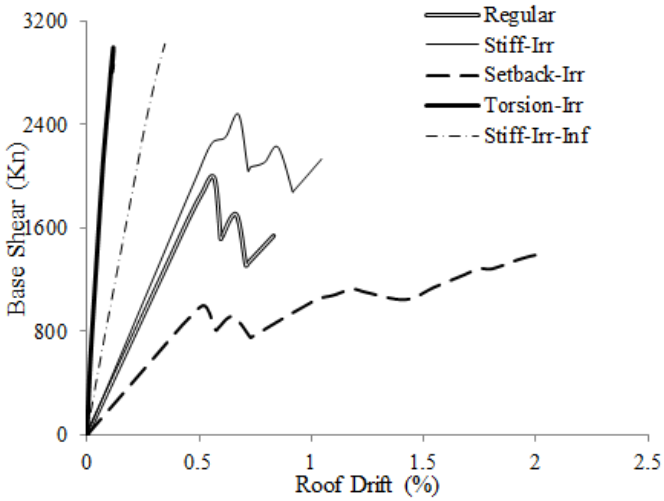

Fig 6.7 Pushover curves for the buildings analysed

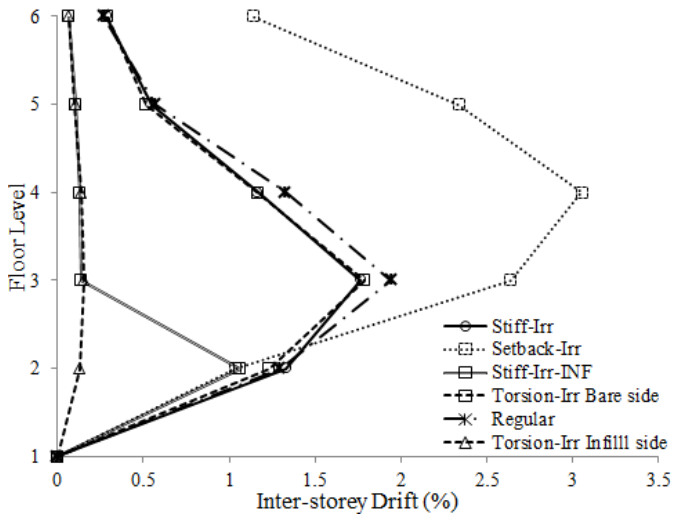

Fig 6.8 Inter-storey drift at floor level of buildings in pushover loading

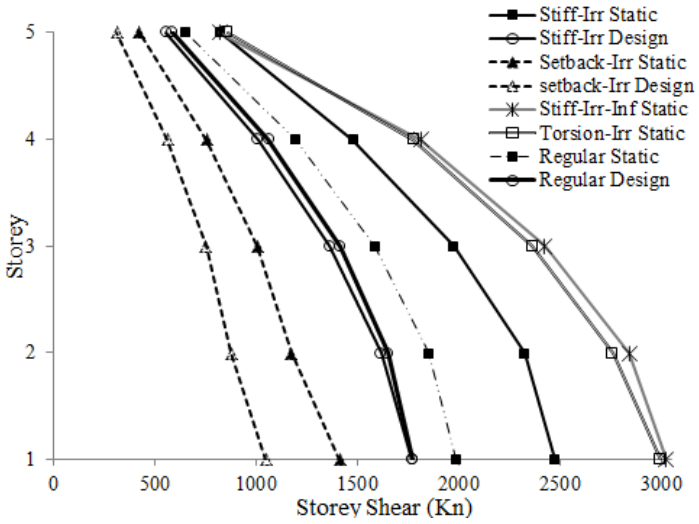

Fig 6.9 Comparison of design shear and pushover storey shear

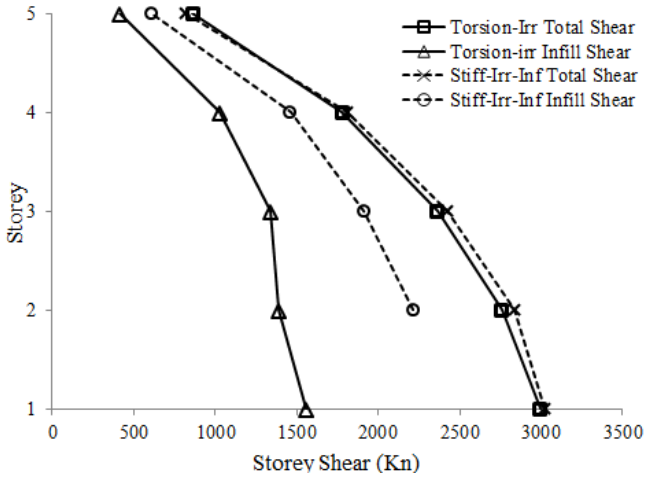

Fig 6.10 Contribution of infill walls in resisting shear force

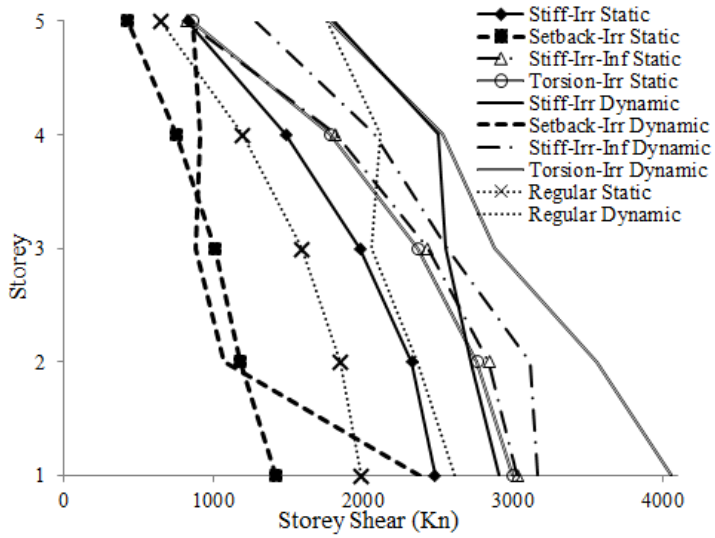

Fig 6.11 Comparison of pushover and dynamic storey shear

CHAPTER 7

7. SUMMARY AND CONCLUSION

Seismic fragility curves were developed as damage assessment tool to evaluate the seismic performance of reinforced concrete frame buildings in Canada. Three different building heights (2-, 5- and 10-storey) were considered. The buildings were designed and analyzed for two different geographic regions; Vancouver, considered as a representative city in Western Canada in a high seismic region and Ottawa, considered as a representative city in Eastern Canada in a medium seismic region. The buildings were designed according to the guideline specified in either the 2010 National Building Code of Canada, representing ductile building stock constructed in the post-1975 era or the 1965 National Building Code of Canada, representing the building stock constructed prior to 1975 in Canada. Analytical models of the buildings were developed with computer software PERFORM-3D. The analytical models were extensively verified against other commercially available computer software. Stiffness degrading hysteretic models were assigned to the members. The level of stiffness degradation was established by examining previous test data. Site specific synthetic seismic records were selected and modified to generate 2010 NBCC compatible records. Incremental dynamic analysis was employed to assess the seismic performance of buildings where spectral acceleration was used as intensity measure and inter-storey drift was considered as damage indicator. Three performance levels were considered: i) Immediate Occupancy, ii) Life Safety and iii) Collapse Prevention. The results of incremental dynamic analysis were used to develop fragility curves for buildings for the performance levels specified. Fragility curves were developed for 2-, 5- and 10-storey buildings designed according to the 2010 NBCC and the 1965 NBCC, as well as 5-storey building with different irregularities, designed according to the 1965 NBCC. Probability of exceeding performance levels as damage states was identified from the fragility curves and used to assess the performance of buildings.

The thesis consists of a series of journal articles presented in a sequence that reflects the progression of the research project. The first article, presented in Chapter 3, describes analytical model development with the validation of the model. The second article, presented in Chapter 4, describes the seismic performance assessment of modern code-compatible buildings in Canada. The third article, presented in Chapter 5, describes the seismic performance assessment of older buildings, also including comparisons with those for the newer buildings. The last article, presented in Chapter 6, describes the seismic performance assessment of older irregular buildings while comparing them with regular buildings of the same era.

The following conclusions are drawn from the investigation and performance evaluation of reinforced concrete frame buildings considered:

- The fragility curves developed for reinforced concrete frame buildings, with different heights, located in different seismic regions having both regular and irregular structural layouts and designed according to different versions of the National Building Code of Canada can be used for probabilistic seismic assessment of buildings. The fragility curves developed in this research represents convenient analytical tools to assess the seismic performance of reinforced concrete frame buildings in Canada.
- PERFORM-3D software produces non-linear building response that is comparable to other available software packages, and hence can be used for fragility analysis.
- Fragility curve developed for the moderately ductile building designed according to the 2010 NBCC and modeled using the deformation limits specified in CSA A23.3-04 showed the same fragility response for immediate occupancy and life safety performance levels as the same building modeled using the deformation limits specified in ASCE 41-13 and ACI 369R-11. However, the probability of exceeding collapse prevention performance level was lower when the latter two standards were used.
- The 2-, 5- and 10-storey buildings designed for Vancouver, following the requirements of the 2010 NBCC, when assessed based on the spectral acceleration at fundamental periods show probabilities of 38%, 42% and 48% at the life safety performance levels, respectively. For the same intensity level, the buildings show 92%, 93% and 95% probability of exceeding immediate occupancy for 2-, 5-, and 10- storey buildings, respectively.

- The 2- and 5-storey buildings for Ottawa, designed according to the requirements of the 2010 NBCC, indicate no probability of exceedance of life safety performance level at spectral accelerations corresponding to fundamental periods, while the 10-storey building shows only 1% probability of exceeding the same performance level. The probability of exceeding the immediate occupancy performance level for the same three buildings are 14%, 10% and 26%, respectively.
- Buildings designed based on pre-1975 editions of NBCC in Vancouver and Ottawa indicate that the collapse prevention limit state is exceeded prior to developing the commonly accepted 2% storey drift limit for life safety. The buildings show higher probabilities of exceedance at the collapse prevention performance level when compared with those buildings designed based on the 2010 NBCC.
- The 2-, 5- and 10-storey buildings designed in Vancouver based on the requirements of 1965 NBCC and assessed based on the 2010 NBCC hazard level spectral accelerations indicate 93%, 97% and 99% probabilities of exceeding immediate occupancy, and 68%, 91% and 88% probabilities of exceeding collapse prevention performance levels.
- The 2-, 5- and 10-storey buildings designed based on the requirements of 1965 NBCC for Ottawa indicate 18%, 11% and 30% probabilities of exceeding immediate occupancy and 1%, 9% and 8% probabilities of exceeding collapse prevention performance levels when assessed based on the 2010 NBCC hazard level spectral accelerations.
- Irregular buildings designed based on pre-1975 editions of NBCC in Vancouver and Ottawa indicate that the collapse prevention limit state of the buildings was exceeded prior to developing the commonly accepted 2% storey drift limit for life safety.
- Irregular buildings, designed for Vancouver according to the 1965 NBCC show similar probabilities of exceeding immediate occupancy performance level as those for regular buildings, though higher probabilities are observed for irregular buildings in Ottawa. At collapse prevention, all irregular buildings, except the buildings with setbacks, showed lower probability of exceeding performance limits because of the higher inter-storey drifts observed at collapse.
- Irregular buildings, designed according to the 1965 NBCC, revealed brittle failure with poor performance in comparison with regular buildings designed to the same code except

for buildings with stiffness irregularity associated with a change in storey height, as this effect was addressed in the 1965 NBCC.

- Buildings with a soft storey developed concentration of damage at the soft storey level, dissipating most of the seismic induced energy within this level. Similarly, buildings with torsional sensitivity developed excessive damage on the flexible side of the building, with most of the energy dissipation taking place in structural elements of the same side.

APPENDIX A

APPENDIX A: SEISMIC VULNERABILITY ASSESSMENT OF A 6-STOREY FRAME BUILDING IN CANADA BY USING THE FRAGILITY CURVES DEVELOPED

A 6-storey reinforced concrete frame building is considered as an illustrative example to assess its seismic vulnerability through the use of seismic fragility curves developed in this research project. The building is taken from the design example of "Seismic Design" chapter of the 2005 Concrete Design Handbook (3rd Edition), published by Cement Association of Canada.

The 6-storey building is an office building located in Vancouver. The building is designed as a ductile moment resisting frame structure and detailed according to the guideline specified in CSA A23.3-04. The horizontal dimension of the building is 42 m by 24 m. The building consisted of 110 mm thick slab with 500 mm square interior and 450 mm square exterior columns. Primary beams have the dimensions of 400 mm (wide) by 600 mm (deep) for the first three storeys and 400 mm (wide) by 550 mm (deep) for upper floors. The secondary beams have dimensions of 300 mm (wide) by 350 mm (deep) for all floors. The plan and elevation views of the building are shown in Figure A1.

Analytical model of the building was developed with software ETABS to determine the effective (cracked) period of the structure. To define the cracked properties of structural members, the effective elastic stiffness was considered as 40% of initial stiffness for beams, and 60% and 70% of initial stiffness for columns at the top three and bottom three levels, respectively. The code defined empirical fundamental period was calculated as 0.759 sec., which could be increased to a maximum of 150 % to define the design period. Hence, the design period of the building was 1.5 X 0.759 = 1.139 sec. However, the effective fundamental period of the building obtained from software ETABS was, T = 1.35 sec.

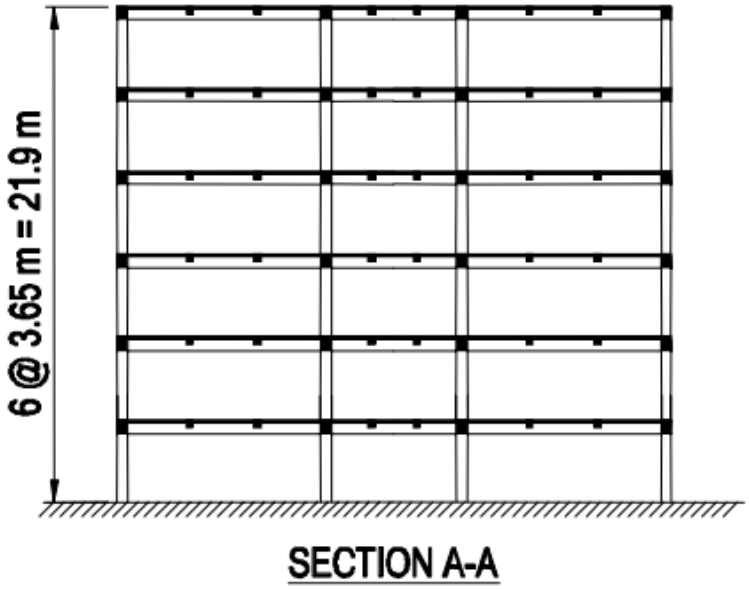

(a)

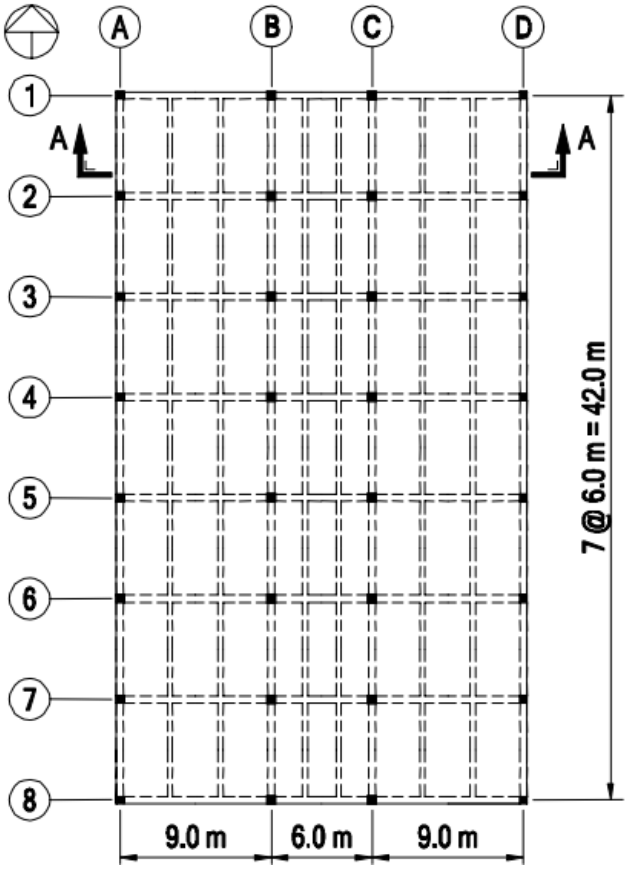

(b)

Fig A.1 (a) Elevation and (b) Plan views of 6-storey building (Concrete Design Handbook 2005)

The building was designed for site soil classification "C" with site coefficients related to acceleration-based (F_a) and velocity-based modification (F_v) as 1.0. From the uniform hazard spectra (UHS) specified in the 2010 National Building Code of Canada for Vancouver, the spectral acceleration corresponding to the fundamental period of the building was calculated as $S_a(T) = 0.274$.

The fragility curves developed in this research project was for site soil classification "C" with $F_a = F_v = 1.0$. Fragility curves developed for the buildings in Vancouver was designed and detailed as ductile reinforced concrete frame buildings according to the guideline specified in CSA A23.3-04. Hence, the site specific parameters for the fragility curves developed in the study are the same as those for the 6-storey building considered here as an illustrative example.

The fundamental period and height used in this study to develop the fragility curves was 2.04 sec. and 20 m for 5-storey regular frame building; and 2.84 sec. and 40 m for 10-storey regular frame building. Fundamental period and height of the 6-storey building considered is 1.35 sec. and 21.9m. It was observed from the current study that the failure mode, location of maximum inter-storey drift and plastic hinge formation in structural members depend on the number of storeys and thus influence the fragility response of a building. Hence it is acceptable to use linear interpolation of fragility response developed in this study for 5-storey and 10-storey buildings to assess the seismic vulnerability of the 6-storey building.

The probability of exceeding Immediate Occupancy (IO), Life Safety (LS) and Collapse Prevention (CP) performance levels for $S_a(T) = 0.274$ were found from the fragility curves for 5-storey buildings, as 56%, 8% and 1%, respectively. This is shown in shown in Figure A2 (a). The probability of exceeding IO, LS and CP performance levels for $S_a(T) = 0.274$, found from fragility curves developed for 10-storey building, are 70%, 29% and 15%, respectively, as shown in Figure A2 (b). From linear interpolation, the probability of exceeding IO performance level for the 6-storey building is $\frac{(70-56)}{(10-5)} X\,(6-5) + 56 = 59\%$. Similarly, the probability of exceeding LS and CP performance levels for the 6-storey building is 12% and 4%. It is noteworthy that the IO and LS limit states were considered as 1% and 2% maximum inter-storey drift ratios. Fragility curves shown in Figure A2 (a) and A2 (b) are taken from Figure 4.10 (e) and (f), respectively, included in Chapter 4 of this thesis. The maximum inter-storey drift observed for 5-storey and 10-storey buildings were 3.91% and 3.07%, respectively. Hence, the

anticipated maximum inter-storey drift for the 6-storey building is 3.74%, as obtained from linear interpolation. This is the maximum inter-storey drift at CP performance level.

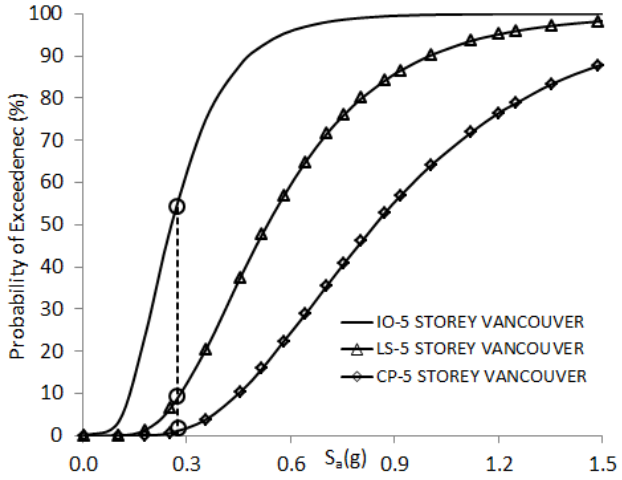

(a)

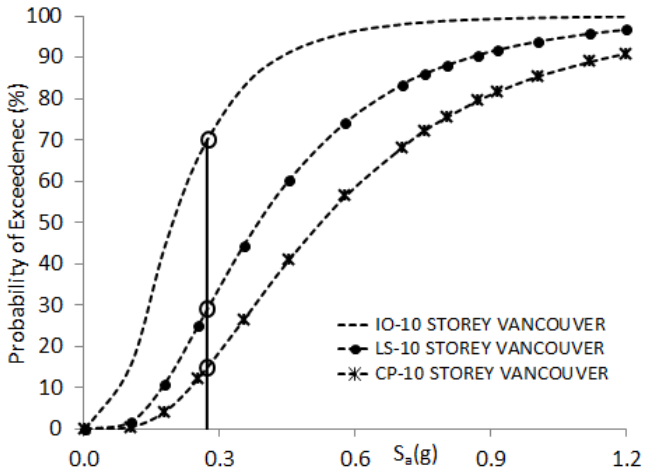

(b)

Fig A.2 Fragility response of 6-storey building from fragility curves of (a) 5-storey and (b) 10-storey buildings